國 立 交 通 大 學

電信工程學系

碩 士 論 文

對角線加權式時空段碼正交分頻多工系統與其通道估計

A Diagonally Weighted Space-Time Block Code OFDM with Channel Estimation

研 究 生：林新詠

指導教授：謝世福 博士

中 華 民 國 九十四 年 十 月

對角線加權式時空段碼正交分頻多工系統與其通道估計

A Diagonally Weighted Space-Time Block Code OFDM with Channel Estimation

研 究 生：林新詠　　Student: S. Y. Lin

指導教授：謝世福　　Advisor: S. F. Hsieh

國立交通大學

電信工程學系碩士班

碩士論文

A Thesis

Submitted to Department of Communication Engineering

College of Electrical Engineering and Computer Science

National Chiao Tung University

In Partial Fulfillment of the Requirements

For the Degree of

Master of Science

in

Electrical Engineering

October, 2005

Hsinchu, Taiwan, Republic of China

中華民國九十四年十月

對角線加權式時空段碼

正交分頻多工系統與其通道估計

學生：林新詠　　指導教授：謝世福

國立交通大學電信工程學系碩士班

摘要

時空段碼正交分頻多工系統因擁高傳輸效率與分集增益(diversity gain)等優勢而於近年來廣受推崇。在本篇論文中，我們針對四根傳輸天線的時空段碼，討論其傳輸矩陣結構是否正交與其傳輸率，並在此提出一種非正交的複數時空段碼 Block Diagonal (BD)。在其通道估計方面，我們應用 Giannakis 所提出的時空正交分頻多工調變之半盲式通道估計，為改善其估計值，phase direct (PD)將被使用以使此通道估計演算法更趨於理想。PD 是在我們得到通道功率(振幅)響應之後解得其相角響應，在時空段碼正交分頻多工中，其通道功率響應必須透過矩陣與向量的運算取得。此外，在非正交複數信號時空段碼中，當傳輸矩陣不可逆時，會無法求得通道功率響應，為解決此問題，我們對時空段碼傳輸矩陣的對角線元素統一乘上一正實常數 k，為公平起見，所有可使用此半盲式通道估計之時空段碼的傳輸矩陣都會經此處理。最後，電腦模擬將會驗證 PD 確實對通道估計有所改善，展示並討論 k 值對於通道估計均方誤差、雜訊與位元錯誤率等的影響。

A Diagonally Weighted Space-Time Block Code OFDM with Channel Estimation

Student: S. Y. Lin Advisor: S. F. Hsieh

Department of Communication Engineering

National Chiao Tung University

Abstract

Space-time block coded orthogonal frequency division multiplexing (STBC OFDM) has become popular recently for its high data rate transmission and diversity gain. In this thesis, we focus on STBCs with four transmit antennas and discuss about whether their transmission matrices are orthogonal and their transmission rate. A novel kind of complex non-orthogonal STBC called Block Diagonal (BD) will be proposed. The semi-blind channel estimation proposed by Giannakis is adopted for the STBC OFDM. To improve the performance of estimator, we use phase direct (PD), which is to solve phase ambiguities after the channel power response is obtained. We get channel power response through matrix and vector computation in STBC OFDM. In complex non-orthogonal STBCs, however, channel power response cannot be obtained when transmission matrix is singular. To solve this problem, we multiply a positive real constant k to the diagonal elements of their transmission matrices, not only in non-orthogonal models but also in all STBCs that can be implemented in the semi-blind channel estimation. Finally, in computer simulations, we can see that PD really improves the estimator. The effect of k on channel estimate mean square error, noise and bit error rate performance will also be exhibited and discussed.

Acknowledgement

首先我要感謝我的指導教授謝世福老師，老師熱心並不厭其煩地引導與指正，讓我獲益良多，老師對於研究嚴謹仔細的思維、深入而廣闊的見解與認真踏實的精神和態度，使我受用無窮。其次要感謝口試委員王逸如老師和廖元甫老師，王老師和廖老師給予我的指點與建議，讓我更瞭解研究領域的廣闊，往後在學習上一定會更加謙卑。

十分感謝實驗室的學長、同學、學弟和我的好朋友們，有你們的支持與鼓勵，我才能順利完成。

最後，由衷地感謝我的父母兄弟，在最困難的時候給我最大的關懷、幫助與安慰，並陪伴我走完這一段路，沒有你們，我絕對不可能完成這一切，僅把這篇論文獻給我的家人們，謝謝你們。

Contents

List of Tables

List of Figures

Chapter 1
Introduction

Orthogonal frequency division multiplexing (OFDM) [1,2] has become a popular technique for transmission of signals over wireless channels. It divides the whole channel into many narrow parallel subchannels to increase the symbol period and reducing or eliminating the inter-symbol interference (ISI) caused by the multipath channel environment. The inter-channel interference (ICI), however, can be eliminated by the independent and orthogonal among subcarriers, which is not easy to obtain in practice. On the other hand, there is higher error probability for those subchannels in deep fades since the dispersive property of wireless channels causes frequency selective fading. Therefore, techniques such as error correction code and diversity [2] have to be used to compensate for the frequency selectivity. In this thesis, we investigate transmitter diversity using space-time block codes for OFDM systems.

Space-time block codes (STBC) [3-9] realize the diversity gains by applying temporal and spatial correlation to the signals transmitted from different antennas without increasing the total transmitted power and transmission bandwidth. They have therefore been attractive means in high data rate transmissions. In fact, there is a diversity gain that results from multiple paths between base station and user terminal, and a coding gain that results from how symbols are correlated across transmit antennas.

Transmitter diversity is an effective technique for combating fading in mobile

wireless communications, especially when receiver diversity is expensive or impractical. Such systems always have more than one transmit-antenna and one receive-antenna and are so-called multi-input single-output (MISO). With single receive end, a well known two-transmit-antenna Alamouti STBC is proposed in [4]. In this thesis, however, we want to look into four-transmit-antenna STBCs. Such model includes real orthogonal [5], complex orthogonal [6,7], and complex non-orthogonal [8,9]. In STBCs with more than two transmit antennas, real orthogonal models guarantee full transmission rate (=1). But the complex orthogonal models cannot achieve full rate [7]. The complex non-orthogonal ones, however, sacrifice the orthogonality to achieve this goal [8,9].

For most STBC transceivers, *multichannel* estimation algorithms are important issues. Training symbols are transmitted periodically in [10] for the receiver to acquire the multi-input multi-output (MIMO) channels. However, training sequences consume bandwidth and, thereby, incur spectral efficiency and capacity loss. For this reason, blind channel estimation methods receive growing attention.

A few works have been proposed until now on blind MIMO and MISO channel estimation that exploits the unique features of STBCs. Blind channel estimation and equalization for MISO STBC systems has been proposed in [11] and for MIMO STBC systems in [12,13]. Just like [14], [13] also introduced the semi-blind channel estimation combining blind method and pilots. A subspace-based semi-blind method is proposed in [15] for estimating the channel relying on redundant modulus precoding responses.

In this thesis, unlike the similar system with two transmit antenna and Alamouti [4] STBC proposed in [15], a linearly precoded STBC OFDM system with four transmit antennas is introduced. Real orthogonal and complex non-orthogonal STBCs are given. The semi-blind channel identification algorithm [15] for frequency-selective

FIR channels through the subspace method is adopted as the channel estimation for this system. Distinct redundant precoders insure that the subspace-based method can estimate multiple channels simultaneously up to one scalar ambiguity [15]. The theoretical mean square error of this estimator derived in [17] will also be mentioned and be compared with the simulation results.

To further improve the subspace-based channel estimates, the “Phase direct (PD)” method based on the finite alphabet property is exploited. The main idea of this method is to solve the channel phase ambiguities after we have gained the channel power response. PD originally works in conventional OFDM [16], which we can acquire the channel power response easily by simple scalar division. But it is quite different in STBC OFDM, since the received data consists of more than one different transmitted data, which are not easy to be separated. So, the main problem we encounter now is how to get the channel power response, which is practically hard to obtain. In this thesis, the method of getting the channel power response for four-antenna STBC OFDM is presented. The modulation classes we focus on are BPSK and QPSK systems.

However, the singular transmission matrices produced by some possible symbol pairs in non-orthogonal STBCs will make getting channel power response unworkable. To solve this problem we modify the structure of transmission matrices of non-orthogonal STBCs by multiplying a real constant gain k on its diagonal elements. Simulation results show that the increase of k will better the subspace estimator. But this will also increase noise power, which will make bit error rate performance worse.

Furthermore, in time-varying channel, a proper window size of received data blocks need to be chosen to get the channel power response and apply it to PD. A trade off is that a shorter window can catch up the channel variation but makes the

system affected by noise more. The preorder form, however, is an issue that should also be noticed behind the algorithm and will be discussed then.

This thesis is organized as follows. In Chapter 2, we show how data is transmitted and received through space-time block code (STBC) and introduce several kinds of STBCs. A novel kind of four-transmit-antenna complex non-orthogonal STBC named Block Diagonal (BD) will be proposed. Four-antenna STBC combined with OFDM system is presented in Chapter 3. A semi-blind channel estimation algorithm for STBC OFDM and its improved method are shown in Chapter 4. Furthermore, Chapter 4 introduces the k -diagonally weighted transmission matrices for complex non-orthogonal STBCs to prevent them from singular and therefore can be adopted in PD. Chapter 5 exhibits simulation results and the effect of diagonal weight k on channel estimate error, noise, and bit error rate. Finally, our conclusions are summarized in Chapter 6.

Chapter 2
Classifications of Space-Time Block Codes

In this chapter, the basic concept of space-time block code (STBC) transceiving process will be given first. We will then introduce several kinds of STBCs. Only the first kind of STBC (Alamouti) is used in the 2-transmission-antenna system. Others are used in 4-transmission-antenna systems, which can be divided into orthogonal and non-orthogonal models. In complex non-orthogonal models, a novel kind of STBC called Block Diagonal (BD) will be proposed. The structure of transmission matrix and transceiving process of each STBC system will also be explained briefly.

2.1 Basic STBC tranceiving process

The following steps are all expressed in the frequency domain, as shown in Fig.2.1.

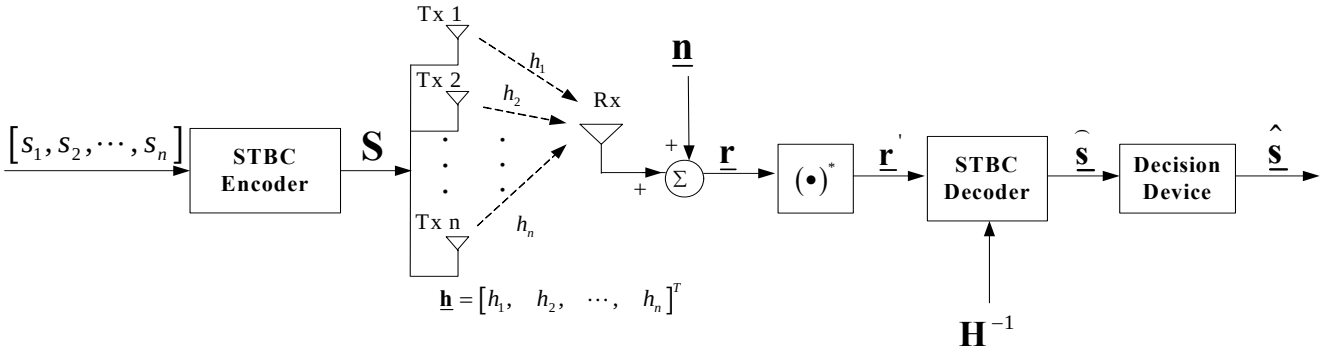

Fig. 2.1 Basic STBC transceiver model in frequency domain

Suppose n transmit antennas are used. STBC transmission matrix is presented as $\mathbf{S}$. n symbol vectors $s_1,\ s_2,\ \cdots,\ s_n$ and their conjugates make up elements of $\mathbf{S}$. Symbols in the same column of $\mathbf{S}$ stand for symbols sent from the same transmit antenna, while symbols in its same row stand for symbols sent in the same time slot.

The channel response vector is denoted by $\underline{\mathbf{h}}$, and the AWGN noise vector by $\underline{\mathbf{n}}$.

$$\underline{\mathbf{h}} = \left[h_1,\ h_2,\ \cdots,\ h_n\right]^T \tag{2.1}$$

$$\underline{\mathbf{n}} = \left[n_1,\ n_2,\ \cdots,\ n_n\right]^T \tag{2.2}$$

where h_i is the channel response and n_i is the AWGN noise. $i \in \{1, 2, \cdots, n\}$.

In the first place, modulated data symbols form the transmission matrices $\mathbf{S}$. Then they are sent through channels. At the receiver end, received data symbol vector $\underline{\mathbf{r}}$ can be presented as:

$$\underline{\mathbf{r}} = \mathbf{S} * \underline{\mathbf{h}} + \underline{\mathbf{n}} \tag{2.3}$$

in frequency domain, where $*$ is the matrix-vector multiplication.

In Eq. (2.3), AWGN are added after the symbols summed from different transmit antennas in the same time slot. In the next step, $\underline{\mathbf{r}}$ is adjusted to $\underline{\mathbf{r}}'$ so that only original data vectors $s_1,\ s_2,\ \cdots\ s_n$ exist here in $\underline{\mathbf{r}}'$ after the adjustment. The terms of h_i and their conjugates are then exchanged with s_i. $\underline{\mathbf{r}}'$ can be written as:

$$\underline{\mathbf{r}}' = \mathbf{H} * \underline{\mathbf{s}} + \underline{\mathbf{n}}' \tag{2.4}$$

where

$$\underline{\mathbf{s}} = \left[s_1,\ s_2,\ \cdots,\ s_n\right]^T \tag{2.5}$$

and $\mathbf{H}$ is the channel state matrix in which $h_1,\ h_2,\ \cdots,\ h_n$ and their conjugates form its elements. Note that during Eq. (2.3) and Eq. (2.4), the characteristic of $\mathbf{S}$ is

going to be transferred into $\mathbf{H}$.

Finally, we can recover $\underline{\mathbf{s}}$ from $\underline{\mathbf{r}}'$ by

$$\hat{\underline{\mathbf{s}}} = \mathbf{H}^{-1} * \underline{\mathbf{r}}' = \mathbf{H}^{-1} * \mathbf{H} * \underline{\mathbf{s}} + \mathbf{H}^{-1} * \underline{\mathbf{n}}' = \underline{\mathbf{s}} + \mathbf{H}^{-1} * \underline{\mathbf{n}}' \tag{2.6}$$

$\hat{\underline{\mathbf{s}}}$ is the soft decision data vector, which is at last sent into decision device to output the hard decision data vector $\hat{\underline{\mathbf{s}}}$.

2.2 Alamouti STBC

A simple STBC model had been proposed by Alamouti in [4]. The transmission matrix of this scheme with two transmission antennas is

$$\mathbf{S} = \begin{bmatrix} s_1 & s_2 \\ -s_2^* & s_1^* \end{bmatrix} \tag{2.7}$$

s_1 and s_2 denote two transmitted symbol vectors that can be any size (including one). As we mentioned in section 2.1, the first and the second column of the matrix denote the data symbol vectors transmitted by the first and the second antenna. While the first and the second rows represent the two time slots it takes in a transmission matrix to transmit the data vectors.

One of its important properties is that the transmission matrix is orthogonal. The word “orthogonal” here means that the product matrix of the multiplication of $\mathbf{S}^H$ and $\mathbf{S}$ is a diagonal matrix, where $\mathbf{S}^H$ is the Hermitian matrix (i.e. its transpose conjugate matrix) of $\mathbf{S}$. Generally, each diagonal element of this product matrix equals to $\sum_{i=1}^{\text{Num\_symbols}} |s_i|^2$. In this model:

$$\mathbf{S}^H * \mathbf{S} = \begin{bmatrix} a_1 & 0 \\ 0 & a_1 \end{bmatrix} \tag{2.8}$$

which corresponds to the definition of orthogonal, and

$$a_1 = \sum_{i=1}^{2} | s_i |^2 \tag{2.9}$$

We also call $\mathbf{S}^H * \mathbf{S}$ the correlation matrix of $\mathbf{S}$.

2.3 Four-by-four Orthogonal STBC

In this section, STBCs with four-by-four transmission matrices are introduced. Four time slots are needed to transmit once (i.e. in a transmission matrix) and four transmit antennas are used in these schemes.

2.3.1 Real Four-by-four Orthogonal (RO) STBC

As are the same in section 2.1, s_1, s_2, s_3, and s_4 can denote four transmitted symbol vectors of any size and form the transmission matrix. The STBC scheme proposed in [5] transmits real symbols, such as PAM and BPSK. Its transmission matrix is shown below:

$$\mathbf{S} = \begin{bmatrix} s_1 & s_2 & s_3 & s_4 \\ -s_2 & s_1 & -s_4 & s_3 \\ -s_3 & s_4 & s_1 & -s_2 \\ -s_4 & -s_3 & s_2 & s_1 \end{bmatrix} \tag{2.10}$$

$\mathbf{S}$ is also orthogonal. With real symbols, it is true that:

$$\sum_{i=1}^{\text{Num\_symbols}} | s_i |^2 = \sum_{i=1}^{\text{Num\_symbols}} (s_i)^2 \tag{2.11}$$

Hence,

$$\mathbf{S}^H * \mathbf{S} = \begin{bmatrix} a_2 & 0 & 0 & 0 \\ 0 & a_2 & 0 & 0 \\ 0 & 0 & a_2 & 0 \\ 0 & 0 & 0 & a_2 \end{bmatrix} \tag{2.12}$$

where

$$a_2 = \sum_{i=1}^{4} (s_i)^2 \tag{2.13}$$

Here, integer Num_symbols presents the number of transmitted symbol vectors s_i in a transmission matrix. The value of Num_symbols is 4 in this subsection. That means four symbol vectors are sent during four time slots in a transmission matrix. So, the *transmission rate* of this STBC is 1 and it is the *maximum achievable transmission rate* in a STBC system. In any arbitrary real signal system, there must exist STBC schemes that have maximum transmission rate with any number of transmission antennas [7].

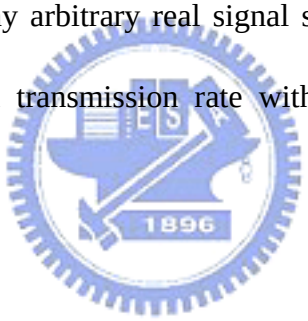

2.3.2 Complex Four-by-four Orthogonal (CO) STBC

In this subsection, the transmission matrix of STBC is also orthogonal. But the complex modulation, such as QAM and PSK, is used. For any kind of complex constellation, the maximal achievable transmission rate is $\frac{\lceil \log_2(N\_Tx) \rceil + 1}{2^{\lceil \log_2(N\_Tx) \rceil}}$ in an N_Tx-transmit-antenna employed orthogonal STBC system [8]. Here, $\lceil x \rceil$ means the minimum integer larger than the real number x. For instance, the maximal transmission rate for a 3 or 4-transmit-antenna system is 3/4. The transmission matrix for a 2-antenna system (section 2.1), however, can always achieves the full transmission rate (=1) whatever with real or complex constellation signals. For

complex signals, it cannot achieve full rate for a STBC when $N\_Tx \geq 3$. But for real signals, however, full rate can be gained with any number of N_Tx [7].

The scheme introduced here, designed by Tarokh et al in [6,7], is a typical complex four-by-four orthogonal STBC. A special feature of this scheme is that it only sends three symbol vectors in every four time slots. Thus, its transmission rate is obviously 3/4, which corresponds to the fact mentioned above. Its transmission matrix structure is:

$$\mathbf{S} = \begin{bmatrix} s_1 & s_2 & \frac{s_3}{\sqrt{2}} & \frac{s_3}{\sqrt{2}} \\ -s_2^* & s_1^* & \frac{s_3}{\sqrt{2}} & -\frac{s_3}{\sqrt{2}} \\ \frac{s_3^*}{\sqrt{2}} & \frac{s_3^*}{\sqrt{2}} & \frac{(-s_1 - s_1^* + s_2 - s_2^*)}{2} & \frac{(-s_2 - s_2^* + s_1 - s_1^*)}{2} \\ \frac{s_3^*}{\sqrt{2}} & -\frac{s_3^*}{\sqrt{2}} & \frac{(s_2 + s_2^* + s_1 - s_1^*)}{2} & -\frac{(s_1 + s_1^* + s_2 - s_2^*)}{2} \end{bmatrix} \quad (2.14)$$

and

$$\mathbf{S}^H * \mathbf{S} = \begin{bmatrix} a_3 & 0 & 0 & 0 \\ 0 & a_3 & 0 & 0 \\ 0 & 0 & a_3 & 0 \\ 0 & 0 & 0 & a_3 \end{bmatrix} \quad (2.15)$$

where

$$a_3 = \sum_{i=1}^{3} |s_i|^2 \quad (2.16)$$

The decoding method for this type of STBC is a little different from that for other types.

2.4 Four-by-four Non-Orthogonal STBC

If it is not acceptable for a decrease in transmission rate, there must be some

sacrifices in other properties of space-time block codes.

One of these sacrifices is that one may reduce the uncoded diversity gain, and rely on coding to exploit the diversity provided by the additional antennas.

Another approach is that the requirement of orthogonality of the space-time block code may be relaxed. Several designs of non-orthogonal space-time block codes will be introduced in the following. With full transmission rate, these designs are also based on 4×4 transmission matrices [8,9].

2.4.1 Spaced Diagonal (SD) STBC

This non-orthogonal (also called quasi-orthogonal) design was proposed by Tirkkonen, Boariu and Hottinen in [8]. s_1, s_2, s_3, s_4 are four complex constellation signals. The STBC transmission matrix is written as:

$$\mathbf{S}=\begin{bmatrix} s_1 & s_2 & s_3 & s_4 \\ -s_2^* & s_1^* & -s_4^* & s_3^* \\ s_3 & s_4 & s_1 & s_2 \\ -s_4^* & s_3^* & -s_2^* & s_1^* \end{bmatrix} \tag{2.17}$$

Thus, its correlation matrix is:

$$\mathbf{S}^H * \mathbf{S}=\begin{bmatrix} a_4 & 0 & b_4 & 0 \\ 0 & a_4 & 0 & b_4 \\ b_4 & 0 & a_4 & 0 \\ 0 & b_4 & 0 & a_4 \end{bmatrix} \tag{2.18}$$

where

$$a_4=\sum_{i=1}^{4}|s_i|^2 \tag{2.19}$$

and

$$b_4=s_1s_3^*+s_3s_1^*+s_2s_4^*+s_4s_2^*=2\,\mathrm{Re}[s_1s_3^*+s_2s_4^*] \tag{2.20}$$

Each of the non-orthogonal parts (b_4) is separated by 0 from the orthogonal parts (a_4) in $\mathbf{S}^H * \mathbf{S}$, so the name "Spaced Diagonal" is given. From the location of b_4, we can see that there are two non-orthogonal pairs in this model: the 1st and 3rd columns, the 2nd and 4th columns.

2.4.2 Dual Diagonal (DD) STBC

Another work was proposed in [9] and developed the second kind of non-orthogonal STBC. The transmission matrix is formed as:

$$\mathbf{S} = \begin{bmatrix} s_1 & s_2 & s_3 & s_4 \\ s_4 & s_3 & s_2 & s_1 \\ s_3^* & -s_4^* & -s_1^* & s_2^* \\ s_2^* & -s_1^* & -s_4^* & s_3^* \end{bmatrix} \tag{2.21}$$

Here, each same kind of symbol in s_1, s_2, s_3, s_4 forms a triangle in $\mathbf{S}$. The correlation matrix of $\mathbf{S}$ is:

$$\mathbf{S}^H * \mathbf{S} = \begin{bmatrix} a_5 & 0 & 0 & b_5 \\ 0 & a_5 & b_5 & 0 \\ 0 & b_5 & a_5 & 0 \\ b_5 & 0 & 0 & a_5 \end{bmatrix} \tag{2.22}$$

where

$$a_5 = \sum_{i=1}^{4} |s_i|^2 \tag{2.23}$$

and

$$b_5 = s_1 s_4^* + s_4 s_1^* + s_2 s_3^* + s_3 s_2^* = 2\,\mathrm{Re}[s_1 s_4^* + s_2 s_3^*] \tag{2.24}$$

The name "Dual Diagonal STBC" comes from that the nonzero elements are located on the diagonal and reverse diagonal, respectively, in its correlation matrix. The two non-orthogonal pairs of DD, however, are absolutely 1st and 4th columns, the

2nd and 3rd columns.

2.4.3 Block Diagonal (BD) STBC

Here, we propose a novel kind of four-by-four non-orthogonal STBC named Block Diagonal. Its may be generated by the general form in [12]. The transmission matrix of this model is:

$$\mathbf{S} = \begin{bmatrix} s_1 & s_2 & s_3 & s_4 \\ -s_3^* & -s_4^* & s_1^* & s_2^* \\ s_2 & s_1 & s_4 & s_3 \\ -s_4^* & -s_3^* & s_2^* & s_1^* \end{bmatrix} \tag{2.25}$$

and

$$\mathbf{S}^H * \mathbf{S} = \begin{bmatrix} a_6 & b_6 & 0 & 0 \\ b_6 & a_6 & 0 & 0 \\ 0 & 0 & a_6 & b_6 \\ 0 & 0 & b_6 & a_6 \end{bmatrix} \tag{2.26}$$

where

$$a_6 = \sum_{i=1}^{4} |s_i|^2 \tag{2.27}$$

and

$$b_6 = s_1 s_2^* + s_2 s_1^* + s_3 s_4^* + s_4 s_3^* = 2\,\mathrm{Re}[s_1 s_2^* + s_3 s_4^*] \tag{2.28}$$

Eq. (2.26) shows that the two non-orthogonal pairs of $\mathbf{S}$ are the 1st and 2nd columns, the 3rd and 4th columns, which are all different from the non-orthogonal pairs of SD and DD. Any two of four columns are in one non-orthogonal pair. Therefore, three STBCs in section 2.4 have a total of $C_2^4 = 6$ different non-orthogonal column pairs, which sit on all 12 non-diagonal locations of $\mathbf{S}^H * \mathbf{S}$ (each occupies two). So these three STBCs contain all possible conditions of

non-orthogonal STBCs with two non-orthogonal pairs.

2.5 Summary

Comparing to the Complex Orthogonal STBC in the same transmission matrix size, the Complex 4-by-4 Non-orthogonal STBCs have poor SER/BER performances at low SNR (<15dB) [8,9] and more complicated equalization matrices at the receive end, in the trade off of higher transmission rate. The basic properties and comparisons of four-antenna STBCs introduced in this chapter are shown in Table. 2.1.

Properties / STBC	Real or Complex ?	Orthogonal ?	Transmission Rate
Real Orthogonal	Real	Yes	1
Complex Orthogonal	Complex	Yes	3/4
Complex Non-Orthogonal	Complex	No	1

Table 2.1 Basic properties and comparisons between four-antenna STBCs

In chapter 3, we will demonstrate how these four-antenna STBCs are combined with the OFDM system. In chapter 4, channel estimation methods for STBC OFDM in chapter 3 will be given. Four types of four-antenna STBC models: RO, SD, DD, BD, will be used.

Chapter 3
Space-Time Block Code OFDM System Model

We will combine STBCs with OFDM system in this chapter. The system we use in this thesis is similar to that in [15,17], which has two transmit antennas, one receive antenna, and Alamouti STBC (section 2.2).

Four transmit antennas are used here in this system, and its model is depicted in Fig. 3.1. Any kind of schemes in section 2.3 and section 2.4 can be chosen as the STBC in this OFDM system.

The symbols are divided into huge block vectors first with size $4K \times 1$ before transmission. Each block is further separated into four smaller parts with each has K symbols. $\underline{s}^{(1)}(n)$ denotes the first K symbols of $\underline{s}(n)$, while $\underline{s}^{(2)}(n)$, $\underline{s}^{(3)}(n)$, $\underline{s}^{(4)}(n)$ denotes its second, third, and last K symbols.

$$\underline{s}(n) = \begin{bmatrix} \underline{s}^{(1)}(n) \\ \underline{s}^{(2)}(n) \\ \underline{s}^{(3)}(n) \\ \underline{s}^{(4)}(n) \end{bmatrix} \tag{3.1}$$

With each one of size $M \times K$ ($M > K$), four different tall matrices $\boldsymbol{\theta}_1$, $\boldsymbol{\theta}_2$, $\boldsymbol{\theta}_3$ and $\boldsymbol{\theta}_4$ (for input block symbols $\underline{s}^{(1)}(n)$, $\underline{s}^{(2)}(n)$, $\underline{s}^{(3)}(n)$, and $\underline{s}^{(4)}(n)$, respectively)

represent four distinct linear block precoders where $\underline{s}(n)$ is first sent to. After precoders, the input symbol block becomes

$$\tilde{\underline{s}}(n)=\begin{bmatrix}\tilde{\underline{s}}^{(1)}(n)\\ \tilde{\underline{s}}^{(2)}(n)\\ \tilde{\underline{s}}^{(3)}(n)\\ \tilde{\underline{s}}^{(4)}(n)\end{bmatrix}=\begin{bmatrix}\theta_1\underline{s}^{(1)}(n)\\ \theta_2\underline{s}^{(2)}(n)\\ \theta_3\underline{s}^{(3)}(n)\\ \theta_4\underline{s}^{(4)}(n)\end{bmatrix}=\begin{bmatrix}\theta_1 & 0 & 0 & 0\\ 0 & \theta_2 & 0 & 0\\ 0 & 0 & \theta_3 & 0\\ 0 & 0 & 0 & \theta_4\end{bmatrix}\begin{bmatrix}\underline{s}^{(1)}(n)\\ \underline{s}^{(2)}(n)\\ \underline{s}^{(3)}(n)\\ \underline{s}^{(4)}(n)\end{bmatrix}=\mathbf{\Theta}\underline{s}(n) \qquad (3.2)$$

where

$$\mathbf{\Theta}=\begin{bmatrix}\theta_1 & 0 & 0 & 0\\ 0 & \theta_2 & 0 & 0\\ 0 & 0 & \theta_3 & 0\\ 0 & 0 & 0 & \theta_4\end{bmatrix} \qquad (3.3)$$

is a $4M\times 4K$ matrix and $\tilde{\underline{s}}(n)$ is of size $4M\times 1$.

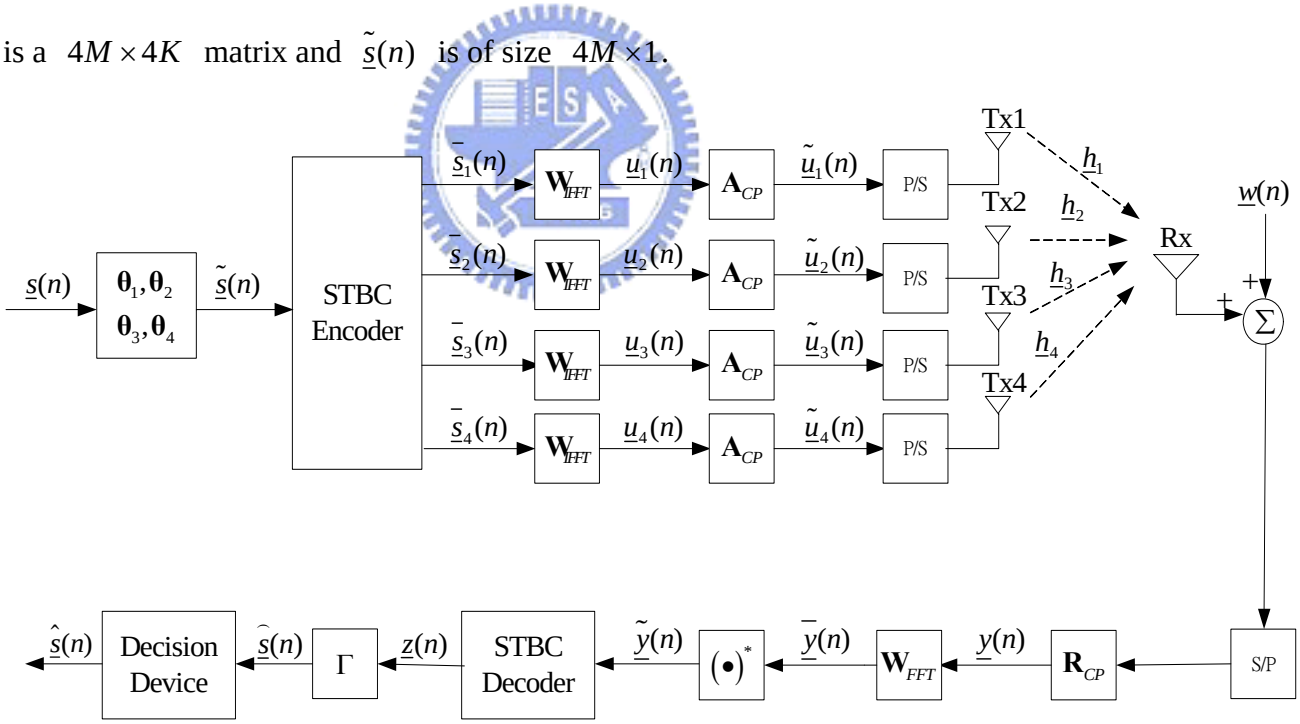

Fig. 3.1 Four-transmit-antenna STBC OFDM transceiver model with block precoders

3.1 STBC Encoder and Transmitter

$\underline{\tilde{s}}(n)$ is then sent to the space-time encoder. Any four-antenna STBC can be used to in the system. The four precoded sub-blocks of $\underline{\tilde{s}}(n)$: $\underline{\tilde{s}}^{(1)}(n)$, $\underline{\tilde{s}}^{(2)}(n)$, $\underline{\tilde{s}}^{(3)}(n)$, and $\underline{\tilde{s}}^{(4)}(n)$ will form a $4M \times 4$ output code matrix of encoder as

$$\left[\underline{\bar{s}_1}(n) \quad \underline{\bar{s}_2}(n) \quad \underline{\bar{s}_3}(n) \quad \underline{\bar{s}_4}(n)\right] = \begin{bmatrix} \underline{\bar{s}_1}^{(1)}(n) & \underline{\bar{s}_2}^{(1)}(n) & \underline{\bar{s}_3}^{(1)}(n) & \underline{\bar{s}_4}^{(1)}(n) \\ \underline{\bar{s}_1}^{(2)}(n) & \underline{\bar{s}_2}^{(2)}(n) & \underline{\bar{s}_3}^{(2)}(n) & \underline{\bar{s}_4}^{(2)}(n) \\ \underline{\bar{s}_1}^{(3)}(n) & \underline{\bar{s}_2}^{(3)}(n) & \underline{\bar{s}_3}^{(3)}(n) & \underline{\bar{s}_4}^{(3)}(n) \\ \underline{\bar{s}_1}^{(4)}(n) & \underline{\bar{s}_2}^{(4)}(n) & \underline{\bar{s}_3}^{(4)}(n) & \underline{\bar{s}_4}^{(4)}(n) \end{bmatrix} = \mathbf{M}(\underline{\tilde{s}}^{(i)}(n)) = \mathbf{S} \tag{3.4}$$

where $i = 1,2,3,4$. $\underline{\bar{s}_i}^{(1)}(n)$, $\underline{\bar{s}_i}^{(2)}(n)$, $\underline{\bar{s}_i}^{(3)}(n)$ and $\underline{\bar{s}_i}^{(4)}(n)$ are all OFDM symbol. $\mathbf{S}$ is the transmission matrix of STBC in chapter 2. Eq. (3.4) shows that the blocks in $\underline{\tilde{s}}(n)$ in Eq. (3.2) are transmitted through four different independent channels in four consecutive time intervals.

After the OFDM symbols encoded by the space-time encoder, they are modulated by M-point IFFT, where the result equals to multiplied by an IFFT matrix $\mathbf{W}_{IFFT}$. Vectors $\underline{u}_i(n)$ are produced ($i = 1,2,3,4$), then.

The size of time domain symbol vector $\underline{u}_i(n)$ is then be expanded by a length L cyclic prefix (CP) to eliminate the effect of inter-block-interference (IBI) caused by channel, and its size becomes $M + L$, then. The CP of $\mathbf{W}_M \underline{\bar{s}_i}^{(l)}(n)$ is the replicas of its last L elements and will be put in front of it, where $l = 1,2,3,4$. The channel order ((number of channel taps)-1) is assumed to be less than or equal to L. The

insertion of CP is represented by $\mathbf{A}_{CP}$ in Fig. 2.1, and the outputs are $\underline{\tilde{u}}_i(n)$. They are finally sent through transmit antenna i sequentially, $i=1,2,3,4$.

3.2 Channel

In the following descriptions, the channels between four transmit antennas and the receive antenna are assumed to be frequency selective and their discrete time baseband equivalent effect is in the form of the FIR linear time-invariant filter, which has the impulse response vector

$$\underline{h}_i = [h_i(0), h_i(1), \ldots, h_i(L)]^T, \quad i=1,2,3,4 \tag{3.5}$$

where $L \geq \max(L_1, L_2, L_3, L_4)$. L_i is the channel order of $\underline{h}_i$, $i=1,2,3,4$.

The FIR channel $\mathbf{H}_i$ is a $(M+L)\times(M+L)$ lower-triangular Toeplitz matrix and its (s,t)th element is $h_i(s-t)$, $s,t \in \{1,2, \cdots ,M+L\}$.

$$\mathbf{H}_i = \begin{bmatrix} h_i(0) & 0 & 0 & 0 & 0 & 0 & 0 \\ h_i(1) & h_i(0) & 0 & 0 & 0 & 0 & 0 \\ h_i(2) & h_i(1) & h_i(0) & 0 & 0 & 0 & 0 \\ \vdots & \vdots & \ddots & \vdots & \vdots & \vdots & \vdots \\ 0 & 0 & 0 & h_i(L) & \cdots & h_i(0) & 0 \\ 0 & 0 & 0 & 0 & h_i(L) & \cdots & h_i(0) \end{bmatrix} \tag{3.6}$$

3.3 Receiver

At the receiver end, an additive white Gaussian noise vector $\underline{w}(n)$ is added to the received block, in the first step. Then the CP is removed by discarding the first L

received symbols. The removing of CP can be described by the matrix $\mathbf{R}_{CP} = [0_{M\times L} \ \ \mathbf{I}_M]$. And the matrix $\widetilde{\mathbf{H}}_i$ represents the equivalent channel matrix without IBI, where

$$\widetilde{\mathbf{H}}_i = \mathbf{R}_{CP}\mathbf{H}_i\mathbf{A}_{CP} \tag{3.7}$$

In Fig. 3.1, the received IBI-free $4M\times 1$ block $\underline{y}(n)$ can be written as:

$$\underline{y}(n) = \begin{bmatrix} \underline{y}^{(1)}(n) \\ \underline{y}^{(2)}(n) \\ \underline{y}^{(3)}(n) \\ \underline{y}^{(4)}(n) \end{bmatrix} \tag{3.8}$$

After removing the CP, the OFDM symbols in $\underline{y}(n)$ are demodulated by M-point FFT, which is presented as being multiplied by the $M\times M$ FFT matrix $\mathbf{W}_{FFT}$ to obtain the received block $\underline{\overline{y}}(n)$,

$$\underline{\overline{y}}(n) = \begin{bmatrix} \underline{\overline{y}}^{(1)}(n) \\ \underline{\overline{y}}^{(2)}(n) \\ \underline{\overline{y}}^{(3)}(n) \\ \underline{\overline{y}}^{(4)}(n) \end{bmatrix} \tag{3.9}$$

We then adjust $\underline{\overline{y}}(n)$ to $\underline{\tilde{y}}(n)$ by

$$\underline{\tilde{y}}(n) = \begin{bmatrix} \underline{\overline{y}}^{(1)}(n) \\ \underline{\overline{y}}^{(2)^*}(n) \\ \underline{\overline{y}}^{(3)}(n) \\ \underline{\overline{y}}^{(4)^*}(n) \end{bmatrix} \tag{3.10}$$

and sent to space-time decoder. The output $\underline{z}(n)$ is a block with diversity gain. After all, the original data symbol $\underline{s}(n)$ is recovered from $\underline{z}(n)$ by applying the equalizer Γ. $\underline{\hat{s}}(n)$ is the soft decision data here, which is perturbed by the noise. It is then put into a decision device. Finally, the hard decision data appears. The frequency domain

version of Fig. 3.1 can then be plotted in Fig. 3.2.

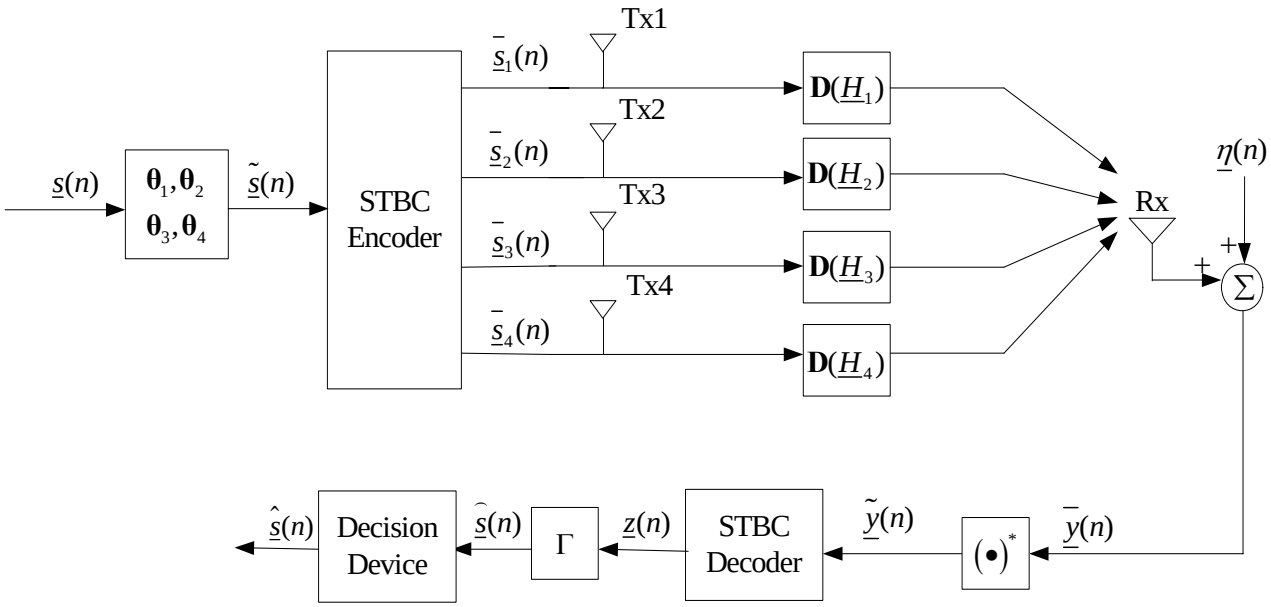

Fig. 3.2. Frequency domain version of four-antenna STBC OFDM transceiver model

The frequency response vector of channel $\underline{h}_i$ in Eq. (3.6) is

$$\underline{H}_i = \mathbf{V}\underline{h}_i \tag{3.11}$$

with matrix $\mathbf{V}$ is the submatrix of the first $L+1$ columns of $\mathbf{W}_{FFT}$.

The equivalent channel matrix in time domain $\widetilde{\mathbf{H}}_i$ can be diagonalized by pre- and post-multiplication with $\mathbf{W}_{FFT}$ and $\mathbf{W}_{IFFT}$:

$$\mathbf{W}_{FFT}\widetilde{\mathbf{H}}_i\mathbf{W}_{IFFT} = \mathbf{D}(\underline{H}_i) \tag{3.12}$$

where $\mathbf{D}(\underline{H}_i)$ denoting the diagonal matrix with $\underline{H}_i$ on its diagonal.

Combining the fact above, Eq. (3.4) and Eq. (3.9) together, we can rewrite $\underline{\bar{y}}(n)$ in Eq. (3.9) as:

$$\underline{\bar{y}}(n)=\begin{bmatrix}\sum_{i=1}^{4}\left[\mathbf{D}(\underline{H}_i)\underline{\bar{s}}_i^{(1)}(n)\right]\\ \sum_{i=1}^{4}\left[\mathbf{D}(\underline{H}_i)\underline{\bar{s}}_i^{(2)}(n)\right]\\ \sum_{i=1}^{4}\left[\mathbf{D}(\underline{H}_i)\underline{\bar{s}}_i^{(3)}(n)\right]\\ \sum_{i=1}^{4}\left[\mathbf{D}(\underline{H}_i)\underline{\bar{s}}_i^{(4)}(n)\right]\end{bmatrix}+\underline{v}(n) \tag{3.13}$$

where

$$\underline{v}(n)=\begin{bmatrix}\underline{v}^{(1)}(n)\\ \underline{v}^{(2)}(n)\\ \underline{v}^{(3)}(n)\\ \underline{v}^{(4)}(n)\end{bmatrix}=\begin{bmatrix}\mathbf{W}_{FFT} & \mathbf{0} & \mathbf{0} & \mathbf{0}\\ \mathbf{0} & \mathbf{W}_{FFT} & \mathbf{0} & \mathbf{0}\\ \mathbf{0} & \mathbf{0} & \mathbf{W}_{FFT} & \mathbf{0}\\ \mathbf{0} & \mathbf{0} & \mathbf{0} & \mathbf{W}_{FFT}\end{bmatrix}\mathbf{R}_{CP}\underline{w}(n) \tag{3.14}$$

3.4 STBC Decoder and Equalizer

Here, let us take BD in section 2.4.3 for example, Eq. (3.10) can be written as:

$$\begin{aligned}\underline{\tilde{y}}(n)&=\begin{bmatrix}\underline{\bar{y}}^{(1)}(n)\\ \underline{\bar{y}}^{(2)^*}(n)\\ \underline{\bar{y}}^{(3)}(n)\\ \underline{\bar{y}}^{(4)^*}(n)\end{bmatrix}\\ &=\begin{bmatrix}\mathbf{D}(\underline{H}_1) & \mathbf{D}(\underline{H}_2) & \mathbf{D}(\underline{H}_3) & \mathbf{D}(\underline{H}_4)\\ \mathbf{D}(\underline{H}_3^*) & \mathbf{D}(\underline{H}_4^*) & -\mathbf{D}(\underline{H}_1^*) & -\mathbf{D}(\underline{H}_2^*)\\ \mathbf{D}(\underline{H}_2) & \mathbf{D}(\underline{H}_1) & \mathbf{D}(\underline{H}_4) & \mathbf{D}(\underline{H}_3)\\ \mathbf{D}(\underline{H}_4^*) & \mathbf{D}(\underline{H}_3^*) & -\mathbf{D}(\underline{H}_2^*) & -\mathbf{D}(\underline{H}_1^*)\end{bmatrix}\begin{bmatrix}\underline{\tilde{s}}^{(1)}(n)\\ \underline{\tilde{s}}^{(2)}(n)\\ \underline{\tilde{s}}^{(3)}(n)\\ \underline{\tilde{s}}^{(4)}(n)\end{bmatrix}+\begin{bmatrix}\underline{v}^{(1)}(n)\\ \underline{v}^{(2)^*}(n)\\ \underline{v}^{(3)}(n)\\ \underline{v}^{(4)^*}(n)\end{bmatrix}\\ &=\overline{\mathbf{D}}\,\mathbf{\Theta}\underline{s}(n)+\underline{\eta}(n)=\mathbf{A}\underline{s}(n)+\underline{\eta}(n)=\underline{x}(n)+\underline{\eta}(n)\end{aligned} \tag{3.15}$$

where

$$\overline{\mathbf{D}}=\begin{bmatrix}\mathbf{D}(\underline{H}_1) & \mathbf{D}(\underline{H}_2) & \mathbf{D}(\underline{H}_3) & \mathbf{D}(\underline{H}_4)\\ \mathbf{D}(\underline{H}_3^*) & \mathbf{D}(\underline{H}_4^*) & -\mathbf{D}(\underline{H}_1^*) & -\mathbf{D}(\underline{H}_2^*)\\ \mathbf{D}(\underline{H}_2) & \mathbf{D}(\underline{H}_1) & \mathbf{D}(\underline{H}_4) & \mathbf{D}(\underline{H}_3)\\ \mathbf{D}(\underline{H}_4^*) & \mathbf{D}(\underline{H}_3^*) & -\mathbf{D}(\underline{H}_2^*) & -\mathbf{D}(\underline{H}_1^*)\end{bmatrix},\quad \underline{\eta}(n)=\begin{bmatrix}\underline{v}^{(1)}(n)\\ \underline{v}^{(2)^*}(n)\\ \underline{v}^{(3)}(n)\\ \underline{v}^{(4)^*}(n)\end{bmatrix} \tag{3.16}$$

$$\mathbf{A} = \overline{\mathbf{D}}\,\Theta, \quad \underline{x}(n) = \mathbf{A}\underline{s}(n) \tag{3.17}$$

If the frequency domain channel state vectors $\underline{H}_1$, $\underline{H}_2$, $\underline{H}_3$ and $\underline{H}_4$ are available at the receiver, $\underline{z}(n)$ can be obtained from $\underline{\tilde{y}}(n)$ by:

$$\begin{aligned} \underline{z}(n) &= \overline{\mathbf{D}}^H \underline{\tilde{y}}(n) \\ &= \overline{\mathbf{D}}^H \overline{\mathbf{D}}\,\mathbf{\Theta}\underline{s}(n) + \overline{\mathbf{D}}^H \underline{\eta}(n) \\ &= \overline{\mathbf{D}_\mathbf{A}}\,\underline{s}(n) + \underline{\xi}(n) \end{aligned} \tag{3.18}$$

where

$$\overline{\mathbf{D}_\mathbf{A}} = \overline{\mathbf{D}}^H \overline{\mathbf{D}}\,\mathbf{\Theta} \tag{3.19}$$

and

$$\underline{\xi}(n) = \overline{\mathbf{D}}^H \underline{\eta}(n) \tag{3.20}$$

In above equations, the decoding step $\overline{\mathbf{D}}^H \overline{\mathbf{D}}$ comes from $\mathbf{S}^H * \mathbf{S}$ of STBCs in chapter 2. Eq. (3.10) will turn the property of orthogonal (or non-orthogonal) of STBCs from $\mathbf{S}$ into $\overline{\mathbf{D}}$. So the correlation matrix can be used in decoding, for simplification. Note that it has been achieved multiantenna diversity of order four.

From Eq. (3.18), we know that $\overline{\mathbf{D}_\mathbf{A}}^H$ and the inverse of $\left(\overline{\mathbf{D}_\mathbf{A}}^H \overline{\mathbf{D}_\mathbf{A}}\right)$ is needed to recover $\underline{s}(n)$ from $\underline{z}(n)$. It is clear that $\left(\overline{\mathbf{D}_\mathbf{A}}^H \overline{\mathbf{D}_\mathbf{A}}\right)$ must be full rank ($=4K$). And thus $\overline{\mathbf{D}_\mathbf{A}}$ in Eq. (3.19) should be full column rank ($=4K$), which means every $M \times M$ submatrix in $\overline{\mathbf{D}_\mathbf{A}}$ (except $\mathbf{0}: M \times K$) must be full column rank ($=4K$).

So the designing of precoders is a main issue. Two important conditions in [15] should be taken into consideration, here:

Condition (3.1) $M > K + L$.

Condition (3.2) $\mathbf{\theta}_i, i \in \{1,2,3,4\}$ is designed so that any K rows of $\mathbf{\theta}_i$ are linearly

independent.

The form of precoders will be mentioned later in chapter 5.

After going through the equalizer Γ, the output is the soft decision data:

$$\begin{aligned}\hat{\underline{s}}(n) &= \Gamma \cdot \underline{z}(n) \\ &= inv\left(\overline{\mathbf{D}_\mathbf{A}}^H \overline{\mathbf{D}_\mathbf{A}}\right)\overline{\mathbf{D}_\mathbf{A}}^H \underline{z}(n) \\ &= inv\left(\overline{\mathbf{D}_\mathbf{A}}^H \overline{\mathbf{D}_\mathbf{A}}\right)\overline{\mathbf{D}_\mathbf{A}}^H \overline{\mathbf{D}_\mathbf{A}}\,\underline{s}(n) + \Gamma \cdot \underline{\xi}(n) \\ &= \underline{s}(n) + inv\left(\overline{\mathbf{D}_\mathbf{A}}^H \overline{\mathbf{D}_\mathbf{A}}\right)\overline{\mathbf{D}_\mathbf{A}}^H \underline{\xi}(n)\end{aligned} \tag{3.21}$$

where

$$\Gamma = inv\left(\overline{\mathbf{D}_\mathbf{A}}^H \overline{\mathbf{D}_\mathbf{A}}\right)\overline{\mathbf{D}_\mathbf{A}}^H \tag{3.22}$$

At last, the soft decision data is put into the decision device and projected onto the finite alphabet to get the hard decision data $\hat{\underline{s}}(n)$.

The channel state information (CSI) in Eq. (3.19) is assumed to be perfectly available at the receiver end. In the next chapter, we will exhibit how to get the channel state information when it is unknown.

Chapter 4

Subspace-based Channel Estimation and the improved method Phase Direct

In four-antenna STBC OFDM systems, the channel estimation method is based on the redundancy caused by four $M \times K$ linear precoders $\boldsymbol{\theta}_1$, $\boldsymbol{\theta}_2$, $\boldsymbol{\theta}_3$, and $\boldsymbol{\theta}_4$, which is similar to the channel estimation in the two-antenna system in [17].

We will first simply describe the main idea of the subspace-based channel estimation. Similar or same methods had been proposed for some two and four-antenna STBCs in [11-14,15,17]. After the description, the design of precoders in our systems is introduced. The theoretical mean square error of this algorithm derived in [17] will then be mentioned.

In section 4.2, an improved finite alphabet method based on the subspace-based channel estimation named phase direct (PD) [16], will be introduced to make the channel estimates better. The PD based on subspace method in [17] only focus on Alamouti STBC [4] with BPSK modulation. Here, we will extend it to four-antenna STBC OFDM systems in section 2.3.1 and 2.4. We will also extend all these three systems from BPSK modulation to QPSK modulation, which will also result in more possible channel power response conditions. Getting channel power is an important

issue in PD. Such issue in the two-antenna Alamouti STBC OFDM system with BPSK was also mentioned in [17]. In four-antenna STBC OFDM systems, because the possible conditions of channel power response become more, the getting of the channel power response is more complicated than that in a two-antenna system. And so is that in QPSK than in BPSK in the same system. The algorithm we use in this thesis to get channel power response is to select the most proper one from all its possible conditions. So we should find out all the possible conditions of its channel power response. Such algorithm is going to be discussed in section 4.2.2.

Furthermore, the feasibility for the algorithm in section 4.2.2 depends on that all possible symbol conditions for $\mathbf{S}$ of STBCs are non-singular. To achieve this goal, we will introduce the diagonally weighted models of STBCs in section 4.2.3. PD for four-antenna STBCs in static channel will be expressed in section 4.2.4.

Finally, in time-varying channel, the choice of window size of received blocks in PD will also be mentioned. This will be shown in section 4.2.5 while the same issue was also taken in [17]. A longer window of received blocks can lessen the effect of noise but cannot follow the varying channel, while a shorter window can follow the channel variance more precisely than a longer one.

4.1 Subspace-based Multichannel Estimation

In the following description in this method, as the same in chapter 3, we also choose Block Diagonal (BD) STBC in 2.4.3 to show the estimation algorithm here.

4.1.1 Subspace-based Multichannel Estimation Method

First, the algorithm starts from the received data vectors in Eq. (3.17), neglecting the noise:

$$\underline{\tilde{y}}(n) = \underline{x}(n) = \mathbf{A}\underline{s}(n) \tag{4.1}$$

N blocks of $\underline{\tilde{y}}(n) = \underline{x}(n)$ are collected and form a matrix $\mathbf{X}_N$ in the size $4M \times N$:

$$\left[\underline{x}(1),\quad \underline{x}(2),\quad \cdots,\quad \underline{x}(N)\right] = \mathbf{X}_N = \mathbf{A}\mathbf{S}_N \tag{4.2}$$

where

$$\mathbf{S}_N = \left[\underline{s}(1),\quad \underline{s}(2),\quad \cdots,\quad \underline{s}(N)\right] \tag{4.3}$$

It is impossible to implement this algorithm on the Complex Orthogonal (CO) STBC system in section 2.3.2, however, because its received data vectors $\underline{\tilde{y}}(n)$ cannot be presented in the form of $\mathbf{A}\underline{s}(n)$ in Eq. (4.1) [11].

Compared to the condition in the two-antenna system in [15,17] that the number of received blocks N should be large enough ($\geq 2K$). N must satisfy the condition that $N \geq 4K$ here in four-antenna systems to guarantee that $\mathbf{S}_N$ is with full rank $4K$.

According to *Condition (3.1)*, *Condition (3.2)*, and the condition above. $\underline{s}(n)$, a $4K \times 1$ independent data vector, will show the fact that $\text{rank}(\mathbf{X}_N) = 4K$, and that the nullity of $\mathbf{X}_N$ $\text{null}(\mathbf{X}_N) = 4M - 4K$. Note that the range space of $\mathbf{X}_N$ $R(\mathbf{X}_N) = R(\mathbf{X}_N\mathbf{X}_N^H) = R(\mathbf{A})$. So the singular value decomposition (SVD) of $\mathbf{X}_N$ can be written as:

$$\mathbf{X}_N = \mathbf{A}\mathbf{S}_N = \begin{bmatrix}\mathbf{U}_x & \mathbf{U}_n\end{bmatrix}\begin{bmatrix}\sum_x & \mathbf{0} \\ \mathbf{0} & \mathbf{0}\end{bmatrix}\begin{bmatrix}\mathbf{V}_x^H \\ \mathbf{V}_n^H\end{bmatrix} \tag{4.4}$$

where $\sum_x = \text{diag}(\sigma_1^2,\ \sigma_2^2,\ \cdots,\ \sigma_{4k}^2)$ are range eigenvalues of $\mathbf{X}_N$, and $\sigma_1^2 \geq \sigma_2^2 \geq \cdots \geq \sigma_{4k}^2$. The null eigenvalues (all zeroes) yield null eigenvectors of $\mathbf{X}_N$, which form the $4M \times (4M - 4K)$ matrix $\mathbf{U}_n$ and column span the null space $N(\mathbf{X}_N)$ caused by redundant preorders.

Next, we use the property that $N(\mathbf{X}_N)$ is orthogonal to $R(\mathbf{X}_N) = R(\mathbf{A})$, it appears that:

$$\underline{u}_k^H \mathbf{A} = \underline{0}, \quad k = 1, 2, \cdots, 4M - 4K \tag{4.5}$$

where $\underline{u}_k$ is the k th column of the null space matrix $\mathbf{U}_n$. It is also the k th null eigenvector of $\mathbf{X}_N$.

Then, we separate the $4M \times 1$ $\underline{u}_k$ into four equal size parts:

$$\underline{u}_k = \begin{bmatrix} \underline{u}_{k\_1st} \\ \underline{u}_{k\_2nd} \\ \underline{u}_{k\_3rd} \\ \underline{u}_{k\_4th} \end{bmatrix} \tag{4.6}$$

where all of its four parts are $M \times 1$ vectors.

Here, we take BD in OFDM for example. By Eq. (3.15) and Eq. (4.5), it can be shown that

$$\begin{aligned} & \underline{u}_k^H \mathbf{A} \\ &= \begin{bmatrix} \underline{u}_{k\_1st}^H & \underline{u}_{k\_2nd}^H & \underline{u}_{k\_3rd}^H & \underline{u}_{k\_4th}^H \end{bmatrix} \begin{bmatrix} \mathbf{D}(\underline{H}_1) & \mathbf{D}(\underline{H}_2) & \mathbf{D}(\underline{H}_3) & \mathbf{D}(\underline{H}_4) \\ \mathbf{D}(\underline{H}_3^*) & \mathbf{D}(\underline{H}_4^*) & -\mathbf{D}(\underline{H}_1^*) & -\mathbf{D}(\underline{H}_2^*) \\ \mathbf{D}(\underline{H}_2) & \mathbf{D}(\underline{H}_1) & \mathbf{D}(\underline{H}_4) & \mathbf{D}(\underline{H}_3) \\ \mathbf{D}(\underline{H}_4^*) & \mathbf{D}(\underline{H}_3^*) & -\mathbf{D}(\underline{H}_2^*) & -\mathbf{D}(\underline{H}_1^*) \end{bmatrix} \begin{bmatrix} \boldsymbol{\theta}_1 & \mathbf{0} & \mathbf{0} & \mathbf{0} \\ \mathbf{0} & \boldsymbol{\theta}_2 & \mathbf{0} & \mathbf{0} \\ \mathbf{0} & \mathbf{0} & \boldsymbol{\theta}_3 & \mathbf{0} \\ \mathbf{0} & \mathbf{0} & \mathbf{0} & \boldsymbol{\theta}_4 \end{bmatrix} \\ &= \underline{0} \end{aligned} \tag{4.7}$$

For any $M \times 1$ vectors $\underline{a}$ and $\underline{b}$, it is true that

$$\underline{a}^H \mathbf{D}(\underline{b}) = \underline{b} \mathbf{D}(\underline{a}^*) \tag{4.8}$$

where $\mathbf{D}(*)$ is as defined in chapter 3.

So we can write Eq. (4.7) as

$$\begin{bmatrix} \underline{H}_1^T & \underline{H}_2^T & \underline{H}_3^H & \underline{H}_4^H \end{bmatrix} \underbrace{\begin{bmatrix} \mathbf{D}(\underline{u}^*_{k\_1st}) & \mathbf{D}(\underline{u}^*_{k\_3rd}) & -\mathbf{D}(\underline{u}_{k\_2nd}) & -\mathbf{D}(\underline{u}_{k\_4th}) \\ \mathbf{D}(\underline{u}^*_{k\_3rd}) & \mathbf{D}(\underline{u}^*_{k\_1st}) & -\mathbf{D}(\underline{u}_{k\_4th}) & -\mathbf{D}(\underline{u}_{k\_2nd}) \\ \mathbf{D}(\underline{u}^*_{k\_2nd}) & \mathbf{D}(\underline{u}^*_{k\_4th}) & \mathbf{D}(\underline{u}_{k\_1st}) & \mathbf{D}(\underline{u}_{k\_3rd}) \\ \mathbf{D}(\underline{u}^*_{k\_4th}) & \mathbf{D}(\underline{u}^*_{k\_2nd}) & \mathbf{D}(\underline{u}_{k\_3rd}) & \mathbf{D}(\underline{u}_{k\_1st}) \end{bmatrix}}_{=\mathbf{G}(\underline{u}_k)} \underbrace{\begin{bmatrix} \boldsymbol{\theta}_1 & \mathbf{0} & \mathbf{0} & \mathbf{0} \\ \mathbf{0} & \boldsymbol{\theta}_2 & \mathbf{0} & \mathbf{0} \\ \mathbf{0} & \mathbf{0} & \boldsymbol{\theta}_3^* & \mathbf{0} \\ \mathbf{0} & \mathbf{0} & \mathbf{0} & \boldsymbol{\theta}_4^* \end{bmatrix}}_{=\boldsymbol{\Psi}} = \underline{0} \tag{4.9}$$

where

$$\mathbf{G}(\underline{u}_k) = \begin{bmatrix} \mathbf{D}(\underline{u}^*_{k\_1st}) & \mathbf{D}(\underline{u}^*_{k\_3rd}) & -\mathbf{D}(\underline{u}_{k\_2nd}) & -\mathbf{D}(\underline{u}_{k\_4th}) \\ \mathbf{D}(\underline{u}^*_{k\_3rd}) & \mathbf{D}(\underline{u}^*_{k\_1st}) & -\mathbf{D}(\underline{u}_{k\_4th}) & -\mathbf{D}(\underline{u}_{k\_2nd}) \\ \mathbf{D}(\underline{u}^*_{k\_2nd}) & \mathbf{D}(\underline{u}^*_{k\_4th}) & \mathbf{D}(\underline{u}_{k\_1st}) & \mathbf{D}(\underline{u}_{k\_3rd}) \\ \mathbf{D}(\underline{u}^*_{k\_4th}) & \mathbf{D}(\underline{u}^*_{k\_2nd}) & \mathbf{D}(\underline{u}_{k\_3rd}) & \mathbf{D}(\underline{u}_{k\_1st}) \end{bmatrix} \tag{4.10}$$

and

$$\boldsymbol{\Psi} = \begin{bmatrix} \boldsymbol{\theta}_1 & \mathbf{0} & \mathbf{0} & \mathbf{0} \\ \mathbf{0} & \boldsymbol{\theta}_2 & \mathbf{0} & \mathbf{0} \\ \mathbf{0} & \mathbf{0} & \boldsymbol{\theta}_3^* & \mathbf{0} \\ \mathbf{0} & \mathbf{0} & \mathbf{0} & \boldsymbol{\theta}_4^* \end{bmatrix} \tag{4.11}$$

Using the relationship between $\underline{h}_i$ and $\underline{H}_i$ in Eq. (3.11), Eq. (4.9) is transformed into

$$\begin{bmatrix} \underline{h}_1^T & \underline{h}_2^T & \underline{h}_3^H & \underline{h}_4^H \end{bmatrix} \underbrace{\begin{bmatrix} \mathbf{V}^T & \mathbf{0} & \mathbf{0} & \mathbf{0} \\ \mathbf{0} & \mathbf{V}^T & \mathbf{0} & \mathbf{0} \\ \mathbf{0} & \mathbf{0} & \mathbf{V}^H & \mathbf{0} \\ \mathbf{0} & \mathbf{0} & \mathbf{0} & \mathbf{V}^H \end{bmatrix}}_{=\mathbf{F}} \mathbf{G}(\underline{u}_k)\boldsymbol{\Psi} = \underline{0} \tag{4.12}$$

where

$$\mathbf{F} = \begin{bmatrix} \mathbf{V}^T & \mathbf{0} & \mathbf{0} & \mathbf{0} \\ \mathbf{0} & \mathbf{V}^T & \mathbf{0} & \mathbf{0} \\ \mathbf{0} & \mathbf{0} & \mathbf{V}^H & \mathbf{0} \\ \mathbf{0} & \mathbf{0} & \mathbf{0} & \mathbf{V}^H \end{bmatrix} \tag{4.13}$$

In Eq. (4.12), the channel states are presented in time domain rather than in frequency domain in Eq. (4.9). The former is adopted because $\mathbf{F}\mathbf{G}(\underline{u}_k)\boldsymbol{\Psi}$ has less number of

rows ($4(L+1)$) than $\mathbf{G}(\underline{u}_k)\mathbf{\Psi}$ has ($4M$), and it can thus reduce computation complexity.

Now, we have every null eigenvector $\underline{u}_k$ in Eq. (4.5) doing all the steps above, with $k = 1, 2, \cdots, 4M - 4K$. And then put them in a row, we can get

$$\underbrace{\begin{bmatrix} \underline{h}_1^T & \underline{h}_2^T & \underline{h}_3^H & \underline{h}_4^H \end{bmatrix}}_{\tilde{\underline{h}}^H} \underbrace{\mathbf{F}\left[\mathbf{G}(\underline{u}_1)\mathbf{\Psi}, \quad \mathbf{G}(\underline{u}_2)\mathbf{\Psi}, \quad \cdots, \quad \mathbf{G}(\underline{u}_{4M-4K})\mathbf{\Psi}\right]}_{\mathbf{Q}} = \underline{0} \qquad (4.14)$$

The zero vector $\underline{0}$ here in Eq. (4.14) has 1 row and $4(L+1)\times[4K\times(4M-4K)]$ columns, and

$$\tilde{\underline{h}}^H = \begin{bmatrix} \underline{h}_1^T & \underline{h}_2^T & \underline{h}_3^H & \underline{h}_4^H \end{bmatrix} \qquad (4.15)$$

$$\mathbf{Q} = \mathbf{F}\left[\mathbf{G}(\underline{u}_1)\mathbf{\Psi}, \quad \mathbf{G}(\underline{u}_2)\mathbf{\Psi}, \quad \cdots, \quad \mathbf{G}(\underline{u}_{4M-4K})\mathbf{\Psi}\right] \qquad (4.16)$$

So,

$$\| \tilde{\underline{h}}^H \mathbf{Q} \|^2 = \tilde{\underline{h}}^H \mathbf{Q}\mathbf{Q}^H \tilde{\underline{h}} = 0 \qquad (4.17)$$

In Eq. (4.17), we can see that the estimated channel can be found as the eigenvector which corresponds to the smallest eigenvalue of $\mathbf{Q}\mathbf{Q}^H$:

$$\tilde{\underline{h}}^H = \arg\min_{\|\tilde{\underline{h}}\|=1} \left\{ \tilde{\underline{h}}^H \mathbf{Q}\mathbf{Q}^H \tilde{\underline{h}} \right\} \qquad (4.18)$$

By Eq. (4.15), the estimated channel is

$$\tilde{\underline{h}} = \begin{bmatrix} \underline{h}_1^* \\ \underline{h}_2^* \\ \underline{h}_3 \\ \underline{h}_4 \end{bmatrix} \qquad (4.19)$$

This algorithm is named subspace-based channel algorithm since it is based on the null space $\mathbf{U}_n$ of received data matrix $\mathbf{X}_N$.

However, in the realistic condition, the white noise is added at the receiver end. In this case, $\mathbf{X}_N$ is replaced with $\mathbf{Y}_N$, and Eq. (4.4) will be in the form as

$$\mathbf{Y}_N = \begin{bmatrix} \tilde{\mathbf{U}}_x & \tilde{\mathbf{U}}_n \end{bmatrix} \begin{bmatrix} \tilde{\sum}_x & \mathbf{0} \\ \mathbf{0} & \tilde{\sum}_n \end{bmatrix} \begin{bmatrix} \tilde{\mathbf{V}}_x^H \\ \tilde{\mathbf{V}}_n^H \end{bmatrix} \tag{4.20}$$

The diagonal matrix $\tilde{\sum}_x$, just as the relation between $\sum_x$ and $\mathbf{X}_N$ in Eq. (4.4), also has range eigenvalues of $\mathbf{Y}_N$ in its diagonal elements. $\tilde{\sum}_n$, however, will have the variance of white noise on its diagonal [15].

As it mentioned in [15,17], in order to simplify the computation, we replace $\mathbf{Y}_N$ in Eq. (4.20) by the sample covariance matrix of $\tilde{\underline{y}}(n)$ in Eq. (3.15):

$$\mathbf{R}_{\tilde{y}} = \frac{1}{N} \sum_{n=1}^{N} \tilde{\underline{y}}(n) \tilde{\underline{y}}^H(n) \tag{4.21}$$

In Eq. (4.19), the estimated channel is not the final estimate because the solution of $\begin{bmatrix} \underline{h}_1^T & \underline{h}_2^T & \underline{h}_3^H & \underline{h}_4^H \end{bmatrix} \mathbf{Q} = \underline{0}$ in Eq. (4.14) is not unique. According to the description about channel identifiability in [15], if distinct precoders (any of the four precoders is different from each other) are used, channel identifiability within one scalar α is guaranteed. For example:

$$\begin{bmatrix} \hat{\underline{h}}_1 \\ \hat{\underline{h}}_2 \\ \hat{\underline{h}}_3 \\ \hat{\underline{h}}_4 \end{bmatrix} = \begin{bmatrix} \alpha\mathbf{I} & \mathbf{0} & \mathbf{0} & \mathbf{0} \\ \mathbf{0} & \alpha\mathbf{I} & \mathbf{0} & \mathbf{0} \\ \mathbf{0} & \mathbf{0} & \alpha^*\mathbf{I} & \mathbf{0} \\ \mathbf{0} & \mathbf{0} & \mathbf{0} & \alpha^*\mathbf{I} \end{bmatrix} \begin{bmatrix} \underline{h}_1 \\ \underline{h}_2 \\ \underline{h}_3 \\ \underline{h}_4 \end{bmatrix} \tag{4.22}$$

holds true in BD, where $\hat{\underline{h}}_i$ is the final estimate of channels, $i = 1,2,3,4$. Here, we use one pair of pre-precoding pilots in [15] to resolve the unknown scalar α.

Other three four-antenna STBCS, however, can also be adopted in the proposed subspace-based channel estimation algorithm. The major steps of this algorithm in realistic environment and simulation are as follows:

Step 1) Collect N received data blocks $\underline{\tilde{y}}(n)$ and compute $\mathbf{R}_{\tilde{y}}$ in Eq. (4.21).

Note that $N \geq 4K$ is the necessary condition in four-antenna systems.

Step 2) Find out the eigenvectors $\underline{u}_k, k = 1, 2, \cdots, 4M - 4K$, corresponding to the smallest $4M - 4K$ eigenvalues of the matrix $\mathbf{R}_{\tilde{y}}$, by proceeding its SVD.

Step 3) Build $\mathbf{Q}$ in Eq. (4.16).

Step 4) Determine the eigenvector corresponding to the smallest eigenvalue of $\mathbf{QQ}^H$ in Eq. (4.18) as the initial estimate.

Step 5) Resolve the scalar ambiguity α and determine the final estimate of channels.

4.1.2 Theoretical Mean Square Error of subspace method

The theoretical mean square error (MSE) for the proposed estimator was derived in [17]. For high SNR and large sample size (large N), an approximation MSE is

$$E(\| \underline{\hat{h}} - \underline{h} \|^2) = E(\| \triangle \underline{h} \|^2) = E\left[trace(\triangle \underline{h} \cdot \triangle \underline{h}^H) \right]$$
$$\approx \frac{\sigma_w^2 \cdot trace(\mathbf{Q}^+ \mathbf{Q}^{+H})}{\sigma_s^2 N} = \frac{\sigma_w^2 \cdot \| \mathbf{Q}^+ \|^2}{\sigma_s^2 N} \tag{4.23}$$

This formula can be adopted in four-antenna systems as well as in the two-antenna system. $\underline{\hat{h}}$ is the estimate of channels and $\underline{h}$ is the real one. Both signals and noise are assume to be i.i.d random variables with zero mean and variance σ_s^2 and σ_w^2, respectively. So we get σ_s^2 / σ_w^2 as SNR. N is the number of sampling received data blocks. And the matrix $\mathbf{Q}^+$, which comes from $\mathbf{Q}$ in Eq. (4.16), will be explained as follows: With noise is added, assuming $\mathbf{Q}$ permits the SVD

$$\mathbf{Q} = \begin{bmatrix} \tilde{\mathbf{U}}_q & \tilde{\mathbf{U}}_{nq} \end{bmatrix} \begin{bmatrix} \tilde{\sum}_q & \mathbf{0} \\ \mathbf{0} & \tilde{\sum}_{nq} \end{bmatrix} \begin{bmatrix} \tilde{\mathbf{V}}_q^H \\ \tilde{\mathbf{V}}_{nq}^H \end{bmatrix} \tag{4.24}$$

where $\mathbf{Q}^{+}$ is computed as

$$\mathbf{Q}^{+} = \tilde{\mathbf{U}}_q \left(\tilde{\sum}_q \right)^{-1} \tilde{\mathbf{V}}_q^{H} \tag{4.25}$$

4.2 Phase Direct (PD)

PD was proposed in conventional (SISO) OFDM [16]. It was then addressed to Alamouti STBC OFDM ([4], section 2.2) in [17]. In this thesis, we will combine it with four-antenna STBC OFDM systems, and based on subspace method to improve channel estimation.

4.2.1 PD in Conventional OFDM

We first show how PD performs in conventional OFDM. The signal modulation types in discussion are P-'ary PSK constellations with size $P: \left\{ \xi_P = e^{j2\pi p/P} \mid p = 1, 2, \cdots, P \right\}$, here. In convention OFDM, the signal at the receive end can be written as

$$y(n,m) = H(\rho_m) s(n,m) + n(\rho_m) \tag{4.26}$$

where $s(n,m)$ and $y(n,m)$ are the transmitted and received data signals, respectively, through the m th subcarrier on the n th received data block. $s(n,m)$ is in the form of P. $H(\rho_m)$ is the channel response of the m th subcarrier in frequency domain and $n(\rho_m)$ is the corresponding noise. A total of M subcarriers and N received data blocks are taken.

For the simplification of getting the power of P to signal in Eq. (4.26), we neglect the noise, and take the expectation to n:

$$E\left\{ y^P(n,m) \right\} = E\left\{ \left[H(\rho_m) s(n,m) \right]^P \right\} = H^P(\rho_m) E\left\{ s^P(n,m) \right\} \tag{4.27}$$

With N received data blocks, the sampling averages of $y(n,m)$ can replace its expectation by $E\{y^P(n,m)\} = \frac{1}{N}\sum_{n=1}^{N} y^P(n,m)$. Assume that $s(n,m)$ and $y(n,m)$ are all known at the receiver, the desired channel power response of $H(\rho_m)$ is

$$H^P(\rho_m) = \frac{\frac{1}{N}\sum_{n=1}^{N} y^P(n,m)}{E\{s^P(n,m)\}} \tag{4.28}$$

Using the property of PSK constellation of size P, expectation of $s(n,m)$ is $E\{s^P(n,m)\} = 1$. Therefore, Eq. (4.28) turns to

$$H^P(\rho_m) = \frac{1}{N}\sum_{n=1}^{N} y^P(n,m) \tag{4.29}$$

One main process in PD is to get the channel phase response from the information of the channel power response in Eq. (4.29). For each $m \in \{1,2,\cdots,M\}$, the estimate of $H(\rho_m)$ is

$$\widehat{H}(\rho_m) = \left[H^P(\rho_m)\right]^{1/P} \lambda_m \tag{4.30}$$

where $\left[H^P(\rho_m)\right]^{1/P}$ is the channel amplitude response, and $\lambda_m \in \{\widehat{\lambda}_m\} = \{e^{j2\pi p/P} \mid p = 1,2,\cdots,P\}$, however, is the phase ambiguity in taking the p th root of $e^{j2\pi/P}$. There are P possible values of phase values, so we need to resolve the phase ambiguity to get the correct channel phase response by comparing all the possibilities in $\{\widehat{\lambda}_m\}$:

$$\lambda_m = \arg\min_{\lambda_m \in \widehat{\lambda}_m} \| H_{est}(\rho_m) - \left[H^P(\rho_m)\right]^{1/P} \widehat{\lambda}_m \|^2 \tag{4.31}$$

$H_{est}(\rho_m)$ here is the frequency-domain initial estimate of channels on the m th subcarrier by some estimated method. We may improve its accuracy through the

following PD steps:

Step 1) Let the estimate from some method as the time-domain initial estimate $\underline{\hat{h}}_{(1)}$ of PD. Transfer it to frequency domain by means of FFT and get $\underline{\widehat{H}}_{(1)}$. Set $H_{est}(\rho_m) = \widehat{H}_{(1)}(\rho_m)$ and $PD\_iter = 1$, for $m = 1, 2, \cdots, M$.

Step 2) Apply Eq. (4.31) in every iteration to resolve phase ambiguities. Produce the phase-compensated channel response estimate vector in frequency domain:

$$\underline{H}_{temp} = \left\{ \left[H^P(\rho_1) \right]^{1/P} \lambda_1, \cdots\cdots, \left[H^P(\rho_M) \right]^{1/P} \lambda_M \right\} \tag{4.32}$$

Note that $H_{est}(\rho_m)$ must be replaced by $\widehat{H}_{(PD\_iter)}(\rho_m)$ in the (PD_iter)th iteration.

Step 3) Add 1 to PD_iter. Then, update channel estinates in time domain:

$$\underline{\hat{h}}_{(PD\_iter+1)} = \mathbf{V}^H \underline{H}_{temp} \tag{4.33}$$

and in frequency domain:

$$\underline{\widehat{H}}_{(PD\_iter+1)} = \mathbf{V} \underline{\hat{h}}_{(PD\_iter+1)} \tag{4.34}$$

$\underline{\widehat{H}}_{(PD\_iter+1)}$ is an important information to use in the next iteration. Matrix $\mathbf{V}$ was defined in section 3. Eq (4.33) and Eq (4.34) together are called denoising. On one hand, Eq (4.33) means that $\underline{H}_{temp}$ is performed an M-point IFFT and keep the first $L+1$ entries (i.e. the multipath length) of $\underline{\hat{h}}_{(PD\_iter+1)}$ through truncation. On the other hand, Eq. (4.34) signifies that an M-point IFFT is performed on the vector formed by $\underline{\hat{h}}_{(PD\_iter+1)}$ after zero-padding.

Step 4) Go to the next ((PD_iter+1)th) iteration. Repeat Step 2 and 3 several times until $\| \underline{\hat{h}}_{(PD\_iter+1)} - \underline{\hat{h}}_{(PD\_iter)} \|^2$ is within some tiny range.

The Signal-flow chart of PD in conventional OFDM is shown in Fig.4.1.

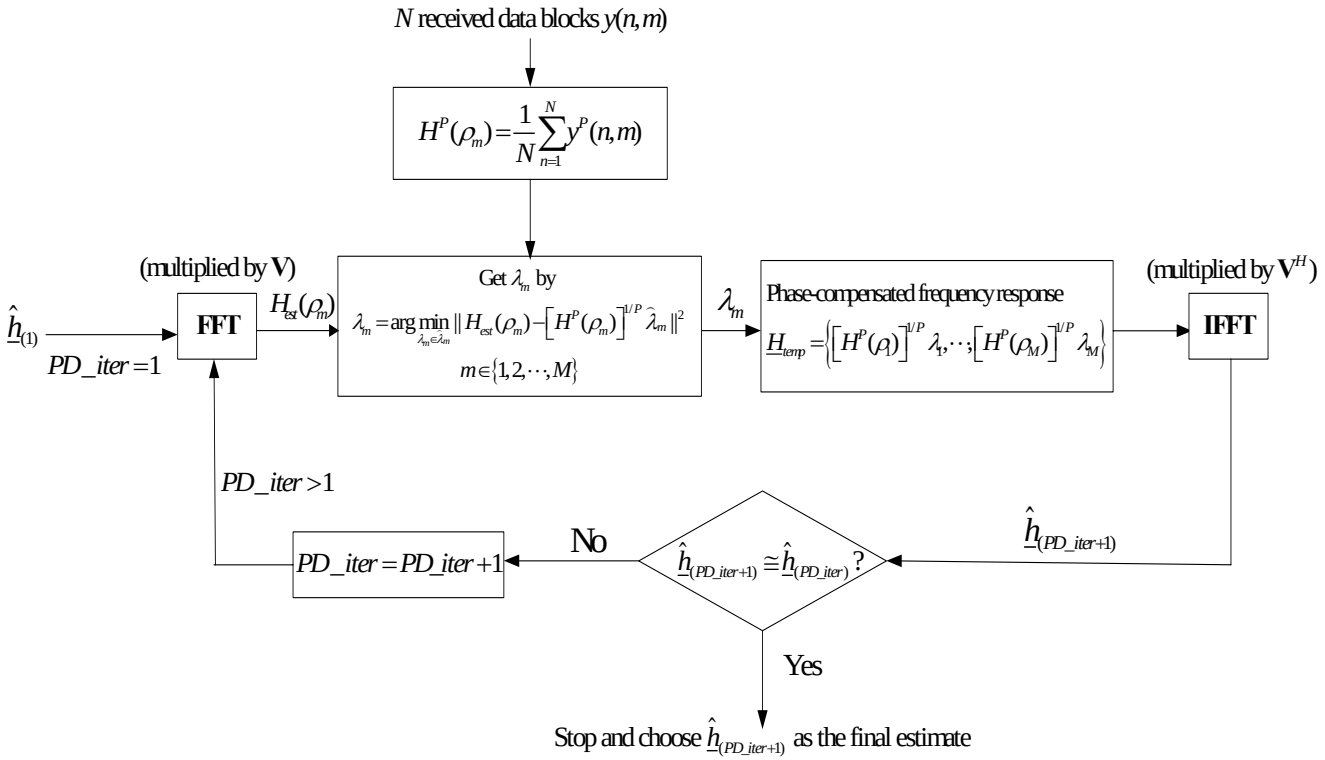

Fig. 4.1 Signal-flow chart of PD in conventional OFDM

4.2.2 Getting Channel Power Response for PD in STBC OFDM

The final purpose of PD is to solve phase ambiguities after getting the channel power response from the information of known data. So the obtainment of channel power response is an important issue in PD. How to get channel power response in conventional OFDM systems is specified in section 4.1 and it is effortless. In STBC OFDM systems, it is not as easy as in conventional OFDM systems since the received data consists of at least two different data. [17] had proposed a sum-difference square method to obtain it in Alamouti model. In the next section, we want to expand the algorithm in gaining channel power response to four-antenna models that fit the subspace method. This algorithm is also theoretically suitable to different kinds of signal constellations but not only to BPSK.

First, we start from the initial received data vector in Eq. (3.13) and according to Eq. (3.4):

$$\underline{\bar{y}}(n)=\begin{bmatrix}\underline{\bar{y}}^{(1)}(n)\\ \underline{\bar{y}}^{(2)}(n)\\ \underline{\bar{y}}^{(3)}(n)\\ \underline{\bar{y}}^{(4)}(n)\end{bmatrix}=\mathbf{S}*\begin{bmatrix}\mathbf{D}_1\\ \mathbf{D}_2\\ \mathbf{D}_3\\ \mathbf{D}_4\end{bmatrix}+\begin{bmatrix}\underline{v}^{(1)}(n)\\ \underline{v}^{(2)}(n)\\ \underline{v}^{(3)}(n)\\ \underline{v}^{(4)}(n)\end{bmatrix} \tag{4.35}$$

Here, we let $\mathbf{D}_i=\mathbf{D}(\underline{H}_i)$, $i=1,2,3,4$, only focus on data through the mth subcarrier, and leave out the noise for the purpose of simplication.

$$\left.\begin{aligned}&s_m^{(i)}(n)=m\text{th data of }\underline{\tilde{s}}^{(i)}(n)\\ &y_m^{(i)}(n)=m\text{th data of }\underline{\bar{y}}^{(i)}(n)\\ &H_i(\rho_m)=\mathbf{D}_i(m,m)\end{aligned}\right\}\text{where}\quad i=1,2,3,4\qquad m=1,2,\cdots,M \tag{4.36}$$

So we can write the variables in Eq. (4.36) as

$$\underline{\mathbf{y_m}}(n)=\begin{bmatrix}y_m^{(1)}(n)\\ y_m^{(2)}(n)\\ y_m^{(3)}(n)\\ y_m^{(4)}(n)\end{bmatrix}=\mathbf{s_m}(n)*\underbrace{\begin{bmatrix}H_1(\rho_m)\\ H_2(\rho_m)\\ H_3(\rho_m)\\ H_4(\rho_m)\end{bmatrix}}_{\underline{\mathbf{H}}(\rho_m)}=\mathbf{s_m}(n)*\underline{\mathbf{H}}(\rho_m) \tag{4.37}$$

$*$ is as defined in chapter 2. $\mathbf{s_m}(n)$ is obviously in the form of transmission matrix $\mathbf{S}$ we introduced also in chapter 2. And the channel power response corresponds to mth subcarrier is computed as

$$\underline{\mathbf{H}}_{\text{CPR}}(\rho_m)=\begin{bmatrix}H_1^P(\rho_m)\\ H_2^P(\rho_m)\\ H_3^P(\rho_m)\\ H_4^P(\rho_m)\end{bmatrix}=\left[\underline{\mathbf{H}}(\rho_m)\right].\wedge P \tag{4.38}$$

So the key point of getting $\underline{\mathbf{H}}_{\text{CPR}}(\rho_m)$ is to determine $\underline{\mathbf{H}}(\rho_m)$, first. We can do this from Eq. (4.37) by

$$\underline{\mathbf{H}}(\rho_m)=\left[\mathbf{s_m}(n)\right]^{-1}*\underline{\mathbf{y_m}}(n) \tag{4.39}$$

if $\mathbf{s_m}(n)$ has its own inverse. Here, $\underline{\mathbf{y_m}}(n)$ is known at receiver. Next, we have to find out each condition of $\mathbf{s_m}(n)$ corresponding to all possible data symbol pairs, $\underline{s_m}(n)$. For instance, in BPSK system, there are two conditions (± 1) for each symbol. And will result in a total of $2^4 = 16$ possible $\underline{s_m}(n)$ (see Eq. (4.40)) in four-antenna STBCs, which has four symbols in one matrix.

$$\underline{s_m}(n) = \left[s_m^{(1)}(n) \quad s_m^{(2)}(n) \quad s_m^{(3)}(n) \quad s_m^{(4)}(n) \right] = [1 \quad 1 \quad 1 \quad 1], [1 \quad 1 \quad 1 \quad -1], \cdots$$
$$\cdots, [-1 \quad -1 \quad -1 \quad -1]$$

(4.40)

So this model has at most 16 possible conditions of $\mathbf{s_m}(n)$, which also yields to at most 16 possible conditions of $\underline{\mathbf{H}}(\rho_m)$ by Eq. (4.39). If we use QPSK in this model, there will be $4^4 = 256$ maximum possible conditions of $\underline{\mathbf{H}}(\rho_m)$ in same models. $\underline{\mathbf{H}}_{\mathrm{CPR}}(\rho_m)$ with many possible conditions are then acquired by Eq. (4.38).

Finally, we can determine the real $H_i^P(\rho_m)$ ($i = 1, 2, 3, 4$) by comparing each possible condition of $\underline{\mathbf{H}}_{\mathrm{CPR}}(\rho_m)$:

$$H_i^P(\rho_m) = \arg \min_{H_i^P(\rho_m)} \| H_{est}^P(\rho_m) - \widehat{H}_i^P(\rho_m) \|^2 \tag{4.41}$$

where $\widehat{H}_i^P(\rho_m) \in \{ i\text{th element of all possible conditions of } \underline{\mathbf{H}}_{\mathrm{CPR}}(\rho_m) \}$, and $H_{est}(\rho_m)$ is the estimated channel via subspace-based method. The signal-flow of how to find $H_i^P(\rho_m)$ is as in Fig.4.2 below.

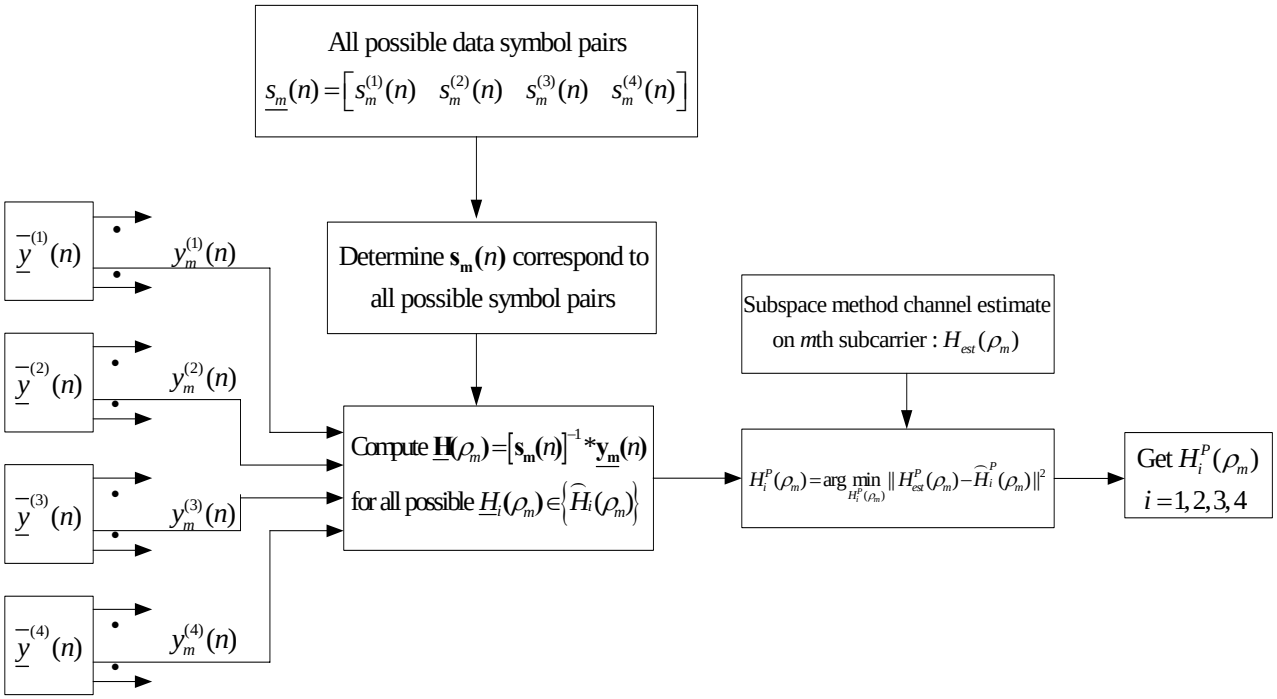

Fig. 4.2 Signal-flow chart of getting channel power response $H_i^P(\rho_m)$ in four-antenna STBC OFDM systems

4.2.3 Diagonally Weighted STBC models

The most important and necessary condition is that $\mathbf{s_m}(n)$ **must be nonsingular corresponding to all possible data symbol pairs**. Because we do not want to miss any possible condition of $\underline{\mathbf{H}}(\rho_m)$ if it cannot be obtained for the inverse of the corresponding $\mathbf{s_m}(n)$ does not exist.

However, we find out that in three non-orthogonal STBC models (SD, DD, and BD), $\mathbf{s_m}(n)$ will be singular in some of the possible symbol pairs. To solve this problem, we modify $\mathbf{S}$ by multiplying their diagonal elements with a positive real index k. Here, let's take BD in section 2.4.3 for instance. The transmission matrix becomes

$$\mathbf{S}=\begin{bmatrix} k*s_1 & s_2 & s_3 & s_4 \\ -s_3^* & k*(-s_4^*) & s_1^* & s_2^* \\ s_2 & s_1 & k*s_4 & s_3 \\ -s_4^* & -s_3^* & s_2^* & k*s_1^* \end{bmatrix} \tag{4.42}$$

and the correlation matrix of $\mathbf{S}$ is

$$\mathbf{S}^H*\mathbf{S}=\begin{bmatrix} a_{61} & b_{61} & c_{61} & 0 \\ b_{62} & a_{62} & 0 & -c_{62} \\ c_{61} & 0 & a_{62} & b_{61} \\ 0 & -c_{62} & b_{62} & a_{61} \end{bmatrix} \tag{4.43}$$

where

$$a_{61}=k^2\,|\,s_1\,|^2+\sum_{i=2}^{4}|\,s_i\,|^2 \tag{4.44a}$$

$$a_{62}=\sum_{i=1}^{3}|\,s_i\,|^2+k^2\,|\,s_4\,|^2 \tag{4.44b}$$

$$b_{61}=k(s_1^*s_2+s_3s_4^*)+(s_1s_2^*+s_3^*s_4) \tag{4.44c}$$

$$b_{62}=k(s_1s_2^*+s_3^*s_4)+(s_1^*s_2+s_3s_4^*) \tag{4.44d}$$

$$c_{61}=(k-1)(s_1^*s_3+s_2^*s_4) \tag{4.44e}$$

$$c_{62}=(k-1)(s_1s_3^*+s_2s_4^*) \tag{4.44f}$$

Compare Eq. (4.43) with Eq. (2.26), we can see that the non-orthogonality of the modified non-orthogonal STBC $(k\neq 1)$ is severe than the original one $(k=1)$ in chapter 2.

Next, we will take BD in BPSK system for an example to show how modified STBC avoid singularity. Let's start from Eq. (4.37), multiply both sides of the equation by $\mathbf{s_m}^H(n)$, we will get

$$\mathbf{s_m}^H(n)*\underline{\mathbf{y_m}}(n)=\mathbf{s_m}^H(n)*\mathbf{s_m}(n)*\underline{\mathbf{H}}(\rho_m)=\mathbf{Cs_m}(n)*\underline{\mathbf{H}}(\rho_m) \tag{4.45}$$

where $\mathbf{Cs_m}(n)$ is the correlation matrix of $\mathbf{s_m}(n)$. Our purpose is to make sure that $\mathbf{Cs_m}(n)$ are non-singular so that

$$\underline{\mathbf{H}}(\rho_m) = \left[\mathbf{Cs_m}(n)\right]^{-1} * \mathbf{s_m^H}(n) * \underline{\mathbf{y_m}}(n) = \left[\mathbf{s_m}(n)\right]^{-1} * \underline{\mathbf{y_m}}(n) \tag{4.46}$$

In BPSK, it is true that $s_m^{(i)*}(n) = s_m^{(i)}(n) \in \{\pm 1\}$. Then, we have a total number of 16 possible symbol pairs $\underline{s_m}(n)$ in Eq. (4.40) and their corresponding $\mathbf{s_m}(n)$, $\mathbf{Cs_m}(n)$. From Eq. (4.43), (4.44 a-f) and substituting 16 kinds of $\underline{s_m}(n)$, we get:

$$\mathbf{Cs_m}(n) = \begin{bmatrix} a & b & c & 0 \\ b & a & 0 & -c \\ c & 0 & a & b \\ 0 & -c & b & a \end{bmatrix} \tag{4.47}$$

where

$$a = k^2 + 3 \tag{4.48a}$$

$$\begin{cases} b = 0\ ,\ c = 0 \\ \quad\text{or} \\ b = \pm 2(k+1),\ c = \pm 2(k-1) \end{cases} \tag{4.48b}$$

Then, we take the determinant of $\mathbf{Cs_m}(n)$:

$$\det\left[\mathbf{Cs_m}(n)\right] = (a^2 - b^2 - c^2)^2 \tag{4.49}$$

According to $a, b,$ and c in functions of k, we discuss about the non-singularity of $\mathbf{Cs_m}(n)$ rather than $\mathbf{s_m}(n)$ in two cases:

Case 1) $a = k^2 + 3,\ b = 0,\ c = 0$:

$$\det\left[\mathbf{Cs_m}(n)\right] = \left\{(k^2+3)^2 + 0^2 + 0^2\right\}^2 = (k^2+3)^4 \neq 0 \tag{4.50}$$

Case 1 guarantees that $\mathbf{Cs_m}(n)$ is non-singular, in which half of 16 possible conditions satisfy.

Case 2) $a = k^2 + 3,\ b = \pm 2(k+1),\ c = \pm 2(k-1)$:

$$\det\left[\mathbf{Cs_m}(n)\right] = \left\{(k^2+3)^2 + \left[\pm 2(k+1)\right]^2 + \left[\pm 2(k-1)\right]^2\right\}^2 = (k^2-1)^4 \tag{4.51}$$

For the purpose of $\mathbf{Cs_m}(n)$ (also $\mathbf{s_m}(n)$) being non-singular, $k^2 - 1 \neq 0$. Hence,

$k \neq \pm 1$ (or $k \neq 1$ for k is positive).

Note that any kind of modulation can be adopted in this algorithm. Nevertheless, there are some constraints in non-orthogonal STBC OFDM when BPSK and QPSK, which we would like to focus on, are used. The numbers of possible symbol pairs that will make $\mathbf{s}_m(n)$ and $\mathbf{C}\mathbf{s}_m(n)$ singular in four-antenna STBCs are shown in Table 4.1 (BPSK) and Table 4.2 (QPSK).

STBC / k	RO	SD	DD	BD
$=1$	0	8	8	8
$\neq 1$	0	0	0	0

Table 4.1 Number of symbol pairs make $\mathbf{s}_m(n)$ and $\mathbf{C}\mathbf{s}_m(n)$ singular in different STBCs in BPSK (Total: 16 pairs, $k > 0$)

STBC / k	SD	DD	BD
$=1$	32	32	32
$\neq 1$	0	0	0

Table 4.2 Number of symbol pairs make $\mathbf{s}_m(n)$ and $\mathbf{C}\mathbf{s}_m(n)$ singular in different STBCs in QPSK (Total: 256 pairs, $k > 0$)

When $k = 1$, $\mathbf{s}_m(n)$ is singular, and this makes channel power getting and PD unavailable. Therefore, the case $k = 1$ of non-orthogonal STBCs can only supply the subspace method, but cannot take part in PD. So we should avoid this situation by letting $k \neq 1$ when performing PD in three non-orthogonal STBC models.

In RO, however, this problem does not exist (see Table 4.1) because its transmission matrix certifies the full rank and non-singularity of $\mathbf{s_m}(n)$ for all possible signal pairs in BPSK and QPSK. Still, this model can also be modified. We will have all the four four-antenna STBCs (RO, SD, DD, and BD) diagonally weighted in computer simulations and set k to the same value when comparing the performances of all these models. Transmission matrices and their correlation matrices of these four diagonally weighted STBC will be mentioned in Appendix.

Another important point should be noticed is that $s_m^{(i)}(n)$, elements of precoders' output $\tilde{\underline{s}}^{(i)}(n)$, must equal to the original input data symbols in $\underline{s}^{(i)}(n)$ in Eq. (3.1) and (3.2) so that the algorithm above can work. For this reason, precoders should be designed carefully. We will specify the proper precoders' form early in the next chapter.

4.2.4 PD in STBC OFDM

PD has been applied to Alamouti STBC [4] OFDM system in [17], based on BPSK baseband modulation. In this thesis, according to the algorithm getting channel power response in the previous section, it can be extended to four-antenna systems, and applied to both BPSK ($P = 2$) and QPSK ($P = 4$) modulations (See Fig.4.3).

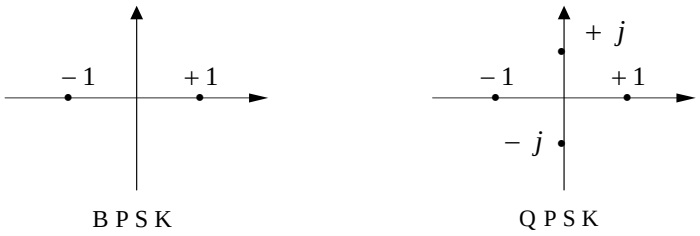

Fig. 4.3 Signal constellations of BPSK and QPSK used in PD

Section 4.2.2 exhibits the method how to get $H_i^P(\rho_m)$, which corresponds to ith

channel and mth subcarrier, where $i \in \{1,2,3,4\}$, $m \in \{1,2,\cdots,M\}$. We receive a total of N data blocks in this algorithm. For the nth block ($n \in \{1,2,\cdots,N\}$) and the ith channel, we should further get all M subcarriers' frequency channel power response

$$\underline{H}_{i,(n)}^{P} = \left[H_{i,(n)}^{P}(\rho_1), H_{i,(n)}^{P}(\rho_2), \cdots, H_{i,(n)}^{P}(\rho_M) \right] \tag{4.44}$$

In static channels (i.e. channel states will always be constant), we average all the $\underline{H}_{i,(n)}^{P}$ to get the average channel power response $\underline{H}_{i}^{P}$ by

$$H_{i}^{P}(\rho_m) = \frac{1}{N} \sum_{n=1}^{N} H_{i,(n)}^{P}(\rho_m), \quad m = 1,2,\cdots,M \tag{4.45}$$

and

$$\underline{H}_{i}^{P} = \frac{1}{N} \sum_{n=1}^{N} \underline{H}_{i,(n)}^{P} \tag{4.46}$$

Then, we apply from Eq. (4.27) to (4.34) by selecting the proper P to perform PD and better the channel estimate accuracy. In Fig.4.4, we can see how it works in static channel, where each received block is

$$\underline{\bar{y}}(n) = \left[\underline{\bar{y}}^{(1)}(n) \quad \underline{\bar{y}}^{(2)}(n) \quad \underline{\bar{y}}^{(3)}(n) \quad \underline{\bar{y}}^{(4)}(n) \right]^{T}, \; n \in \{1,2,\cdots,N\}. \tag{4.47}$$

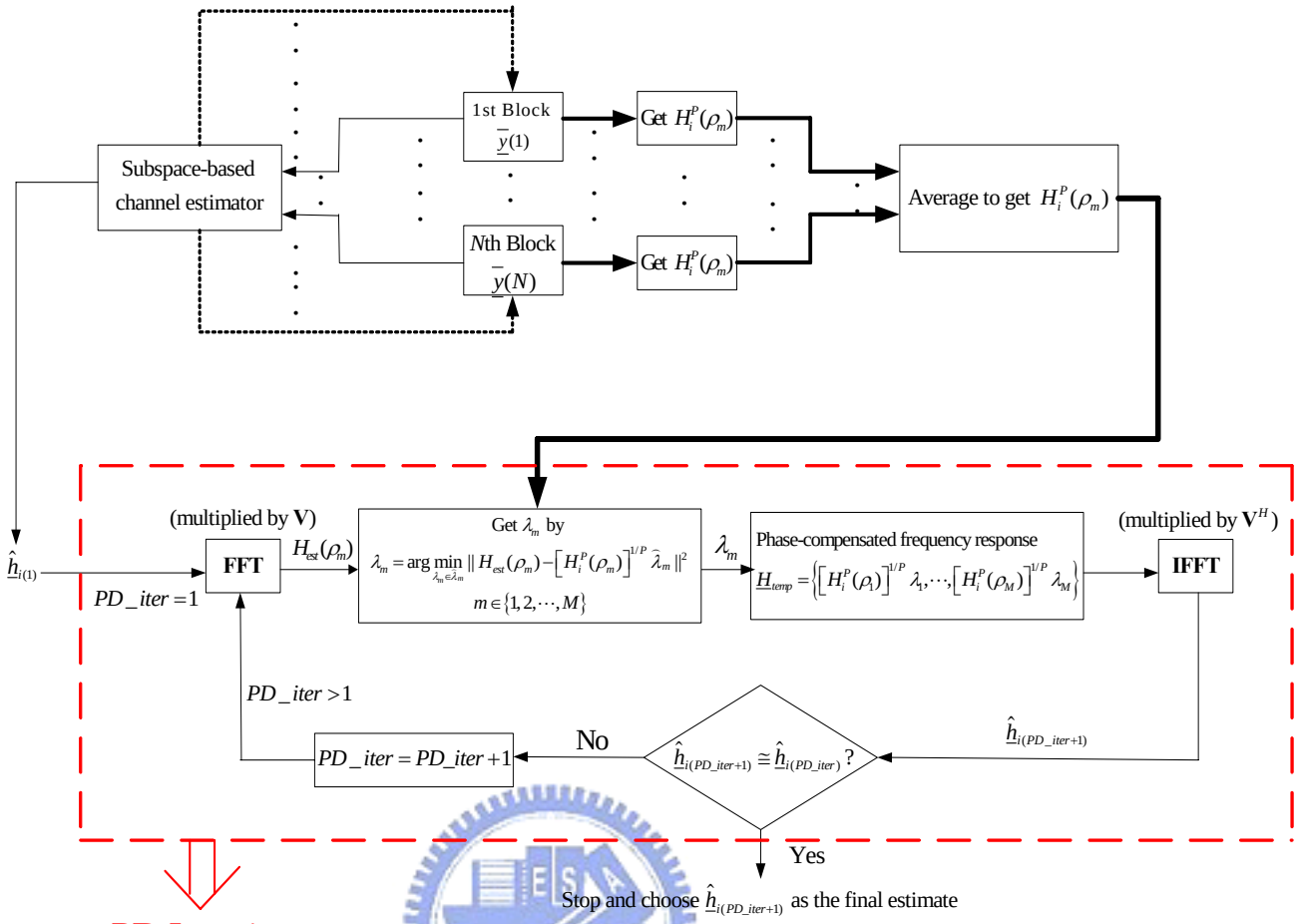

Fig. 4.4 Signal-flow chart of PD in STBC OFDM in static channel

Combining with BPSK and QPSK, the simulation in channel estimation MSE of all the three models will be performed and simulation results will be shown in chapter 5.

4.2.5 Choice of received blocks window size in time-varying channel

In time-varying channel, however, we use several same system flows instead of using only one flow in Fig.4.4. The number of system flows depends on how many received blocks are averaged each time (also called window size). Because the

channel states change, the received data will then be influenced. The method in section 4.2.4 thus will cause bigger estimation error. It is apparent that if the length of window size is N_{win}, it will cause a number of (N / N_{win}) system flow. Suppose N_{win} is selected that (N / N_{win}) becomes a positive integer.

As the case stands, a system with a shorter window size can follow the changes of channel. But it cannot fight against the noise as well as the system with a longer window size does. How to choose a proper window size relies on the changing speed of channels. Fig.4.5 displays the signal-flow chart of PD in STBC OFDM in time-varying channels with the window size $= (N / 3)$. Note that the system block "PD Iteration" here was specified in Fig.4.4.

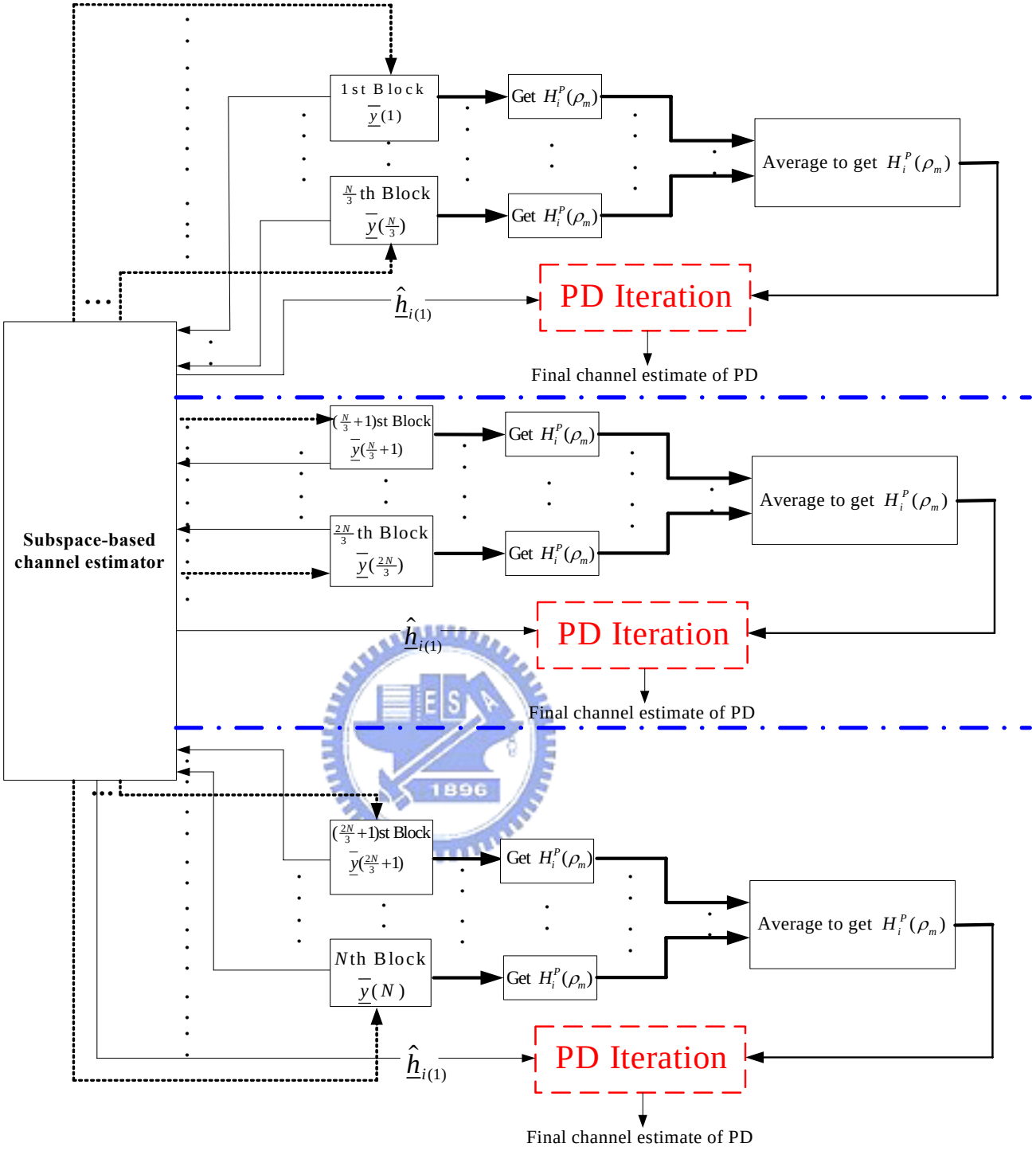

Fig. 4.5 Signal-flow chart of PD in STBC OFDM in time-varying channel

Chapter 5
Computer Simulations

In this chapter, computer simulations are implemented to verify four four-antenna STBCs: RO, SD, DD, and BD, along with OFDM system and algorithms proposed in chapter 4. We assume that all of four channels h_1, h_2, h_3, and h_4 are i.i.d and are normalized (i.e. $\sum_{i=1}^{4} |h_i|^2 = 1$) at any time. Channel estimation error performances are exhibited in section 5.1. First, simulations of subspace-based method discussed in section 4.1 are displayed in section 5.1.1. Next, we will show the performance of PD in both BPSK and QPSK systems in section 5.1.2. At last, in section 5.1.3, all these methods and models are performed in time-varying channels. Bit error rate performances of these STBC models are exhibited in section 5.2.

Before simulation results are illustrated, we should determine several things ahead. First, the figure of performance for channel estimation is defined in frequency domain:

$$\frac{\|\underline{\hat{h}} - \underline{h}\|^2}{\|\underline{h}\|^2} = \frac{\|\Delta\underline{h}\|^2}{\|\underline{h}\|^2} \tag{5.1}$$

where $\underline{\hat{h}}$ is the estimate of channel and $\underline{h}$ is the real one. We call this in Eq. (5.1) the normalized mean-squares channel error (NMSCE) in frequency domain. Although the value of the result in this equation equals to the NMSCE in time domain, we will compute it in frequency domain.

Next, we demonstrate the form of our precoders. With $M = 32,\ K = 24$, we design four $M \times K$ linear distinct precoders as

$$\boldsymbol{\theta}_1 = \left[\mathbf{I}_K(14:21,:);\mathbf{I}_K\right],\quad \boldsymbol{\theta}_2 = \left[\mathbf{I}_K(15:22,:);\mathbf{I}_K\right]$$

$$\boldsymbol{\theta}_3 = \left[\mathbf{I}_K(16:23,:);\mathbf{I}_K\right],\quad \boldsymbol{\theta}_4 = \left[\mathbf{I}_K(17:24,:);\mathbf{I}_K\right] \tag{5.2}$$

where $\mathbf{I}_K$ represents a $K \times K$ ($K = 24$, here) identity matrix. The matlab form $\left[\mathbf{I}_K(a:b,:);\mathbf{I}_K\right]$ means $\left[\mathbf{I}^T_{K(a\sim b)}\ \ \mathbf{I}^T_K\right]^T$ in the matrix form. Where the matrix form $\mathbf{I}^T_{K(a\sim b)}$ of the matlab form $\mathbf{I}_K(a:b,:)$ is the submatrix of $\mathbf{I}_K$ which contains from the ath to the bth row of $\mathbf{I}_K$. $\boldsymbol{\theta}_1$, $\boldsymbol{\theta}_2$, $\boldsymbol{\theta}_3$, and $\boldsymbol{\theta}_4$ are all used in four-antenna STBC OFDM systems. Precoders in these forms can keep the algorithm in section 4.2.2 works successfully [17].

5.1 Channel Estimate Error Performance

5.1.1 Subspace-based Method

In section 5.1 and 5.2, static channels are used in examining the estimator error. We want to see how the subspace method performs in different SNR. Several basic simulation setups are as follows:

- $N = 100$
- $M = 32,\quad K = 24$
- Rayleigh fading channels
- $L = 4$ ($5-$ray channels)
- BPSK or QPSK (in section 5.2) modulation

We first illustrate the tests of theoretical and simulated subspace method in four STBC models. The theoretical result follows Eq. (4.23). Fig.5.1 shows the theoretical result of subspace method in diagonally weighted RO and BD STBC OFDM. As SNR becomes higher, the performance becomes better. This property appears in all four STBCs and will be shown in the following figures. Fig.5.1 also shows that BD outperforms RO under the same k.

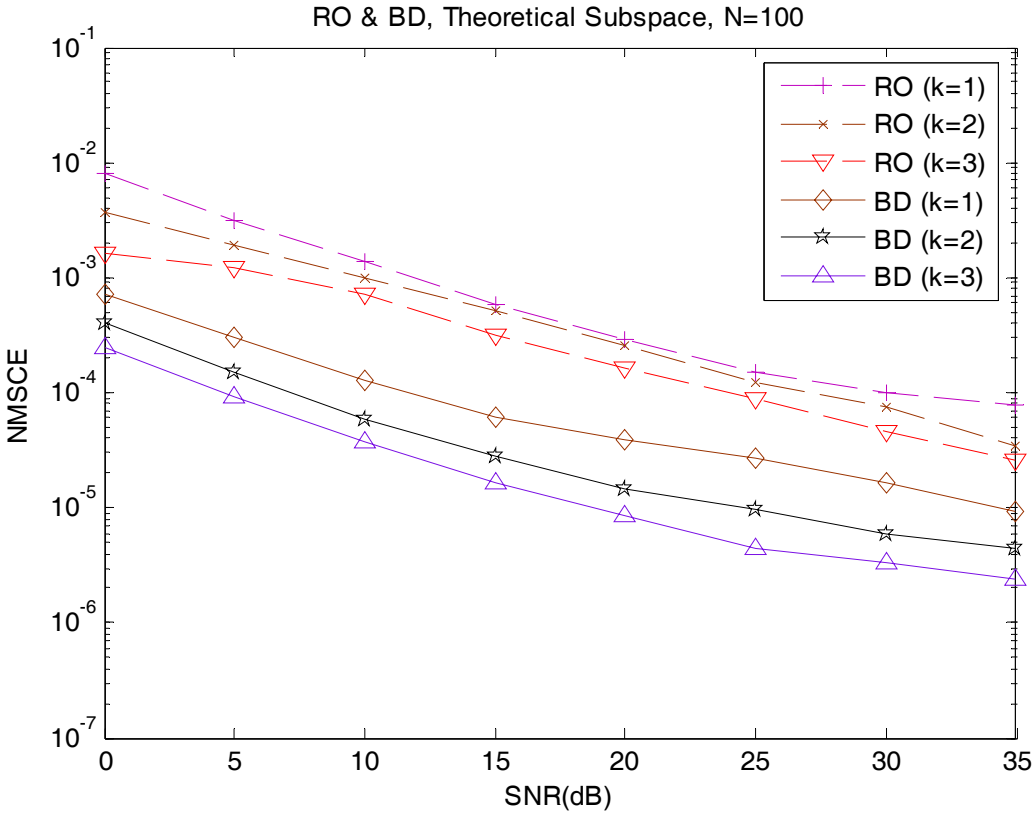

Fig. 5.1 RO & BD, Theoretical Subspace NMSCE

From Fig.5.2 to Fig.5.5, theoretical and simulated subspace NMSCE are exhibited in diagonally weighted STBCs RO, SD, DD, and BD. k=1 and 2 is set. In these figures, we can see that the simulated result is worse than the theoretical one. However, as SNR increases, the simulated result approaches the theoretical one, which fits the assumption of Eq. (4.23) in high SNR condition.

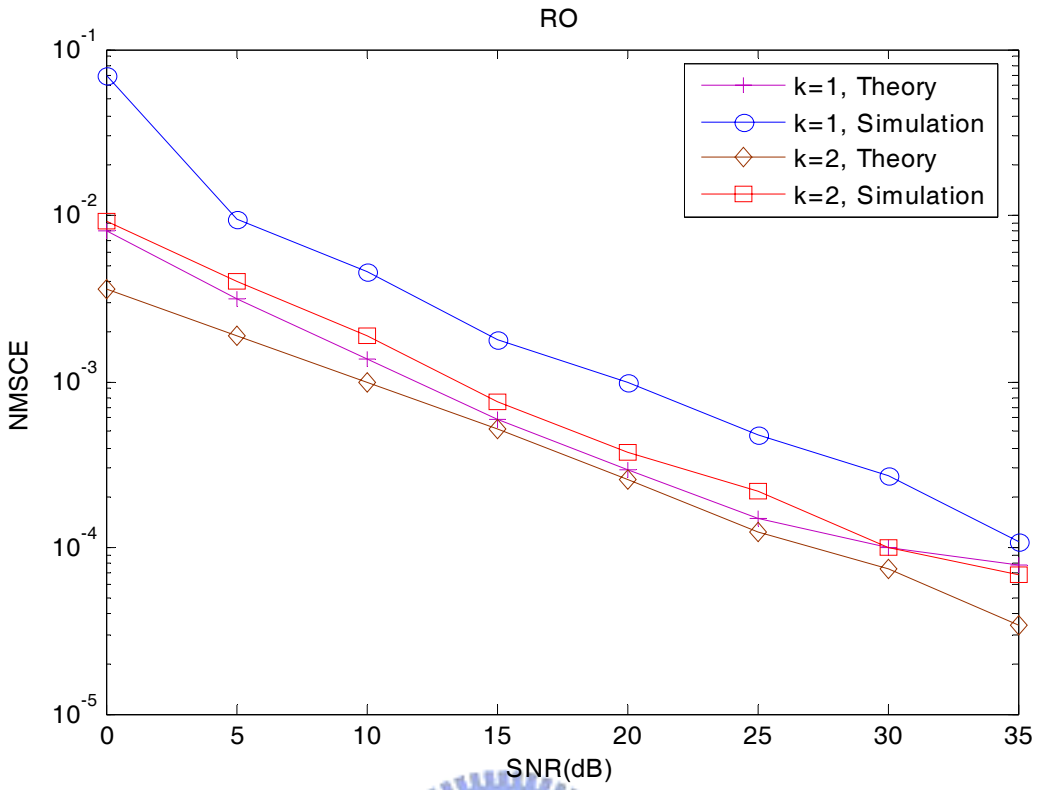

Fig. 5.2 RO, Theoretical and Simulated Subspace NMSCE

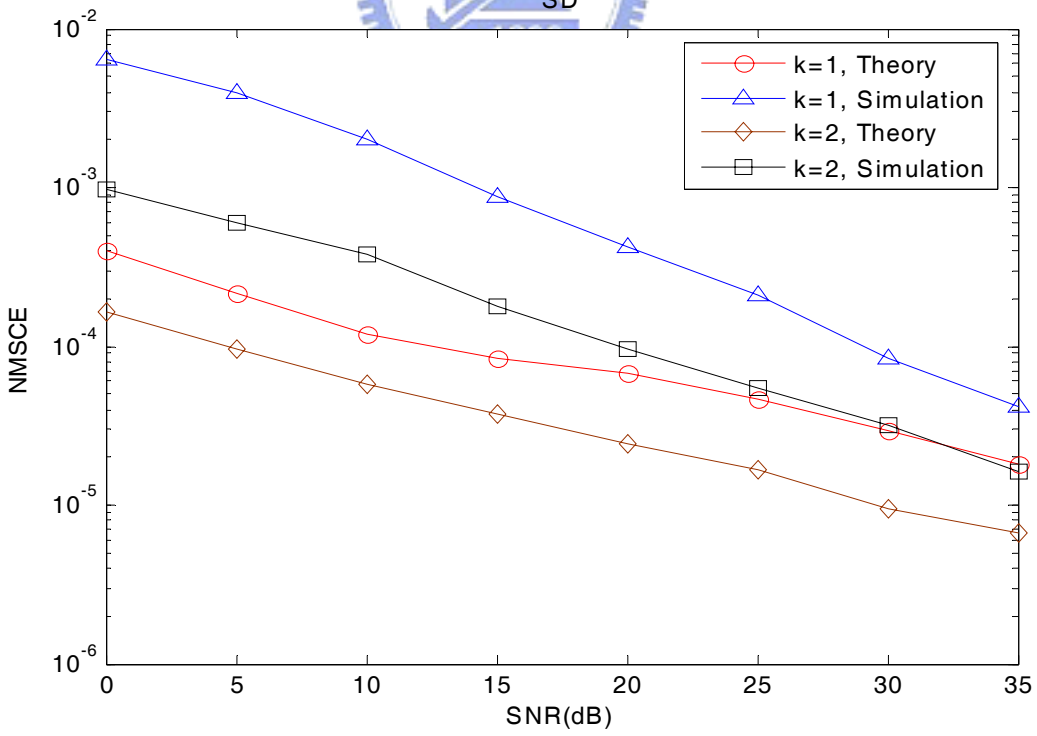

Fig. 5.3 SD, Theoretical and Simulated Subspace NMSCE

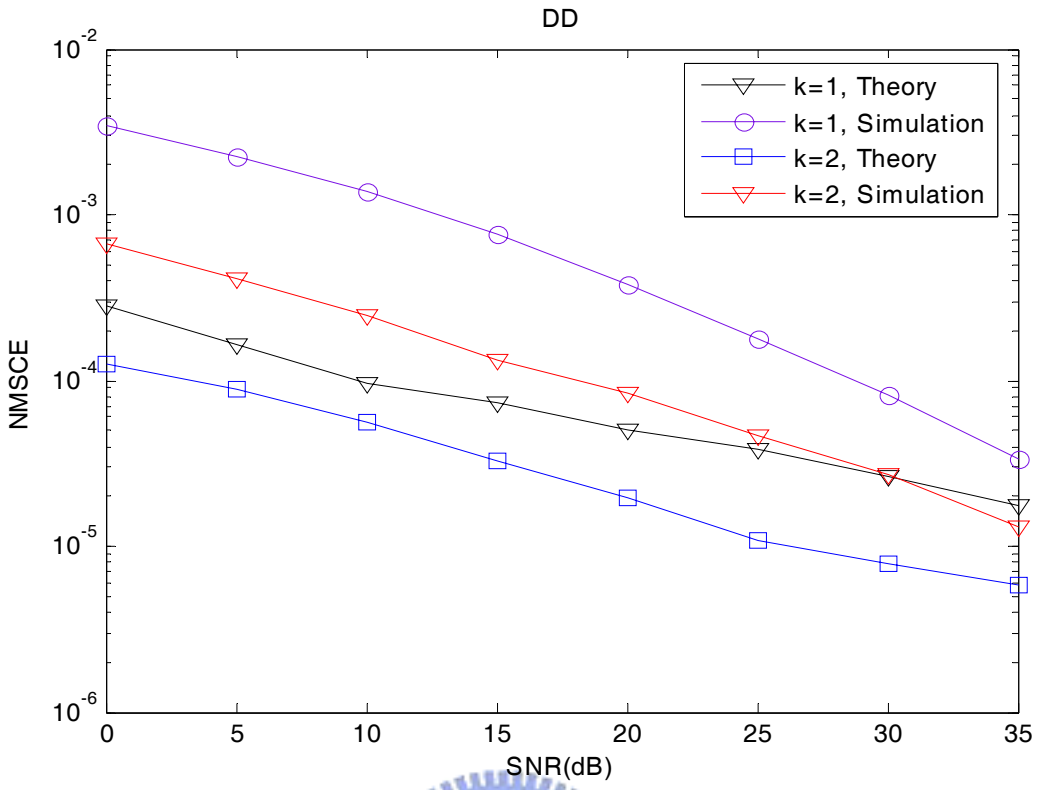

Fig. 5.4 DD, Theoretical and Simulated Subspace NMSCE

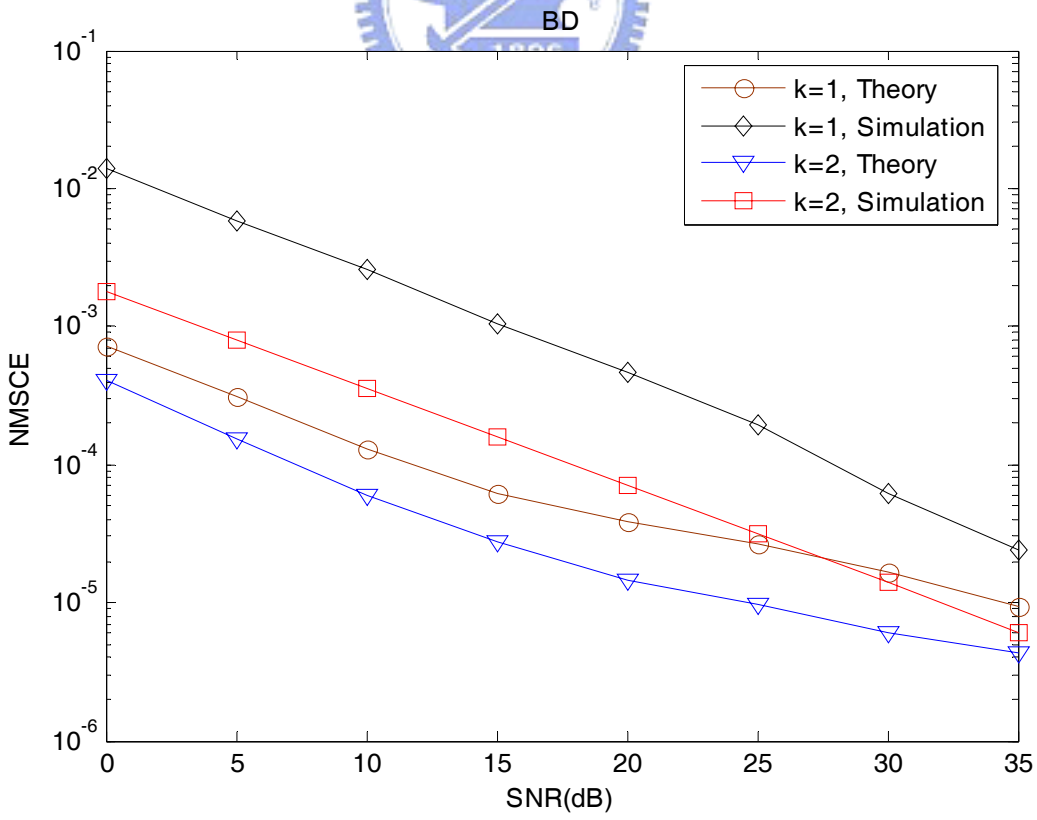

Fig. 5.5 BD, Theoretical and Simulated Subspace NMSCE

The performance of Subspace method of four-antenna STBCs in BPSK is shown in Fig.5.6 ($k=2$, $k=1$ also for RO). It shows that RO is worse than three complex non-orthogonal models.

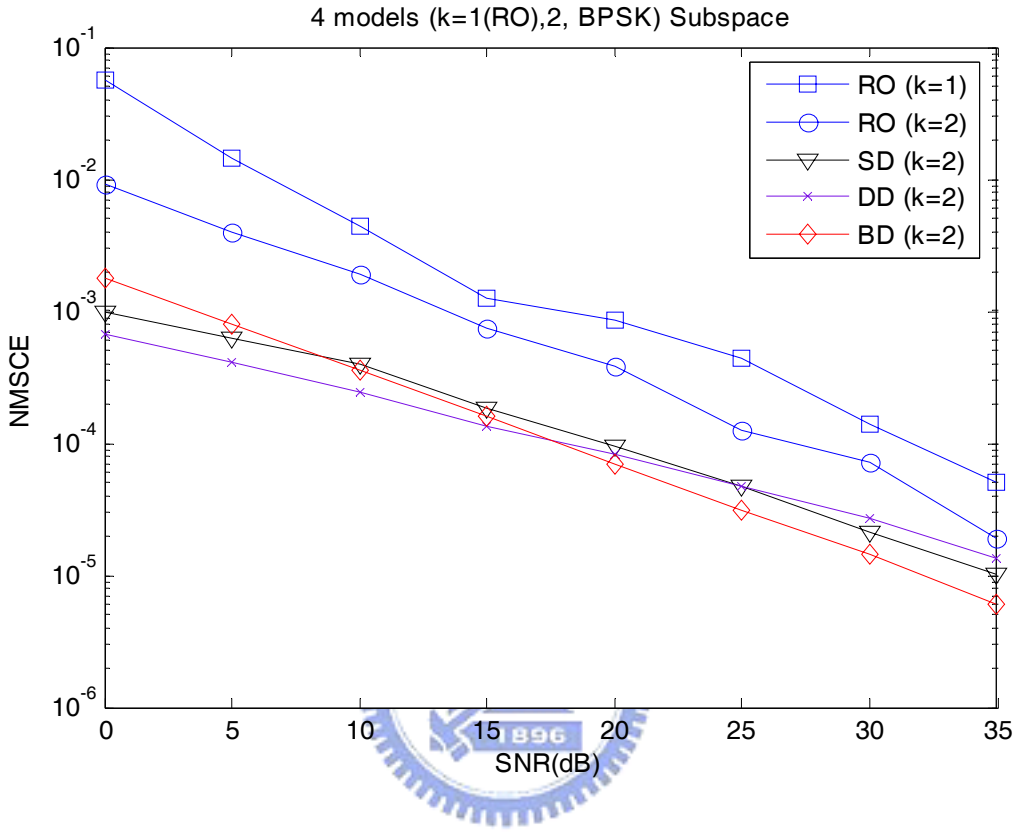

Fig 5.6 Four models, $k=2$ ($k=1$ for RO), Subspace

Since the theoretical value of Eq. (4.23) derived in [17] is an approximation for the channel estimate MSE for high SNR, there is a difference gap between theoretical and simulated results in all four models, which will become smaller when SNR increases.

Another property of diagonally weighted STBCs shown in Fig.5.1~5.5 is that in the same kind of STBC, the estimated error performance becomes better when k is larger. Let's discuss about it from Eq. (4.23), (4.24), and (4.25), as the diagonal elements of $\tilde{\sum}_q$ in Eq. (4.24) become larger, those of $\left(\tilde{\sum}_q\right)^{-1}$ in Eq. (4.25) will become smaller, and thus will cause the estimated mean square error in Eq. (4.23)

smaller. We had observed that when k grows, diagonal elements in $\tilde{\sum}_q$ also increase, which makes a better estimator. NMSCE in different k when SNR = 15 dB in RO with BPSK is shown in Fig.5.7. The results of three non-orthogonal models are similar to that of RO.

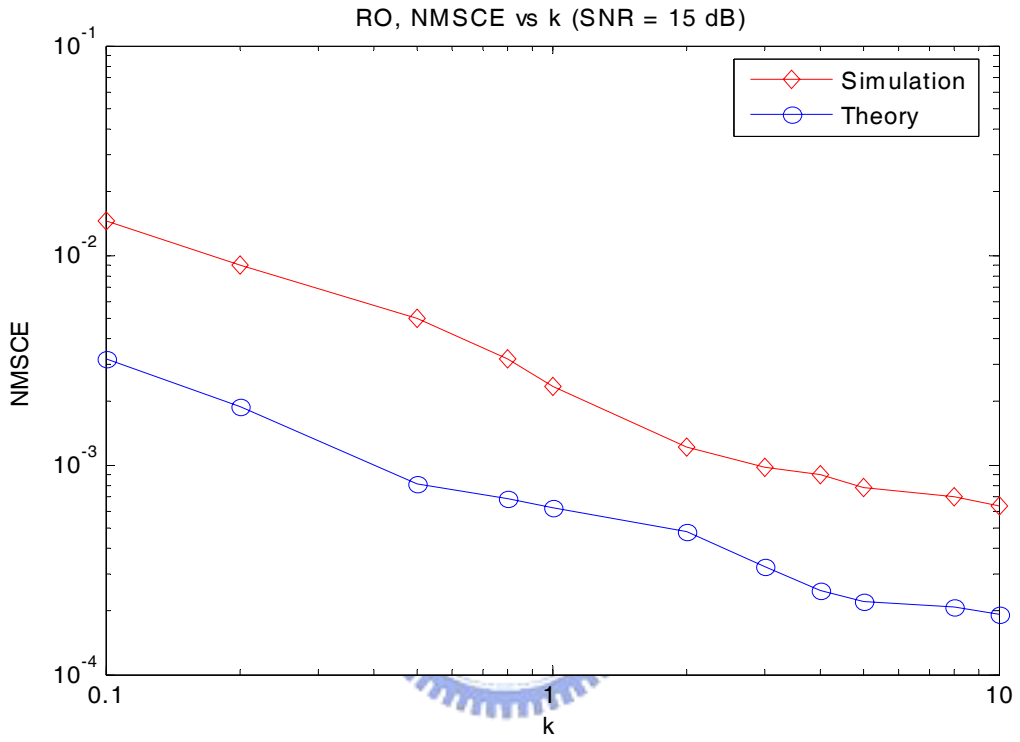

Fig. 5.7 RO, NMSCE vs. k (SNR = 15 dB)

5.1.2 Performance of PD

The performance of the improved method on subspace method, PD, will be illustrated and compared with subspace method both in BPSK and QPSK systems. First, we demonstrate the performance of PD of four-antenna STBCs in BPSK (Fig.5.8, $k=2$, $k=1$ also for RO) and in QPSK (Fig.5.9, $k=2$, no RO). Fig.5.8 shows that in BPSK, RO always has the worst performance, while DD has the best at low SNR. The second is SD and the third BD. At high SNR, however, the better and the worse performance orders of three non-orthogonal STBCs are different from that at low SNR. Such situation is the same in QPSK in Fig.5.9.

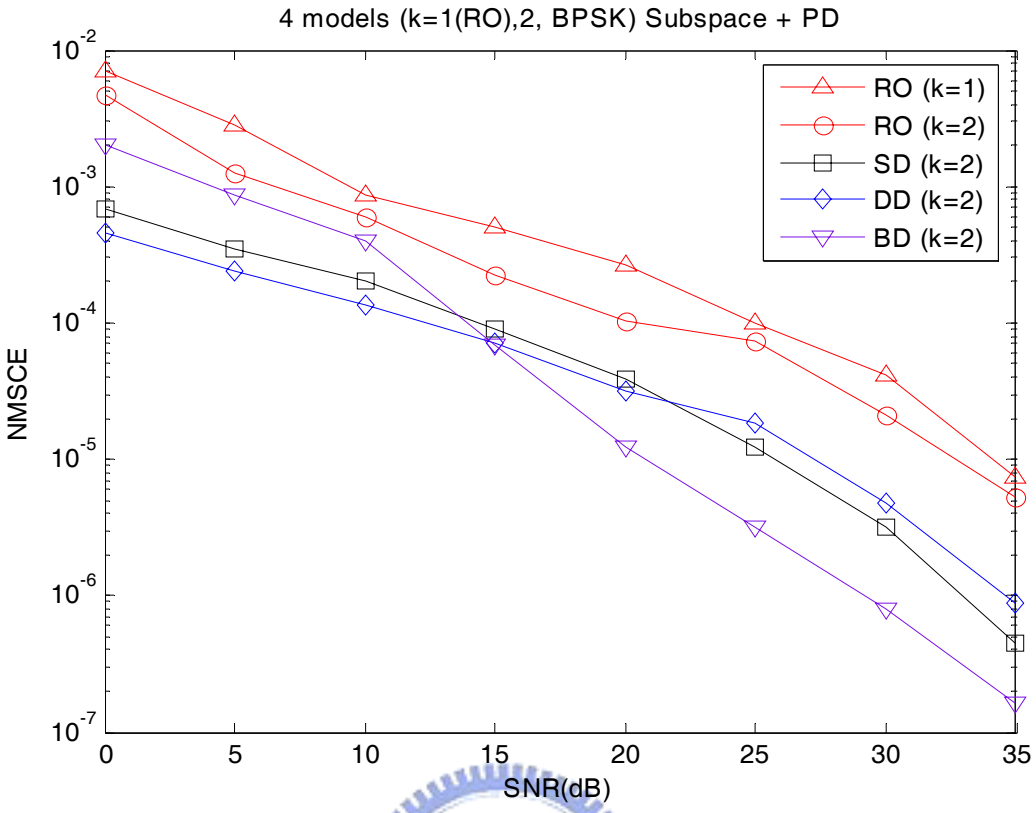

Fig. 5.8 Four models, $k=2$ ($k=1$ for RO), Subspace + PD BPSK

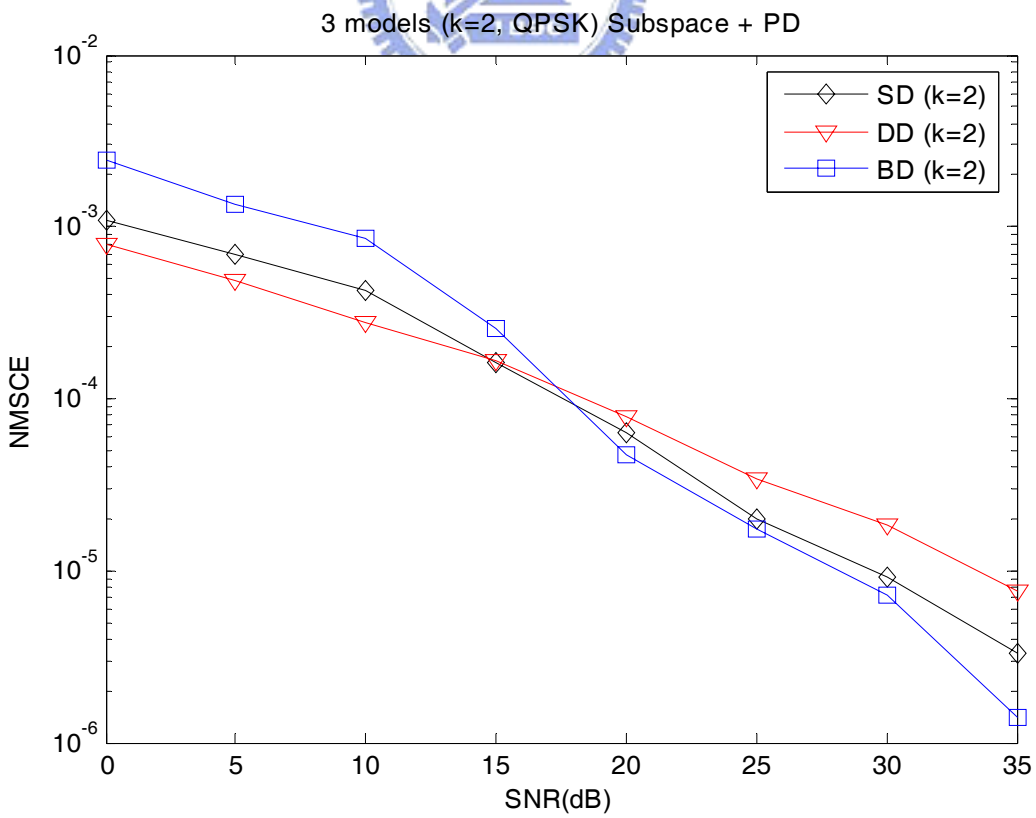

Fig. 5.9 Three models, $k=2$, Subspace + PD in QPSK

Performance comparisons between subspace method and subspace with PD in four models are displayed in Fig.5.10~5.13. Note that in RO, only BPSK is used and $k=1$, 2 is set in simulation. In other three non-orthogonal models, $k=2$ and both BPSK and QPSK are used

We can see that PD does improve the subspace method of all the four models in BPSK and SD, DD, BD in QPSK. Besides, the estimator in BPSK is better than that in QPSK in same conditions.

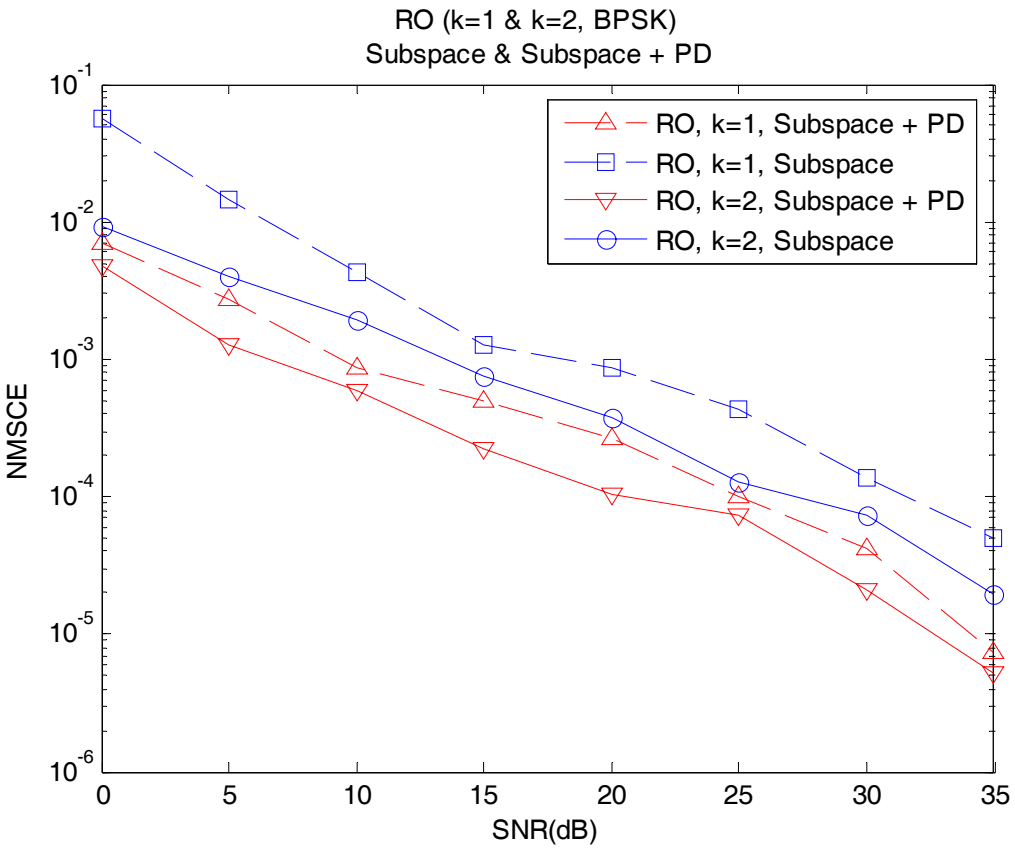

Fig. 5.10 RO, $k=1,2$, Subspace & Subspace + PD in BPSK

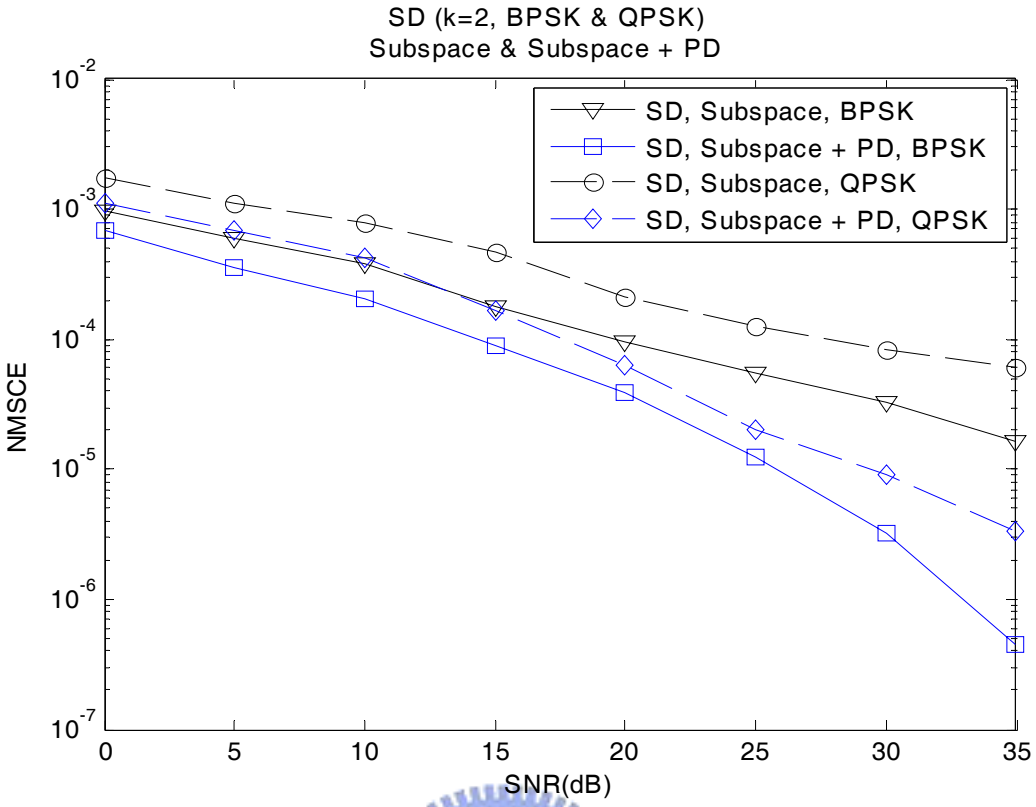

Fig. 5.11 SD, $k = 2$, Subspace & Subspace + PD in BPSK & QPSK

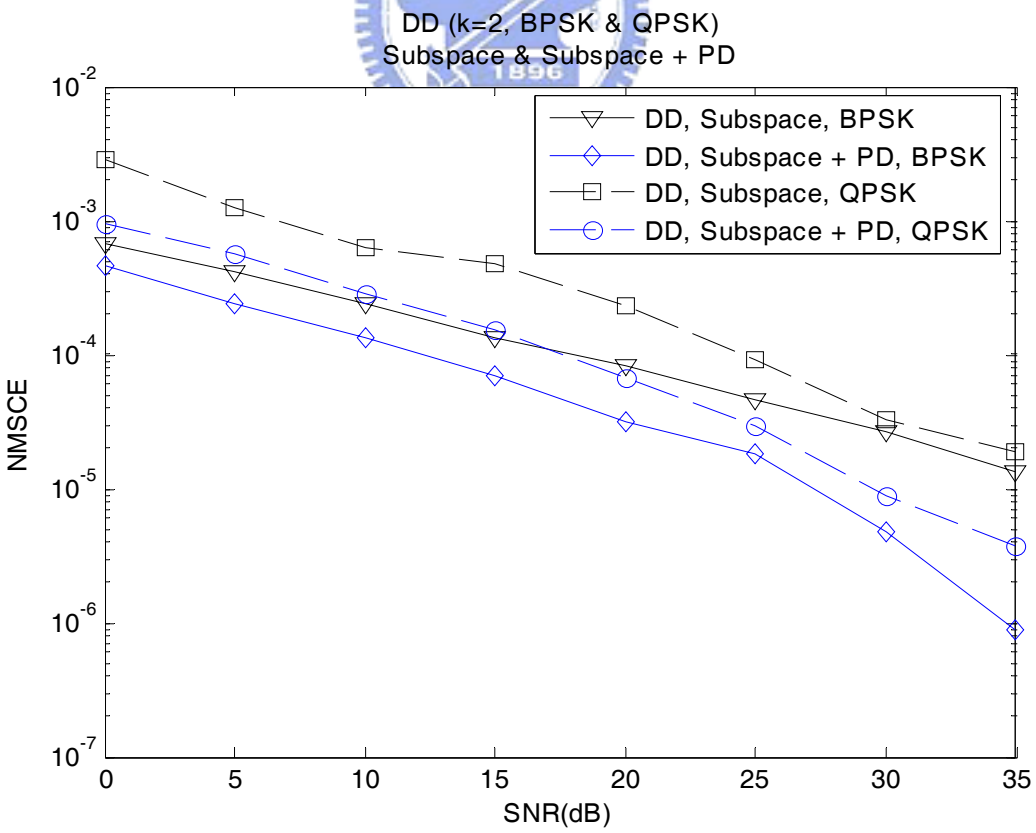

Fig. 5.12 DD, $k = 2$, Subspace & Subspace + PD in BPSK & QPSK

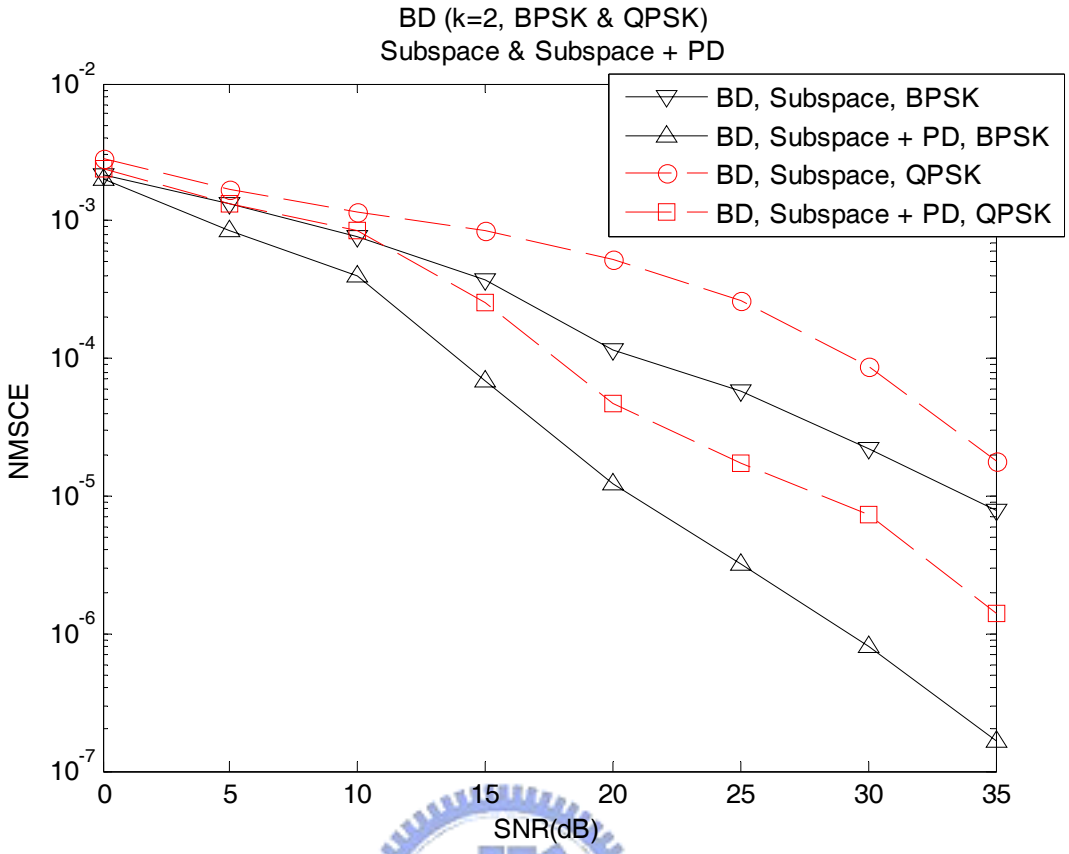

Fig. 5.13 BD, $k=2$, Subspace & Subspace + PD in BPSK & QPSK

We also show how PD acts here with different multipath lengths. $k=2$ and BPSK are used, here. With $L=4$ and $L=5$, subspace method performs in four models from Fig.5.14 to Fig.5.17. In the model of larger CP length, it will be less sensitive to channel noise variation, and will lead to a poorer performance. It is shown that PD is immune to multipath length.

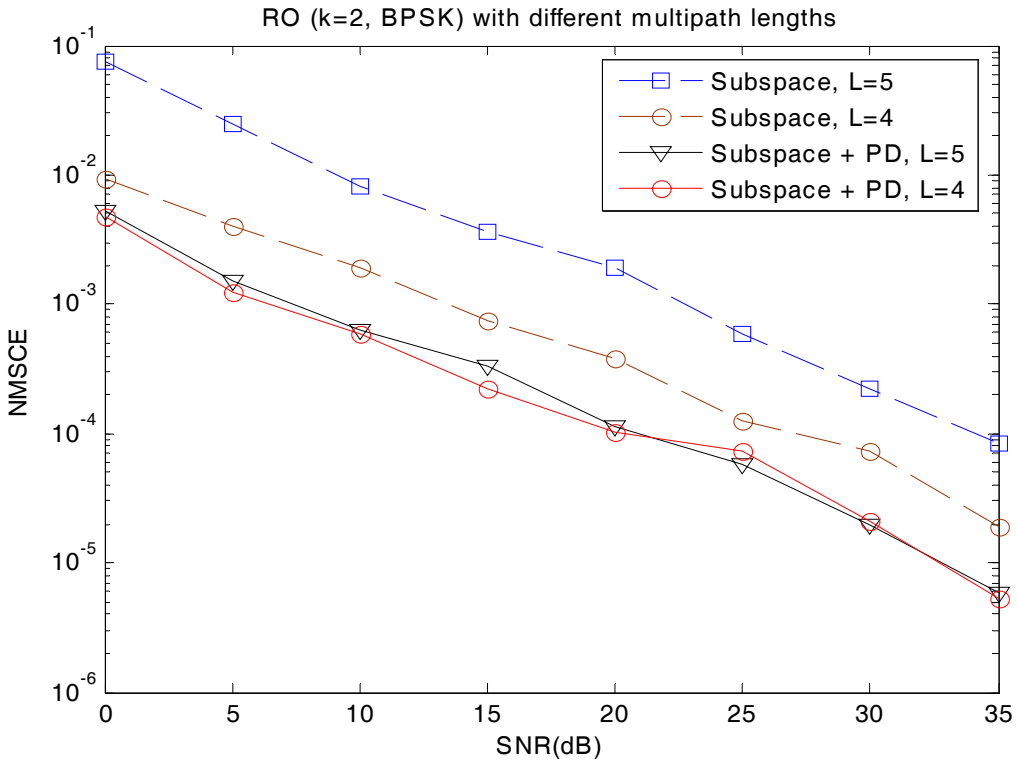

Fig. 5.14 RO, $k = 2$, BPSK, Subspace & Subspace + PD with different multipath lengths

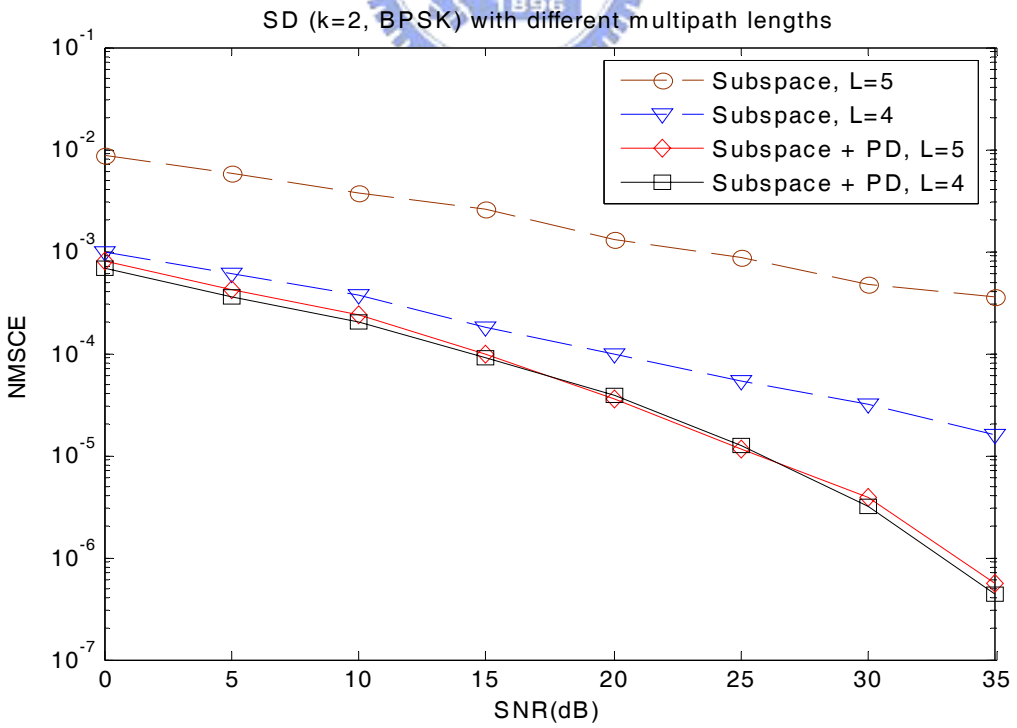

Fig. 5.15 SD, $k = 2$, BPSK, Subspace & Subspace + PD with different multipath lengths

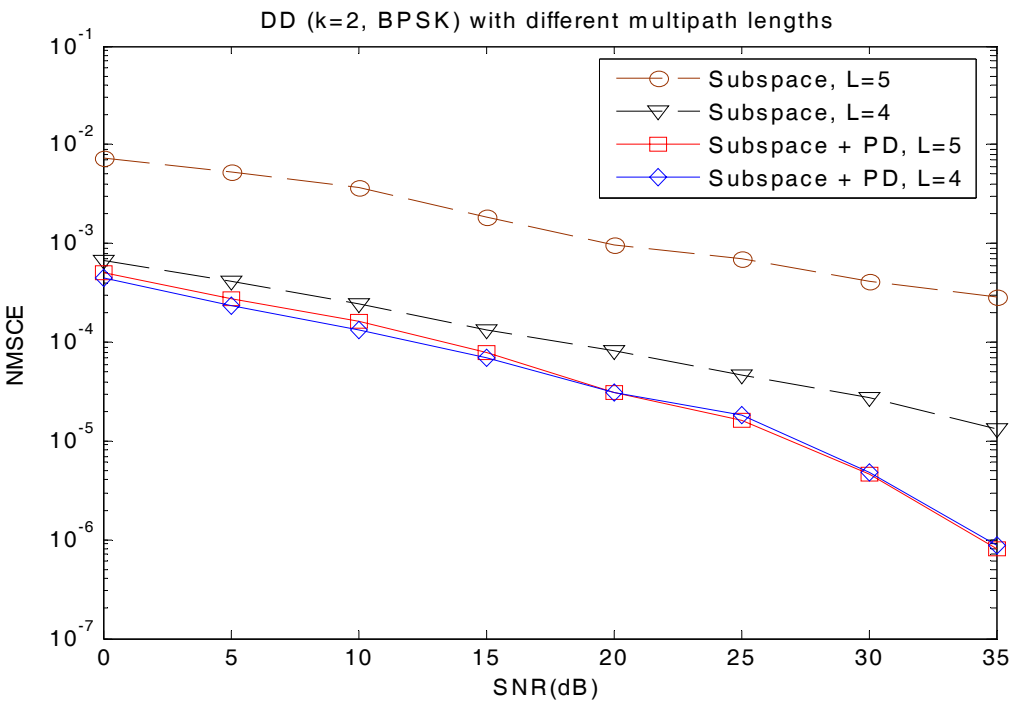

Fig. 5.16 DD, $k = 2$, BPSK, Subspace & Subspace + PD with different multipath lengths

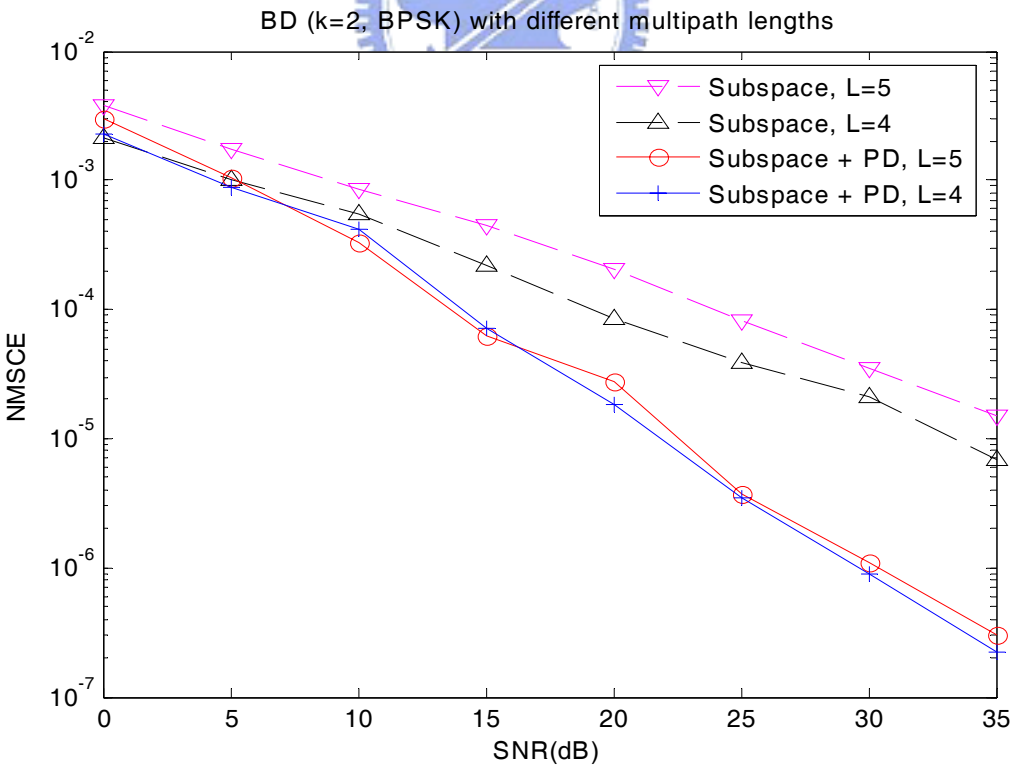

Fig. 5.17 BD, $k = 2$, BPSK, Subspace & Subspace + PD with different multipath lengths

5.1.3 Time-varying channel estimation

The time-varying channel environment we use here is based on Jake's model. In this simulation, it produces FIR channel taps at sampling rate 1 MHz. BPSK is used for all simulations in this section.

We first test the performances of subspace method in four STBC models in time-varying channels with different Maximum Doppler Frequencies (fd): 10Hz (Fig. 5.18), 50Hz (Fig. 5.19), 100Hz (Fig. 5.20), and 200Hz (Fig. 5.21). $N = 100$, $k = 2$ and BPSK are used.

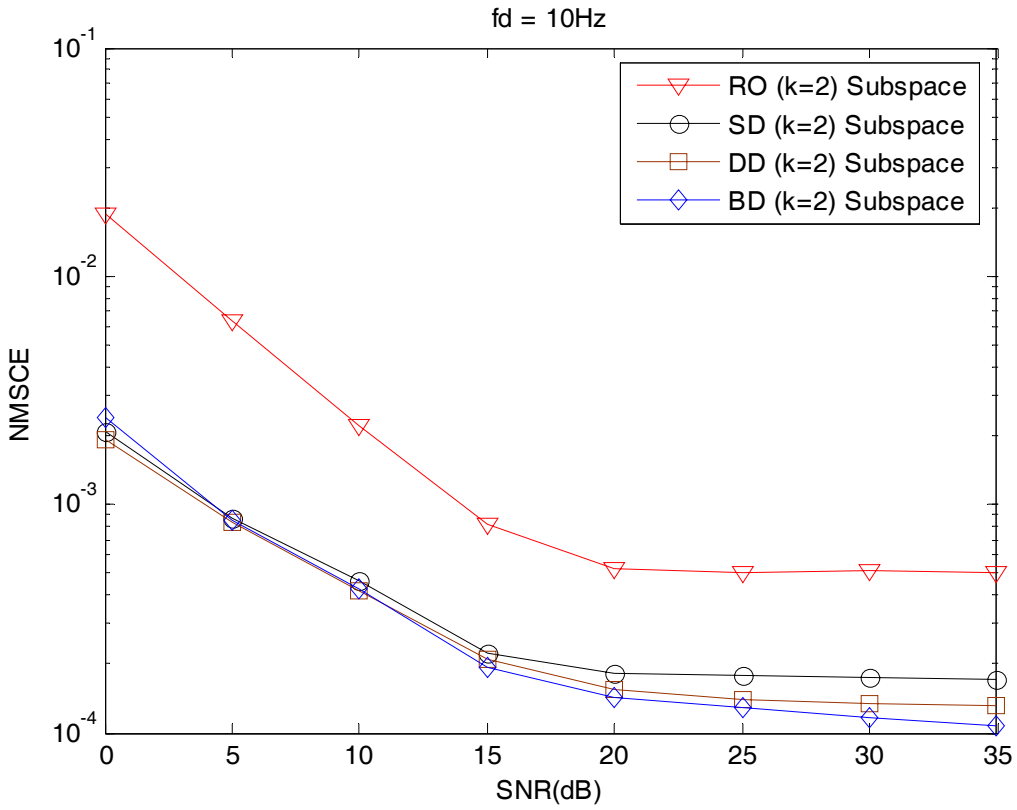

Fig. 5.18 Four models, $k = 2$, BPSK, Subspace with fd = 10Hz

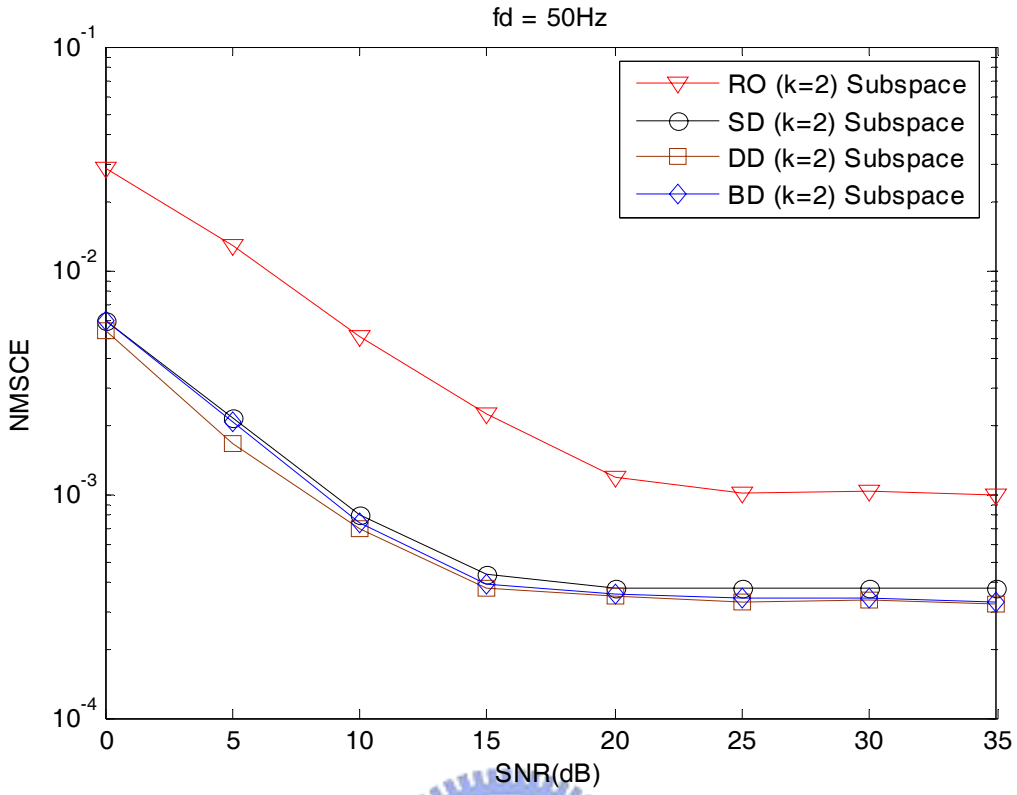

Fig. 5.19 Four models, $k = 2$, BPSK, Subspace with fd = 50Hz

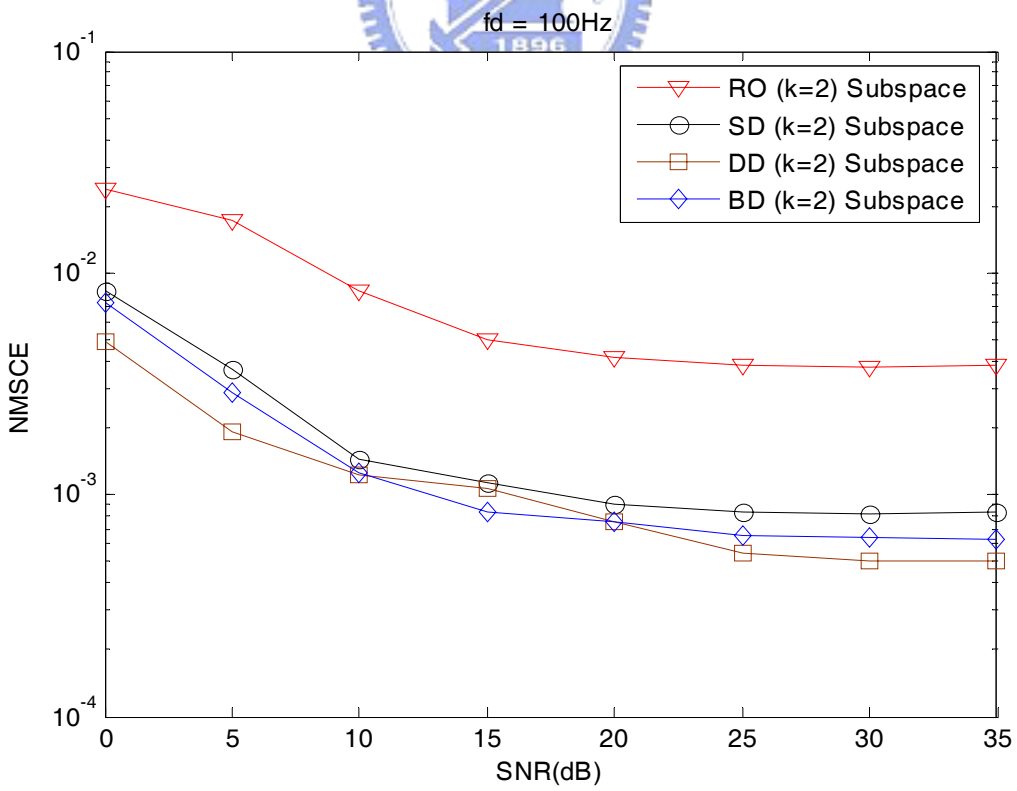

Fig. 5.20 Four models, $k = 2$, BPSK, Subspace with fd = 100Hz

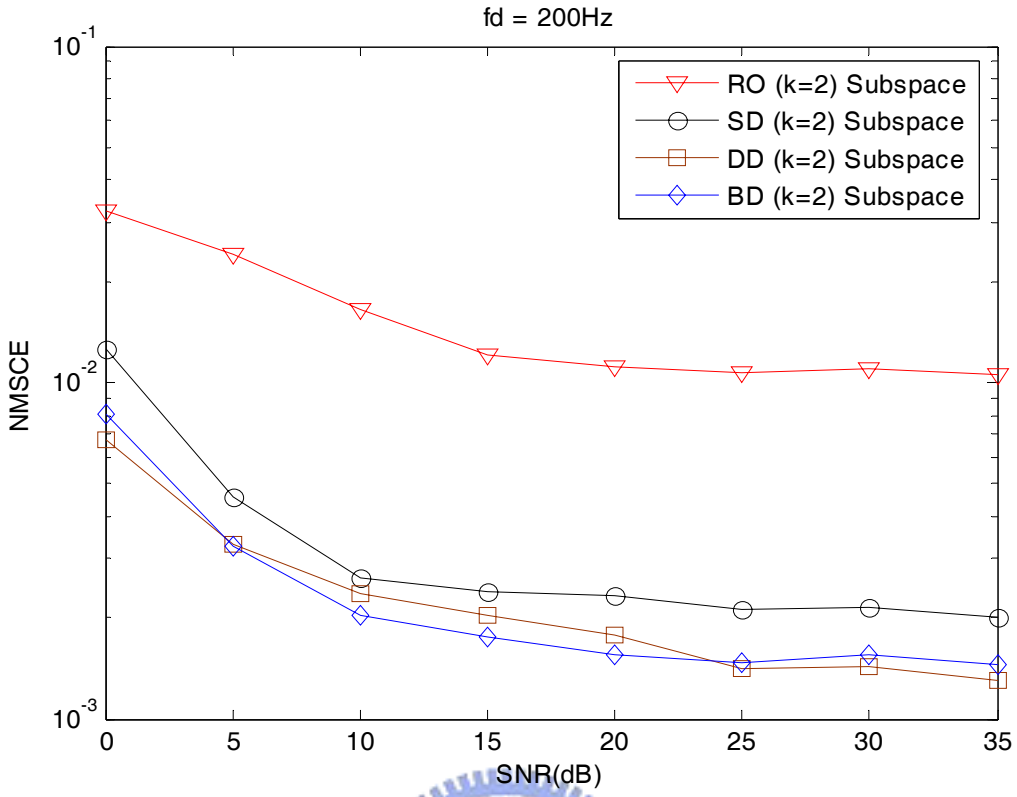

Fig. 5.21 Four models, $k = 2$, BPSK, Subspace with fd = 200Hz

When fd is higher, the estimator error is worse and all of them bring on error floors, which are caused by the phase shifting from Doppler Frequencies.

Then, we want to see how PD combined with small windows of received data blocks performs. Fig.5.22 presents that PD surely improves the subspace method estimator in time-varying channel, where $k = 2$, fd = 50Hz and $N = 100$ is set. The performance is better as a smaller window size is used. Since channel varies rapidly, a smaller window size means that there are more groups of channel information in PD to update the changing channel. We can see that the case window size = 1 makes the achievement of following the channel variation and it eliminates error floors in all STBC models. However, when the window is too small, it will suffer from the noise. So we choose 50 as a proper window size with which large enough to suppress noise and can also follow channel variation, as is shown in Fig.5.22 for RO and BD.

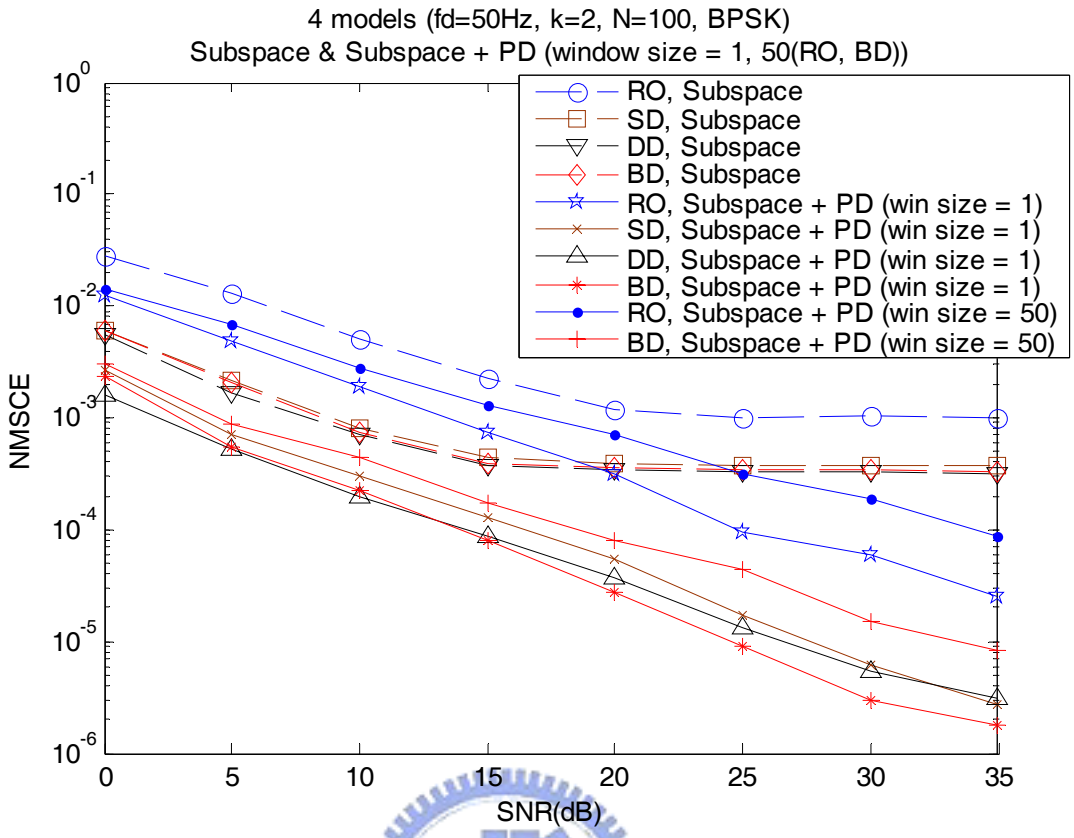

Fig. 5.22 Four models, $k = 2$, BPSK, fd = 50Hz,

Subspace & Subspace + PD (win size = 1, 50(RO, BD))

5.2 Bit Error Rate Performance

In this section, we will show the bit error rate performance in four STBCs with different k. BPSK and static channel are used. We will also discuss about the effect of k value on estimated channel error and noise.

From Fig. 5.23~5.26, BER performances in four models are exhibited. $k = 1,\ 2,$ and 0.8 are given. In same k, using the ideal channel state information (CSI) deservedly gets the best BER. With channel estimate error, subspace CSI gets a worse BER than ideal CSI. CSI from subspace with PD method, however, is better than subspace CSI for its improvement in channel estimation but is still worse than ideal CSI.

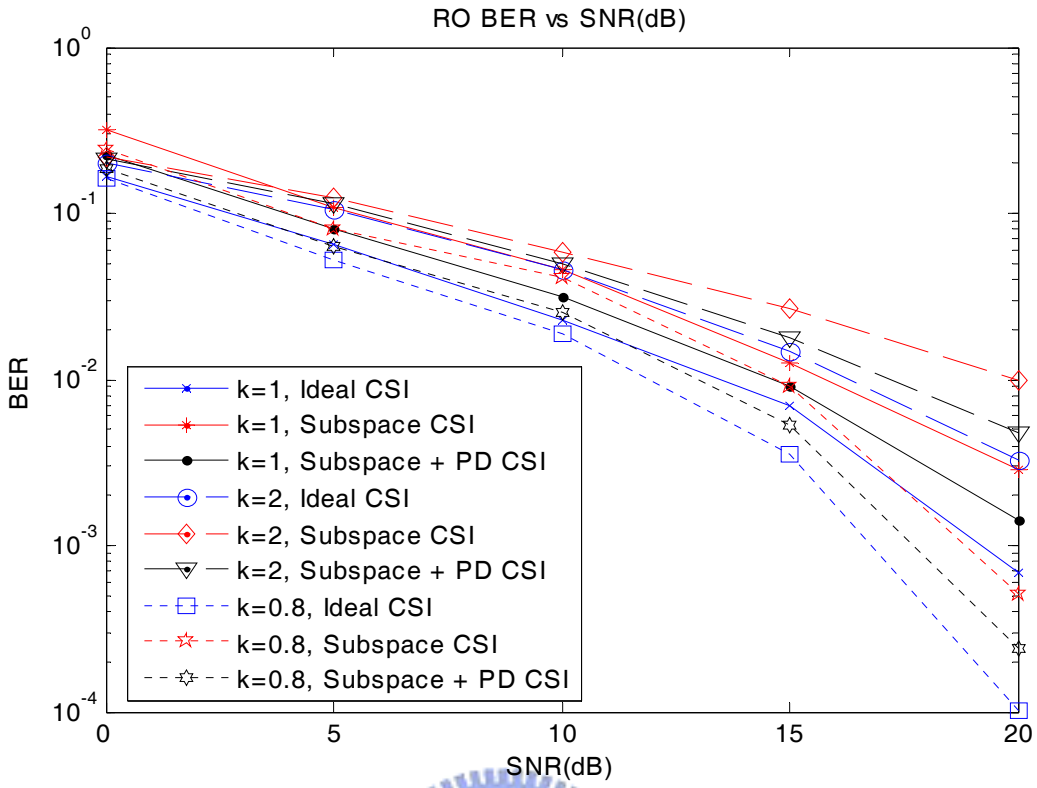

Fig. 5.23 RO, BER vs. SNR ($k = 1,\ 2,\ 0.8$)

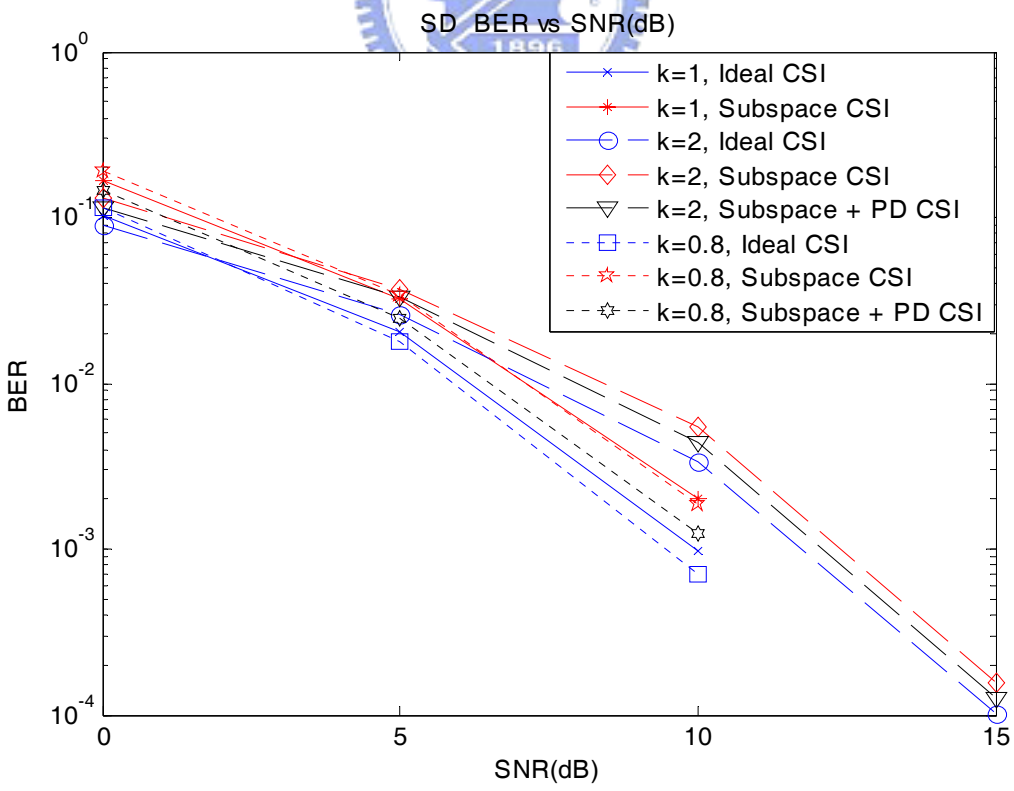

Fig. 5.24 SD, BER vs. SNR ($k = 1,\ 2,\ 0.8$)

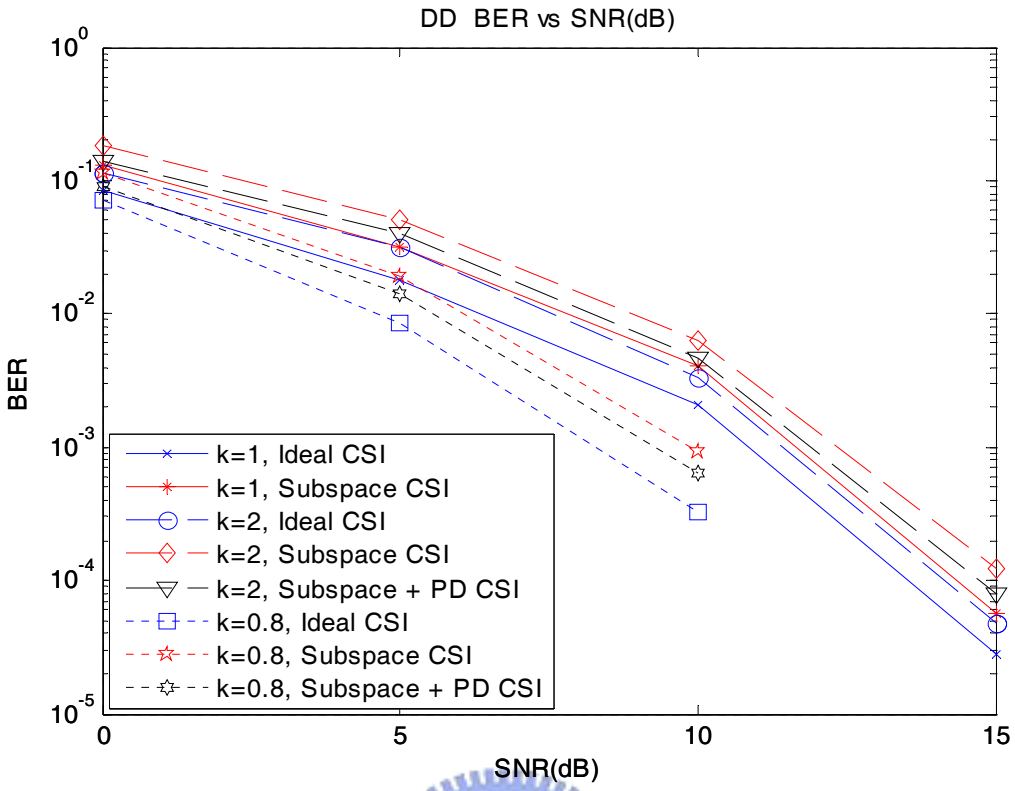

Fig. 5.25 DD, BER vs. SNR ($k = 1,\ 2,\ 0.8$)

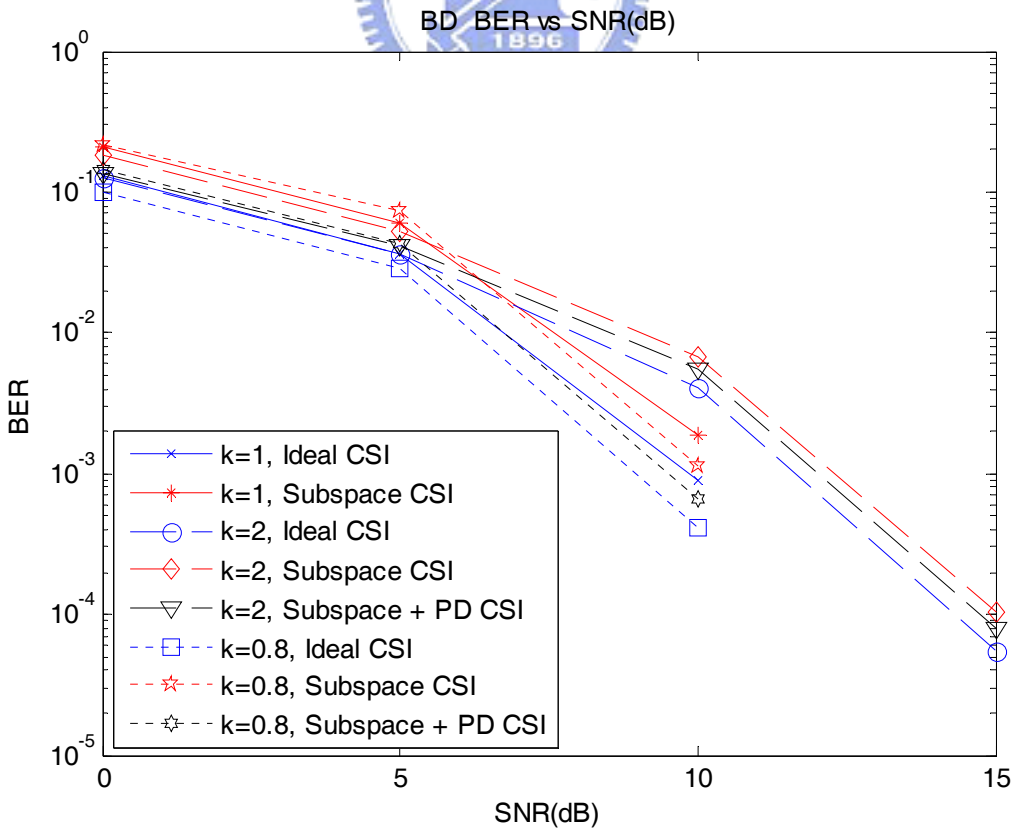

Fig. 5.26 BD, BER vs. SNR ($k = 1,\ 2,\ 0.8$)

The comparisons of BER between four models are shown in Fig.5.27 ($k=1$) and Fig.5.28 ($k=2$). We can see that the BER performance of RO is the worst and those of three complex non-orthogonal models are very close to each other.

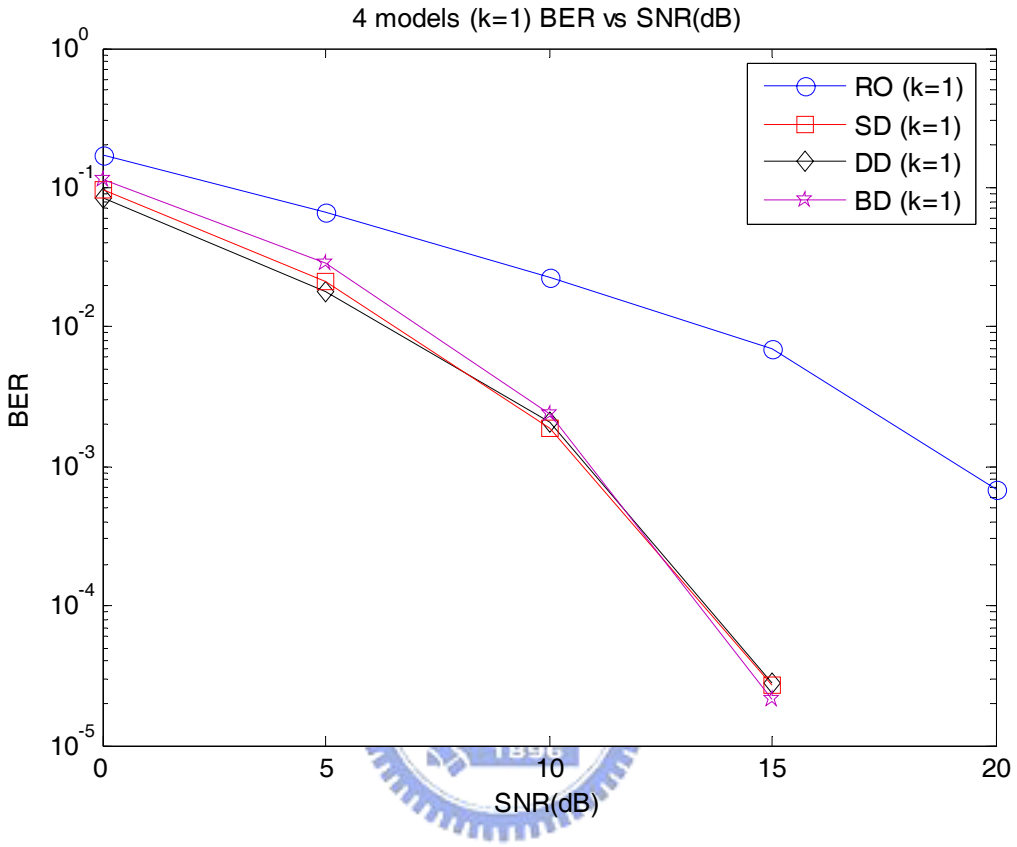

Fig. 5.27 Four models, BER vs. SNR ($k=1$)

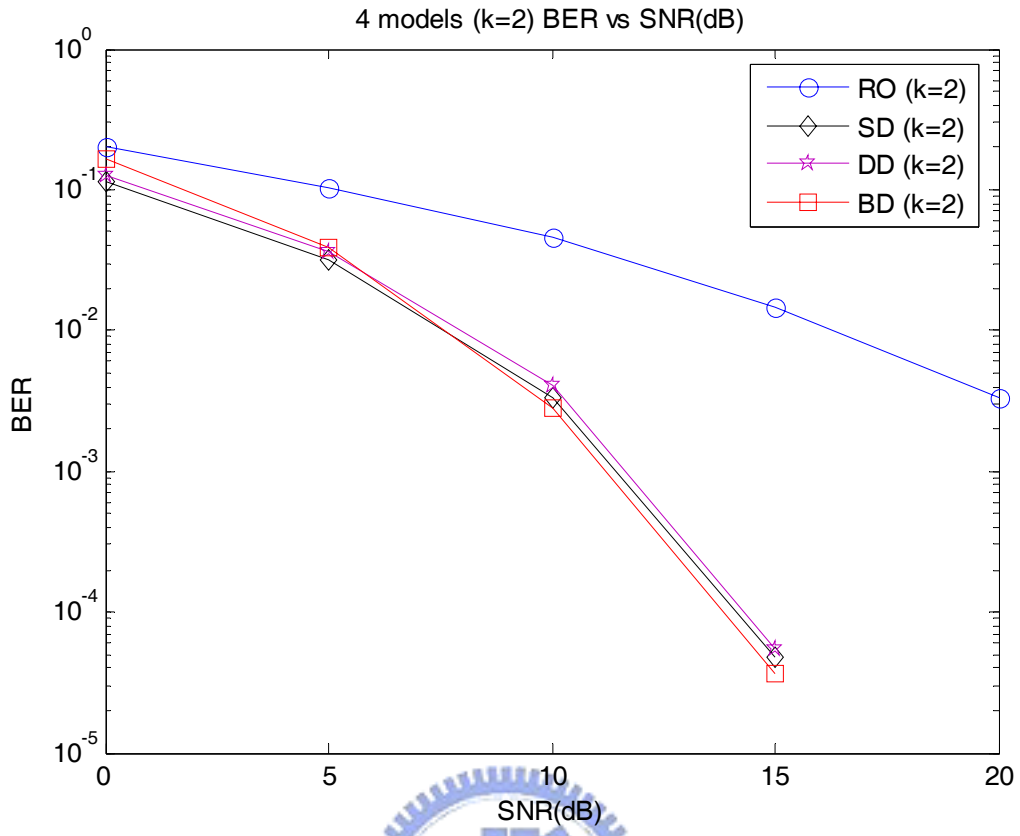

Fig. 5.28 Four models, BER vs. SNR ($k = 2$)

Note that the BER of $k = 2$ is bigger than that of $k = 1$ (the original STBCs). This is because the received signal power is enlarged when $k > 1$, and thus increase the noise power. On the contrary, the BER becomes smaller when $k < 1$ since noise power is decreased. This is a critical problem because the estimator performs better with the increase of k. This is a tradeoff. The effect of k is discussed in the following.

In diagonally weighted STBCs, the value of k affects channel estimate error, signal and noise power. Theoretically MSE in Eq. (4.23) can be written as a function of k:

$$E(\| \hat{\underline{h}} - \underline{h} \|^2) = E(\| \triangle \underline{h} \|^2) \approx \frac{\sigma_w^2 \| \mathbf{Q}^+ \|^2}{\sigma_s^2 N} = \frac{\sigma_w^2 \| \mathbf{Q}^+(k) \|^2}{\sigma_s^2 N} \tag{5.3}$$

where k affects matrix $\mathbf{Q}^{+}$ and the whole theoretically MSE. However, in comparison with noise value, the estimated error needs to be modified. Since from Eq. (2.3), if we substitute estimate $\hat{\underline{\mathbf{h}}} = \underline{\mathbf{h}} + \triangle\underline{\mathbf{h}}$ for realistic $\underline{\mathbf{h}}$, we will get:

$$\underline{\mathbf{r}} = \mathbf{S} * \hat{\underline{\mathbf{h}}} + \underline{\mathbf{n}} = \mathbf{S} * (\underline{\mathbf{h}} + \triangle\underline{\mathbf{h}}) + \underline{\mathbf{n}} = \mathbf{S} * \underline{\mathbf{h}} + \mathbf{S} * \triangle\underline{\mathbf{h}} + \underline{\mathbf{n}} \tag{5.4}$$

Note that k affects both signal and estimated error. So we have to modify the channel estimated error from $\triangle\underline{\mathbf{h}}(k)$ to the equivalent channel estimate error $\mathbf{S}(k) * \triangle\underline{\mathbf{h}}(k)$ to compare with noise $\underline{\mathbf{n}}(k)$.

Here, using the information in Eq. (5.3), we want to derive the theoretical average equivalent channel estimate error power as a function of k in frequency domain.

$$\begin{aligned}
P_{\mathbf{S}*\triangle\underline{\mathbf{h}}}(k) &= E\left[|\mathbf{S} * \triangle\underline{\mathbf{h}}|^2 \right]_{\textit{time domain}} = E\left[|\mathbf{S} \cdot \triangle\underline{\mathbf{h}}|^2 \right]_{\textit{frequency domain}} \\
&= tr\left\{ E\left[\left(\mathbf{S} \cdot \triangle\underline{\mathbf{h}}\right) \cdot \left(\mathbf{S} \cdot \triangle\underline{\mathbf{h}}\right)^{H} \right] \right\} = tr\left\{ E\left[\mathbf{S} \cdot \triangle\underline{\mathbf{h}} \cdot \triangle\underline{\mathbf{h}}^{H} \cdot \mathbf{S}^{H} \right] \right\} \\
&= E\left\{ tr\left[\mathbf{S} \cdot \triangle\underline{\mathbf{h}} \cdot \triangle\underline{\mathbf{h}}^{H} \cdot \mathbf{S}^{H} \right] \right\} = E\left\{ tr\left[\triangle\underline{\mathbf{h}} \cdot \triangle\underline{\mathbf{h}}^{H} \cdot \mathbf{S}^{H} \cdot \mathbf{S} \right] \right\} \\
&= tr\left\{ E\left[\triangle\underline{\mathbf{h}} \cdot \triangle\underline{\mathbf{h}}^{H} \cdot \mathbf{S}^{H} \cdot \mathbf{S} \right] \right\} = tr\left\{ E\left[\triangle\underline{\mathbf{h}} \cdot \triangle\underline{\mathbf{h}}^{H} \right] \cdot E\left[\mathbf{S}^{H} \cdot \mathbf{S} \right] \right\} \\
&= tr\left\{ E\left[\triangle\underline{\mathbf{h}} \cdot \triangle\underline{\mathbf{h}}^{H} \right] \cdot \left[\left(k^2 + 3\right) \cdot I_{4\times 4} \right] \right\} \\
&= \left(k^2 + 3\right) \cdot tr\left\{ E\left[\triangle\underline{\mathbf{h}} \cdot \triangle\underline{\mathbf{h}}^{H} \right] \right\} \\
&= \left(k^2 + 3\right) \cdot E(\| \triangle\underline{\mathbf{h}} \|^2) \\
&\approx \left(k^2 + 3\right) \cdot \frac{\sigma_w^2 \| \mathbf{Q}^{+}(k) \|^2}{\sigma_s^2 N}
\end{aligned} \tag{5.5}$$

k also influences signal power and noise power. In k diagonally weighted STBCs with BPSK, the received signal in frequency domain can be written as:

$$\begin{bmatrix} r_1 \\ r_2 \\ r_3 \\ r_4 \end{bmatrix} = (\pm 1) \begin{bmatrix} k & 1 & 1 & 1 \\ 1 & k & 1 & 1 \\ 1 & 1 & k & 1 \\ 1 & 1 & 1 & k \end{bmatrix} \begin{bmatrix} h_1 \\ h_2 \\ h_3 \\ h_4 \end{bmatrix} = (\pm 1) \begin{bmatrix} kh_1 + h_2 + h_3 + h_4 \\ h_1 + kh_2 + h_3 + h_4 \\ h_1 + h_2 + kh_3 + h_4 \\ h_1 + h_2 + h_3 + kh_4 \end{bmatrix} \tag{5.6}$$

For all channels are uncorrelated (i.e. $h_i^* * h_j = 0,\ \forall i \neq j$) and normalized (i.e.

$\sum_{i=1}^{4}|h_i|^2=1$), the average received signal power is:

$$\sum_{i=1}^{4}|r_i|^2=\frac{1}{4}\left[(k^2+3)(\sum_{i=1}^{4}|h_i|^2)\right]=\frac{k^2+3}{4} \tag{5.7}$$

So the theoretical average noise power is:

$$P_{\underline{\mathbf{n}}}(k)=\frac{k^2+3}{4}\cdot\frac{\sigma_w^2}{\sigma_s^2} \tag{5.8}$$

where σ_s^2/σ_w^2 is the signal-to-noise ratio.

The theoretical power of total perturbation of both equivalent channel estimate error and noise can therefore be written as:

$$\begin{aligned}P_{\text{total}}(k)&=P_{\mathbf{S}^*\triangle\underline{\mathbf{h}}}(k)+P_{\underline{\mathbf{n}}}(k)\\&\approx(k^2+3)\cdot\frac{\sigma_w^2\,\|\mathbf{Q}^+(k)\|^2}{\sigma_s^2 N}+\frac{k^2+3}{4}\cdot\frac{\sigma_w^2}{\sigma_s^2}\\&=(k^2+3)\cdot\frac{\sigma_w^2}{\sigma_s^2}\cdot\left[\frac{\|\mathbf{Q}^+(k)\|^2}{N}+\frac{1}{4}\right]\end{aligned} \tag{5.9}$$

The effect of k on power of noise, channel estimate error, the total perturbation and its theoretical value in BPSK at SNR = 10, 15dB in RO and BD are shown in Fig.5.29 and 5.30, respectively. We can see that low SNR will cause larger total perturbation. We find out that power of total perturbation becomes smallest when k is about 0.5. Therefore, to solve the problem that k enlarges the noise, we can choose k as this value to lessen BER with a little sacrifice of channel estimator.

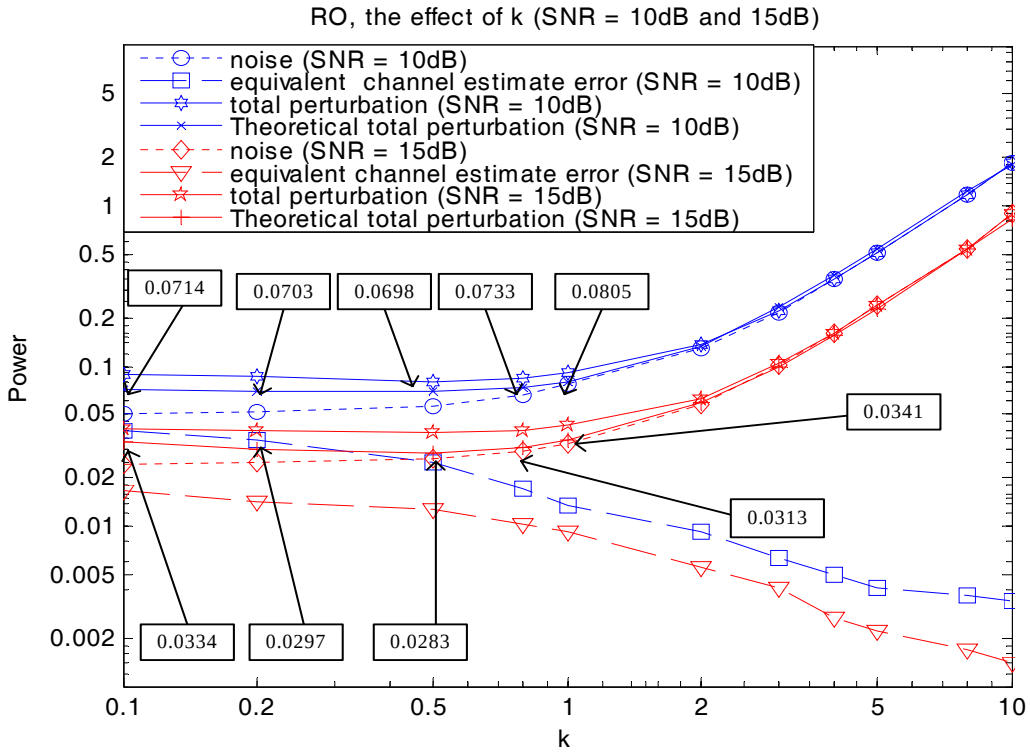

Fig. 5.29 RO, the effect of k on power of perturbations (SNR = 10, 15dB)

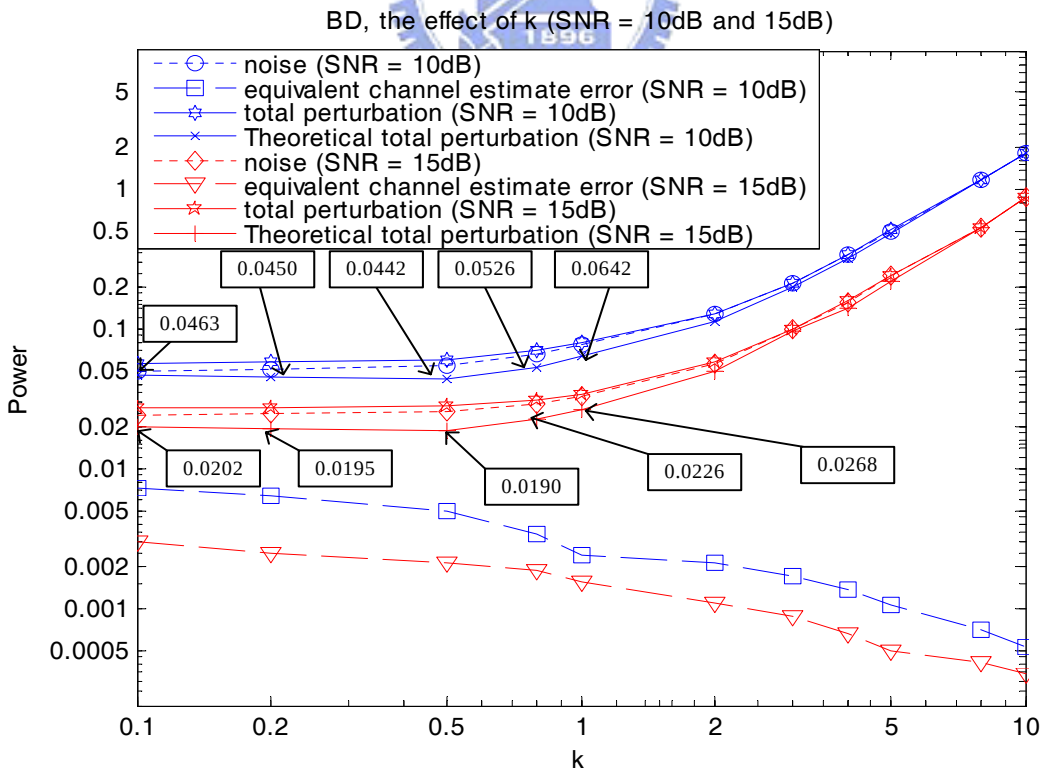

Fig. 5.30 BD, the effect of k on power of perturbations (SNR = 10, 15dB)

5.3 Summary and the related work

In this chapter, we have shown the channel estimate mean square error in some different conditions and the bit error performances in static channel for all the four kinds of STBCs. An important issue is to compare these performances of three complex non-orthogonal models SD, DD and BD. See Table 5.1.

Models / Performances	SD	DD	BD
Subspace MSE	Moderate (High & Low SNR)	Best (Low SNR) Worst (High SNR)	Best (High SNR) Worst (Low SNR)
Subspace+PD MSE	Moderate (High & Low SNR)	Best (Low SNR) Worst (High SNR)	Best (High SNR) Worst (Low SNR)
BER	Moderate	Moderate	Moderate

Table 5.1 Performances comparison between three complex non-orthogonal models

The diagonal weight value k affects channel estimate error, equivalent channel estimate error power, noise power and bit error rate. The increasing of k will decrease the first one but enlarge all the others. So the most appropriate value of k should be selected. From all the simulation results above, $k \approx 0.5$ is a proper value.

k will also change the power of probably only some of data symbols in transmission matrix, and will thus make the change of symbol power not uniform. To solve this problem, the even weight over each data symbol is also a method to prevent from singularity in PD for STBCs. Take diagonally weighted BD for example, only s_1 and s_4 on the diagonal are multiplied by k in Eq. (4.42). If we weight $s_1 \sim s_4$ each by one k as in Eq. (5.10), it can ensure nonsingularity when $k \neq 1$ for PD and

evenly distribute power to each symbol.

$$\mathbf{S}=\begin{bmatrix} k*s_1 & s_2 & s_3 & s_4 \\ -s_3^* & k*(-s_4^*) & s_1^* & s_2^* \\ s_2 & s_1 & s_4 & k*s_3 \\ -s_4^* & -s_3^* & k*s_2^* & s_1^* \end{bmatrix} \tag{5.10}$$

We name this kind of weighted BD the Uniformly Weighted BD, the comparisons of performances between Uniformly Weighted BD and Diagonally Weighted BD in simulated Subspace channel estimation and bit error rate are as follows. We can see that the performances of two BD models are close to each other.

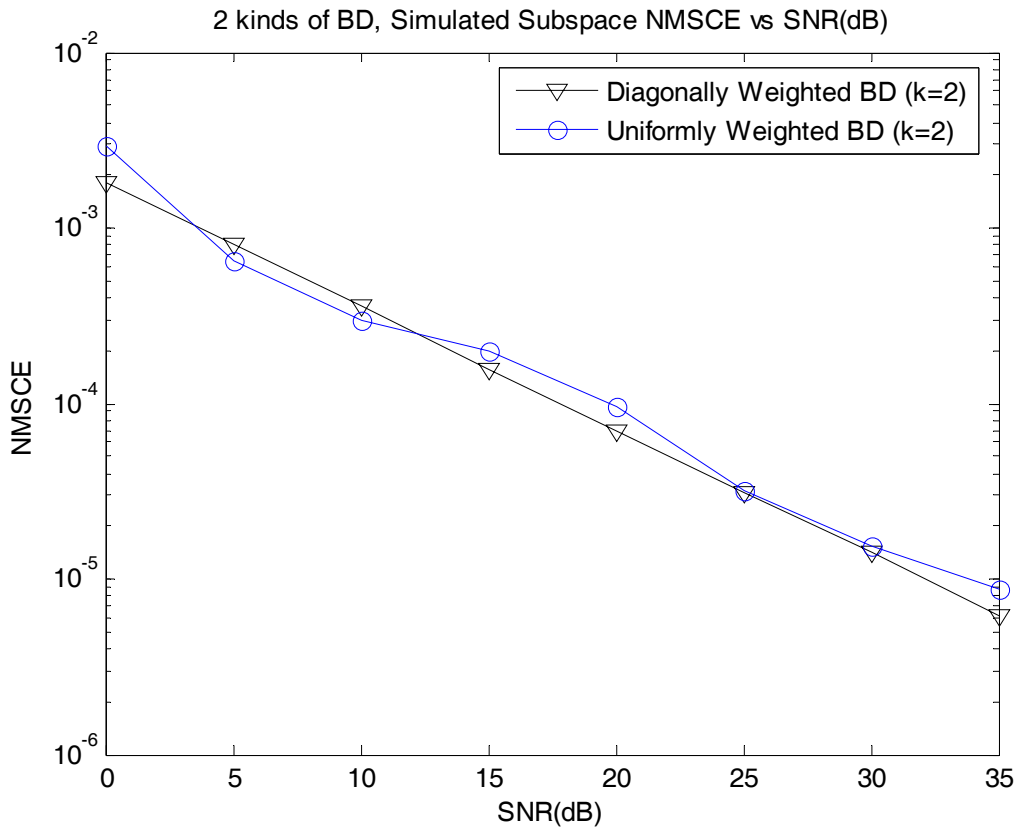

Fig. 5.31 Two different kinds of weighted BD, Subspace ($k=2$)

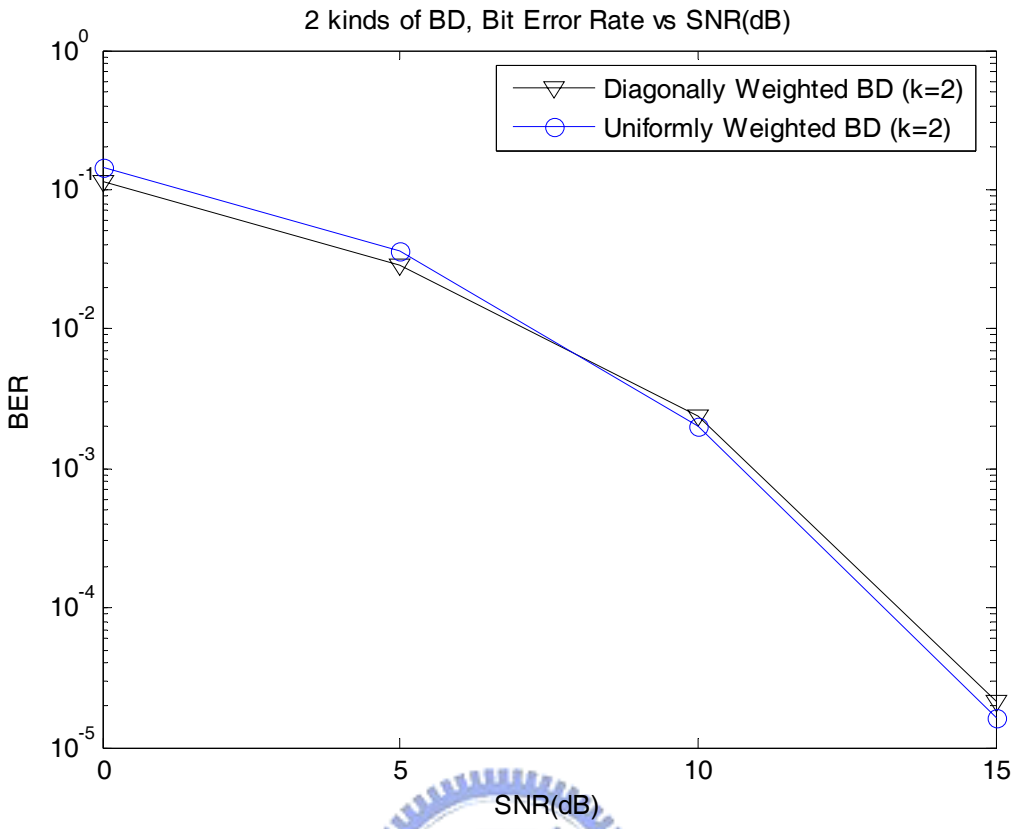

Fig. 5.32 Two different kinds of weighted BD, BER vs. SNR ($k = 2$)

Chapter 6
Conclusions

STBC OFDM offers diversity gain, which is an advantage in high data rate transmission. In STBCs with more than two transmit antennas, real symbol models can always achieve full transmission rate. But complex orthogonal models cannot attain this goal. Complex non-orthogonal models, however, sacrifice orthogonality to gain the full rate. We focus on four-transmit-antenna models in this thesis.

Multichannel estimation algorithms are important issues for STBC transceivers. By blind methods to estimate channels, we can avoid the problem of bandwidth consumption in using training sequences. A subspace-based channel estimation method is shown in which real orthogonal and complex non-orthogonal models can be adopted.

To further better the subspace channel estimates, we exploit a finite alphabet based method “PD”. PD is to solve channel phase ambiguities after getting the channel power response. In STBC OFDM, we need to compare all the possible data symbol pairs in obtaining the channel power response. Simulations have shown that PD does improve the NMSCE of subspace method.

However, the singular transmission matrices caused by some possible symbol pairs in complex non-orthogonal models will make getting channel power response and PD unavailable. We multiply the diagonal elements of their transmission matrices by a positive real weight k to solve this problem. Simulation results show that the value

of k affects both subspace estimator and bit error rate: When k is larger, the estimator becomes better, but incurs a larger noise and worse bit error performance. We can choose the value of k about 0.5 for the smallest total perturbation power to get a better bit error performance and a fairish estimator. The effect of k on power noise, channel estimate error, and total perturbation of RO and BD are also displayed.

In time-varying channel, received data block window size can be chosen combined with PD to track channel variation. It can also resolve the error floor of subspace estimator. A shorter window size can follow the change of channel accurately but will make the estimator suffer from noise more.

The PD method in this thesis for STBC OFDM is only utilized in BPSK and QPSK systems. In high-level modulations, it will become much more complex for the numerous number of possible symbol pairs. Therefore, the simplify mode of this method may be studied in the future.

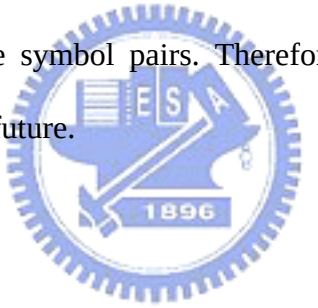

Appendix

Diagonally Weighted STBCs

In this appendix, transmission matrices ($\mathbf{S}$) and their correlation matrices ($\mathbf{S}^H * \mathbf{S}$) of k-diagonally weighted four-antenna STBCs are exhibited.

1. Real 4-by-4 Orthogonal (RO) STBC

$$\mathbf{S} = \begin{bmatrix} k*s_1 & s_2 & s_3 & s_4 \\ -s_2 & k*s_1 & -s_4 & s_3 \\ -s_3 & s_4 & k*s_1 & -s_2 \\ -s_4 & -s_3 & s_2 & k*s_1 \end{bmatrix} \tag{A.1.1}$$

and

$$\mathbf{S}^H * \mathbf{S} = \begin{bmatrix} a_{\mathrm{RO}} & 0 & 0 & 0 \\ 0 & a_{\mathrm{RO}} & 0 & 0 \\ 0 & 0 & a_{\mathrm{RO}} & 0 \\ 0 & 0 & 0 & a_{\mathrm{RO}} \end{bmatrix} \tag{A.1.2}$$

where

$$a_{\mathrm{RO}} = k^2 s_1^2 + s_2^2 + s_3^2 + s_4^2 \tag{A.1.3}$$

2. Spaced Diagonal (SD) STBC

$$\mathbf{S} = \begin{bmatrix} k*s_1 & s_2 & s_3 & s_4 \\ -s_2^* & k*s_1^* & -s_4^* & s_3^* \\ s_3 & s_4 & k*s_1 & s_2 \\ -s_4^* & s_3^* & -s_2^* & k*s_1^* \end{bmatrix} \tag{A.2.1}$$

and

$$\mathbf{S}^H * \mathbf{S} = \begin{bmatrix} a_{SD} & 0 & b_{SD} & 0 \\ 0 & a_{SD} & 0 & b_{SD} \\ b_{SD} & 0 & a_{SD} & 0 \\ 0 & b_{SD} & 0 & a_{SD} \end{bmatrix} \quad \text{(A.2.2)}$$

where

$$a_{SD} = k^2 |s_1|^2 + |s_2|^2 + |s_3|^2 + |s_4|^2 \quad \text{(A.2.3.1)}$$

$$b_{SD} = 2\,\mathrm{Re}\left[k * s_1 s_3^* + s_2 s_4^*\right] \quad \text{(A.2.3.2)}$$

3. Dual Diagonal (DD) STBC

$$\mathbf{S} = \begin{bmatrix} k*s_1 & s_2 & s_3 & s_4 \\ s_4 & k*s_3 & s_2 & s_1 \\ s_3^* & -s_4^* & k*(-s_1^*) & s_2^* \\ s_2^* & -s_3^* & -s_4^* & k*s_3^* \end{bmatrix} \quad \text{(A.3.1)}$$

and

$$\mathbf{S}^H * \mathbf{S} = \begin{bmatrix} a_{DD1} & b_{DD1} & 0 & c_{DD1} \\ b_{DD2} & a_{DD2} & c_{DD1} & 0 \\ 0 & c_{DD2} & a_{DD1} & -b_{DD2} \\ c_{DD2} & 0 & -b_{DD1} & a_{DD2} \end{bmatrix} \quad \text{(A.3.2)}$$

where

$$a_{DD1} = k^2 |s_1|^2 + |s_2|^2 + |s_3|^2 + |s_4|^2 \quad \text{(A.3.3.1)}$$

$$a_{DD2} = |s_1|^2 + |s_2|^2 + k^2 * |s_3|^2 + |s_4|^2 \quad \text{(A.3.3.2)}$$

$$b_{DD1} = (k-1)(s_1^* s_2 + s_3 s_4^*) \quad \text{(A.3.3.3)}$$

$$b_{DD2} = (k-1)(s_1 s_2^* + s_3^* s_4) \quad \text{(A.3.3.4)}$$

$$c_{DD1} = k(s_1^* s_4 + s_2 s_3^*) + (s_1 s_4^* + s_2^* s_3) \quad \text{(A.3.3.5)}$$

$$c_{DD2} = k(s_1 s_4^* + s_2^* s_3) + (s_1^* s_4 + s_2 s_3^*) \quad \text{(A.3.3.6)}$$

4. Block Diagonal (BD) STBC

$$\mathbf{S}=\begin{bmatrix} k*s_1 & s_2 & s_3 & s_4 \\ -s_3^* & k*(-s_4^*) & s_1^* & s_2^* \\ s_2 & s_1 & k*s_4 & s_3 \\ -s_4^* & -s_3^* & s_2^* & k*s_1^* \end{bmatrix} \quad \text{(A.4.1)}$$

and

$$\mathbf{S}^H*\mathbf{S}=\begin{bmatrix} a_{\mathrm{BD1}} & b_{\mathrm{BD1}} & c_{\mathrm{BD1}} & 0 \\ b_{\mathrm{BD2}} & a_{\mathrm{BD2}} & 0 & -c_{\mathrm{BD2}} \\ c_{\mathrm{BD1}} & 0 & a_{\mathrm{BD2}} & b_{\mathrm{BD1}} \\ 0 & -c_{\mathrm{BD2}} & b_{\mathrm{BD2}} & a_{\mathrm{BD1}} \end{bmatrix} \quad \text{(A.4.2)}$$

where

$$a_{\mathrm{BD1}}=k^2\,|\,s_1\,|^2+\sum_{i=2}^{4}|\,s_i\,|^2 \quad \text{(A.4.3.1)}$$

$$a_{\mathrm{BD2}}=\sum_{i=1}^{3}|\,s_i\,|^2+k^2\,|\,s_4\,|^2 \quad \text{(A.4.3.2)}$$

$$b_{\mathrm{BD1}}=k(s_1^*s_2+s_3s_4^*)+(s_1s_2^*+s_3^*s_4) \quad \text{(A.4.3.3)}$$

$$b_{\mathrm{BD2}}=k(s_1s_2^*+s_3^*s_4)+(s_1^*s_2+s_3s_4^*) \quad \text{(A.4.3.4)}$$

$$c_{\mathrm{BD1}}=(k-1)(s_1^*s_3+s_2^*s_4) \quad \text{(A.4.3.5)}$$

$$c_{\mathrm{BD2}}=(k-1)(s_1s_3^*+s_2s_4^*) \quad \text{(A.4.3.6)}$$

Bibliography

[1] R. van Nee, R. Presad, “OFDM wireless multimedia communications,” Artech House, Boston London, 2000.

[2] G.. L. Stuber, J. R. Barry, S. W. Mclaughlin, Y. Li, M. A. Ingram, and T. G. Pratt, “Broadband MIMO-OFDM wireless communications,” in *Proc. IEEE*, vol. 92, pp. 271 – 294, February 2004.

[3] T. H. Liew, and Lajos Hanzo, “Space-Time codes and concatenated channel codes for wireless communications,” in *Proc. IEEE*, vol. 90, February 2002, pp.187 – 219.

[4] S. M. Alamouti, “A simple transmit diversity technique for wireless communications,” *IEEE J. Select. Areas Communications*, vol. 16, pp. 1451—1458, October 1998.

[5] B. Vucetic, J. Yuan, “Space-Time Coding,” Wiley, Chichester England, 2003.

[6] V. Tarokh, H. Jafarkani , and A. R. Calderbank, “Space-Time block coding for wireless communications: Performance Results,” *IEEE J. Select Areas Communications*, vol. 17, pp. 451 – 460, March 1999.

[7] V. Tarokh, H. Jafarkani , and A. R. Calderbank, “Space-Time block codes from orthogonal designs,” *IEEE Trans. Information Theory*, vol. 45, pp. 1456 – 1467, July 1999.

[8] O. Tirkkonen, A. Boariu, and A. Hottinen, “Minimal non-orthogonality rate 1 space-time block code for 3+ Tx antennas,” *IEEE 2000 6th International Symp*, vol. 2, pp. 429 – 432, September 2000.

[9] R. Ran, J. Hou, and M. H. Lee, “Triangular non-orthogonal space-time block code,” *IEEE 57th Semiannual*, vol. 1, pp. 292 – 295, April 2003.

[10] Y. Li, N. Seshadri, and S. Ariyavisitakul, “Channel estimation for OFDM systems with transmitter diversity in mobile wireless channels,” *IEEE J. Select. Areas Communications*, vol. 17, pp.461 – 471, March 1999.

[11] E. Beres, and R. Adve, “Blind channel estimation for orthogonal STBC in MISO systems,” *IEEE Comm Society*, vol. 4, pp.2323–2328, Dec 2004.

[12] N. Nefedov, “Channel estimation for space-time block codes in frequency-flat channels,” *IEEE 15th CAS Symp*, vol. 1, pp.301–305, Sept 2004.

[13] Z. Ding and D. B. Ward, “Subspace approach to blind and semi-blind channel estimation for space-time block codes,” *IEEE Trans. Wireless Communications*, vol. 4, pp. 357–362, March 2005.

[14] J. Choi, “Equalization and semi-blind channel estimation for space-time block coded signals over a frequency-selective fading channel,” *IEEE Trans. Signal Processing*, vol. 52, pp. 774–785, March 2004.

[15] S. Zhou, and G. B. Giannakis, “Subspace-Based (Semi-) blind channel estimation for block precoded space-time OFDM,” *IEEE Trans. Signal processing*, vol. 50, pp.1215 – 1228, May 2002

[16] S. Zhou, and G. B. Giannakis, “Finite-Alphabet Based Channel Estimation for OFDM and Related Multicarrier Systems,” *IEEE Trans. on Communications*, vol. 49, pp.1402 – 1415, Augest 2001

[17] T. Y. Wu, “Blind Channel Estimation for Space-Time OFDM”, *NCTU Master Thesis*, July 2004